Characterization, Quantification and Modification of Starch Nanoparticles

by

Duncan Man Heen Li

A thesis
presented to the University of Waterloo
in fulfilment of the
thesis requirement for the degree of
Master of Science
in
Chemistry

Waterloo, Ontario, Canada, 2014

Author's Declaration

I hereby declare that I am the sole author of this thesis. This is a true copy of the thesis.

I understand that my thesis may be made electronically available to the public.

Abstract

Natural polymers, such as polysaccharides, have the potential to replace petroleum-based polymers in certain industrial applications. Ecosphere® starch nanoparticles (ENPs), produced by EcoSynthetix Inc., are starch-based and considered as a natural polymer. ENPs are produced by reactive extrusion of a thermoplastic melt of starch and glycerol in the presence of glyoxal which acts as a crosslinker. Aqueous dispersions of the ENPs, called Biolatex®, are used as a replacement for petroleum-based styrene-butadiene and styrene-acrylate copolymer latex emulsions in paper making. The objectives of this research were two-fold. The first objective was to explore the nature of the glyoxal crosslink in the ENPs. The second objective was to modify the ENPs with cationic groups and characterize the modified starches using nuclear magnetic resonance (NMR). Multidimensional NMR techniques, such as heteronuclear multiple-quantum correlation spectroscopy (HMQC) and heteronuclear multiple-bond correlation spectroscopy (HMBC) were the primary techniques used to learn more about the presence of a crosslink, the stability of the crosslink and the location of the crosslink in water, DMSO, and DMSO/water mixtures. Cationic modifications were accomplished by reacting the ENPs with reagents such as 2,3-epoxypropylalkylammonium chloride or 3-chloro-2-hydroxypropyltrialkylammonium chloride, which are used extensively in the cationic modification of starch and other polysaccharides. Reactions conditions such as the temperature, solvent, reagent and substrate concentrations were varied to control the degree of substitution. These modified ENPs were characterized by NMR to determine their degrees of substitution.

Acknowledgements

I would like to express my gratitude and appreciation to my supervisor, Dr. Scott Taylor for all his support, guidance and encouragement. I would like to extend thanks to the members of my committee, Dr. Jean Duhamel, and Dr. Mario Gauthier. I would also like to acknowledge all the ECO-WIN group members and Taylor group members for their help and support. Lastly I would like to thank my family and friends for their ongoing support and encouragement.

Table of Contents

List of Figures

Chapter 1 – Starch and Starch Nanoparticles

Chapter 2 – Characterization of ENPs using NMR

Chapter 3 – Dry Cationic Modification of ENPs

List of Abbreviations

Abbreviation	Full Name
AGU	Anhydroglucose unit
BOD	Biological oxygen demand
CASNs	Citric acid crosslinked starch nanoparticles
CHPTMA	3-Chloro-2-hydroxylpropyl trimethylammonium chloride
CMS	Carboxymethyl starch
DEPT-135	Distortionless enhancement by polarization transfer-135
DLS	Dynamic light scattering
DS	Degree of substitution
ENPs	EcoSphere™ starch nanoparticles
EPTAC	2,3-Epoxypropyl trialkylammonium chloride
GPS	Glycerol plasticized starch matrix
GTAC	Glycidyl trimethylammonium chloride
GX	Glyoxal
GY	Glycerol
HMBC	Heteronuclear multiple-bond correlation spectroscopy
HMQC	Heteronuclear multiple-quantum correlation spectroscopy
MWCO	Molecular weight cut off
NMR	Nuclear magnetic resonance
QNP	Quattro resonance X1+X2+X3 decoupling inverse probe

SNPs	Starch nanoparticles
TXI	Triple resonance X1+X2 nucleus decoupling inverse probe

Chapter 1

Starch and Starch Nanoparticles

1.1 Starch

Starch is the world's second most abundant biopolymer found in nature, and is produced by almost all plants as a source of stored energy.[1-9] The attractive properties of starch include its natural abundance, renewability, biodegradability, nontoxicity and inexpensive cost.[1-9] All these advantages have driven scientists to develop new products and new materials using starch substrates.[1-9] The use of bio-based polymers such as starch as starting material also has the fundamental advantage of having a reduced carbon footprint.[10] Oil shortages and the desire to replace petrochemically derived polymers with more environmentally benign bio-based polymers have also driven the development of new starch-based polymers and materials.[6]

Starch exists as water-insoluble granules in plants.[3] The starch granules contain birefringent semi-crystalline regions and amorphous regions.[2,7,10,11] The granules are composed of two types of polysaccharides, amylose and amylopectin.[2,7,8,10,11] Amylose is a linear polysaccharide consisting of α-1,4 glycosidic linkages (Figure 1.1).[2,10,11] Amylopectin is a branched polysaccharide consisting of linear α-1,4 glycosidic bonds and branches generated via α-1,6 glycosidic linkages (Figure 1.2).[2,7,10,11] In the starch granules, amylose and the branching points of amylopectin form the amorphous regions whereas the short amylopectin chains form the crystalline component.[2,7,12,13] High amylose starch composed of few branching points have predominantly linear chains with a molecular weight in the range of 10^5-10^6 g/mol.[7] Amylopectin starch is a highly branched starch polymer with numerous α-1,6 glycosidic linkages and typically

with molecular weights greater than 10^7 g/mol.[7] The ratio of amylose to amylopectin determines the molecular weight of the starch but because this ratio varies within different starches, the molecular weight distributions are typically very broad.[7] Although it is known that starch contains amylose and amylopectin, the molecular organization of granules is not well understood.[14] Many physical and chemical properties such as viscosity, gelation and adhesion are influenced by the amylose:amylopectin ratio in the granules. The size and morphology of starch granules depend very much on the botanical source, region and season.[14]

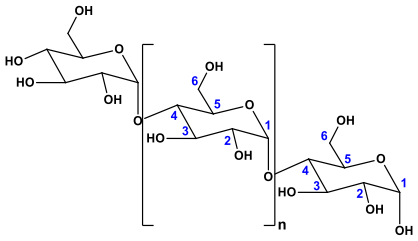

Figure 1.1. Amylose structure

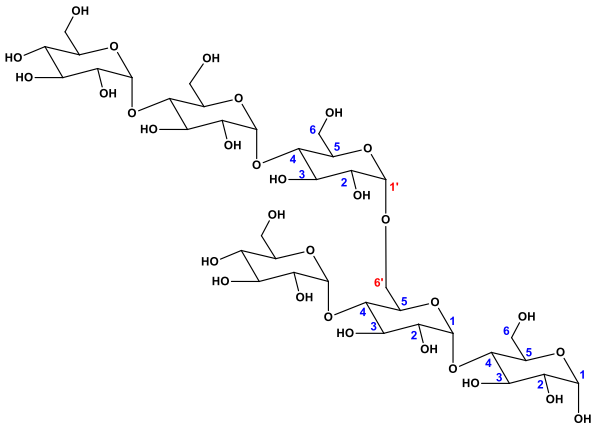

Figure 1.2. Amylopectin structure

When subjecting the starch granules to heat (60 °C), gelatinization occurs where the granules swell irreversibly to many times their original size.[10] During this process, the amylose

becomes soluble and the crystallinity and birefringence properties of the granules diminish.[10] At temperatures below 100 °C and in the absence of mechanical shear, the granule integrity is maintained.[10] Concentrated suspensions of gelatinized starch become viscoelastic (demonstrating high viscosity and elastic properties).[10] The viscoelastic properties are explained by temporary intermolecular networks formed by the concentrated and swollen (gelatinized) granules.[10] Upon cooling to room temperature the concentrated starch dispersion forms an opaque starch-gel. This process is known as retrogradation.[10]

The melting point of native starch is higher than its decomposition temperature, which means that a plasticizer is required when using starch in a liquid form, as the starch would decompose otherwise.[2] Commonly used plasticizers such as glycerol, water, or sorbitol convert starch into a thermoplastic material that is moldable above a certain temperature but returning to a solid state after cooling.[2] Starch in the presence of a plasticizer combined with high temperature and shear will lose its semi-crystalline granular structure and exhibit thermoplastic behaviour.[8]

1.2 Starch Modification

1.2.1 Types of Starch Modifications

Raw starch has limited applications due to its poor solubility in cold water, tendency to retrograde and high viscosity once gelatinized.[15] Therefore, raw starch is usually modified to enhance certain properties before it is used in industry.[15]

Starch is very amenable to modification because it possesses multiple hydroxyl groups.[16] The hydroxyl groups allow for the incorporation of various chemical groups onto its backbone to

obtain polyfunctional colloidal systems.[16] Starch has been modified in a variety of ways. Some examples include oxidation (to produce carboxylated starch), etherification (to produce hydrophobic, cationized or carboxymethylated starch), esterification (i.e. nitration, phosphorylation, sulfation, boration, silylation, acylation) and halogenation.[17] These modifications alter the starch properties, enabling them to be used in a variety of applications. For example, carboxymethyl starch (CMS) results in the addition of hydrophilic, anionic groups to the starch backbone.[18] The modified polymer was shown to have a reduced tendency to retrograde, improved cold water solubility and was less prone to thermal and microbial damage.[18] CMS is used in food, medicine, pharmaceuticals, textiles, printing, electrodes, ceramics, and drilling fluids.[18] Another example of modified starch that is used in industry is acetylated starch. Acetylated starch has improved properties over its native form mainly because of improved stability and resistance to retrogradation.[6] Acetylated starch is widely used in the food industry as a thickening agent.[6]

1.2.2 Cationic Modification of Starch

This thesis focuses specifically on the cationic modification of starch. Although starch has been modified with several types of cationic groups such as phosphonium and sulfonium groups, by far the most common type of cationic modification is via introduction of ammonium groups. The cationic modified starches are used in a wide variety of applications in the paper, textile and oil industries.[19-22] Other potential applications for cationic starches are also being explored. For example, cationic starches are effective flocculants and thus are examined as potential binding agents for treating organic and inorganic matter in wastewater.[19,22,23] Most of the flocculants used today for treating wastewater are synthetic polymers such as poly(acrylamide-co-N,N,N-

trimethylammonium ethyl acrylate)chloride and poly(diallyldimethylammonium)chloride.[23,24] However, it has been shown that these synthetic flocculants contain toxic additives and monomer that remains from the synthesis.[22,24] In addition, they also exhibit poor biodegradability.[22] In Germany, the disposal of flocculated sludge with polyacrylamide derivatives on agrarian surfaces was strictly prohibited since the end of 2013. Flocculants based on natural renewable polymers, especially cationic starches, are alternatives to synthetic flocculants. They are non-toxic and biodegradable. They are already used in the treatment of both waste and drinking water.[22,24] However, although natural polymers have been labeled as low cost, the cost-to-performance ratio of synthetic flocculants is considerably more favourable than for natural (starch-based) flocculants because of the high molar masses required for synthetic flocculants.[25]

The flocculation behaviour of cationic starches depends strongly on the degree of substitution (DS) and the content of amylopectin.[26] Cationic starches prepared from amylopectin-rich and amylose-rich starches produced the highest and lowest degrees of dewatering (removal of water from solid material), respectively.[26] This result was attributed to the higher DS that could be attained with amylopectin-rich starch.[26] Cationic starches were synthesized by Haack et al. by reacting starch with 3-chloro-2-hydroxypropyltrimethylammonium chloride (CHPTMA) in a sodium hydroxide solution at 60 °C for 6 h.[26] They obtained a DS of up to 1.05, but they were unable to surpass this DS even with higher reagent concentrations.[25] At higher reagent concentrations, the reaction efficiencies dropped from 52% to 23%.[25] As the reaction starts off in a highly swollen state, the addition of excess reagent hinders the mixing of the reaction mixture.[25] The mixing could be made easier by diluting the mixture; but, the increased water

content caused increased formation of the glycol (diol).[25,60] These cationic starches alone did not outperform the synthetic flocculants, but when used in combination with synthetic flocculants, there was an increased dewatering efficiency as compared to the pure synthetic flocculants.[25] Cationic starches are unable to compete with synthetic flocculants because the DS that are currently being obtained are not high enough.[25] Finding a solution to this limitation could lead to the preparation of a bio-based flocculant with the potential for complete replacement of synthetic flocculants.

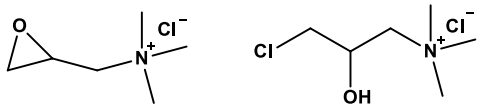

1 2

Figure 1.3. Chemical structure of (**1**) glycidyltrimethylammonium chloride (GTAC) and (**2**) 3-chloro-2-hydroxypropyltrimethylammonium chloride (CHPTMA)

Cationic starches are widely used in the paper making process where they are used as additives for controlling the retention of pigments, paper smoothness, light scattering ability, gloss, and as fillers to improve paper strength.[27] Although different types of starches have been used for the above purposes, it was reported that cationic and amphoteric starches were superior to other modified starches.[28]

In paper making, the usefulness of positively charged starch derivatives arises from their affinity for negatively charged species.[29] They also act as colloidal stabilizers for negatively charged pigments and increase filler retention and the drainage rate of the pulp.[30,56] They are also useful in lowering the biological oxygen demand (BOD) of white water when used as a wet-end additive.[30,56] BOD represents the amount of dissolved oxygen required by aerobic biological

organisms to break down organic materials present in water samples.[30,56] It can be used to gauge the effectiveness of wastewater treatment plants.[30,56]

Two of the most common reagents used for preparing cationic starches are GTAC or CHPTMA.[23] Their chemical structures are shown in Figure 1.3. These reagents contain a quaternary nitrogen and therefore bear a permanent positive charge that is independent of pH. These reagents are commercially available as aqueous solutions. Under basic conditions, CHPTMA is converted into GTAC, which then reacts with free hydroxyl groups to produce cationic starch. An example of such a reaction using CHPTMA is shown in Figure 1.4. With CHPTMA, the base is used in reagent quantities, since the epoxide must be formed. If GTAC is used to modify the starch then no conversion into an epoxide is necessary and so the base is only required in catalytic quantities, though typically reagent quantities are used.

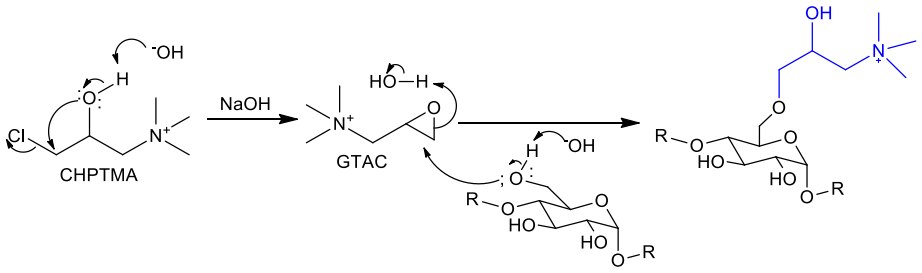

Figure 1.4. Conversion of CHPTMA to GTAC and then reaction with starch. The reaction is shown at the 6-OH; however, modification could also occur at the 2- or 3-OH groups.

Heinze et al. reported that the reaction is not entirely dependent on the concentration of NaOH.[26] Upon reaching a threshold, an excess amount of NaOH started to decrease the reaction efficiency and effectively lowered the DS.[26] At high base concentrations, the epoxide was

hydrolyzed to the diol (as shown in Figure 1.5).[26] It was important for the base to be present to activate the starch but equally as important to minimize the hydrolysis of the reagent to a diol.[26]

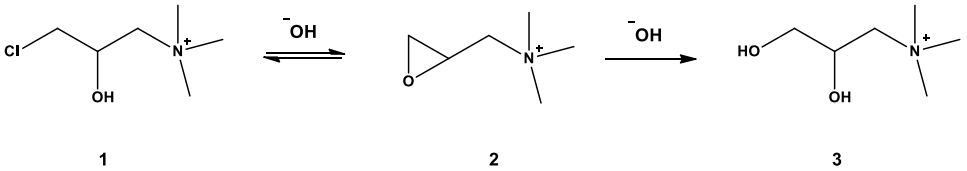

Figure 1.5. Chemical reaction demonstrating the hydrolysis of GTAC to 2,3-dihydroxylpropyltrimethylammonium chloride. (**1**) CHPTMA (**2**) GTAC (**3**) 2,3-dihydroxypropyltrimethylammonium chloride

When starch is modified using CHPTMA in water suspensions, the DS is highly dependent on the molar ratio of the reagents and the type of starch used.[31] Cationic starches modified with CHPTMA had DS between 0.03 to 0.88.[31] Reaction efficiencies were below 47%.[31] The modification of starch in suspension with GTAC yielded higher reaction efficiencies (40-76%) with a DS of 0.38 – 1.05.[31] When the starch was dissolved in DMSO and reacted with GTAC, the reaction efficiencies were similar to those obtained in water (40-76%) but the DS fell to 0.35 – 0.57.[31] An increased amount of sodium hydroxide did not enhance the yield because hydrolysis of the epoxy groups was increased as the sodium hydroxide levels exceeded 0.4 mole/Anhydroglucose unit.[31] The reaction efficiency was found to depend on the sodium hydroxide concentrations, temperature, starch concentrations and reaction time.[30]

1.2.3 Starch Modification via Crosslinking

A common approach to improve the performance of starch is through the introduction of crosslinks. The key to crosslinking starch is by taking advantage of its abundant hydroxyl groups to create ester or ether linkages.[32] Starch has been crosslinked with various agents such as

phosphorus oxychloride, sodium trimetaphosphate, sodium tripolyphosphate, epichlorohydrin, 1,2,3,4-diepoxybutane, dicarboxylic acids, anhydrides, and dialdehydes.[4,32] Crosslinking starch altered the physical properties of starch in numerous ways.[5,6,32,57,58] It increased the physical strength (tensile strength) of the polymer by introducing chemical bonds that act as bridges between starch chains.[6] The increased tensile strength caused an increased resistance to swelling because the crosslinks limit water absorption by restricting the mobility of the starch chains in the amorphous regions.[6,57,58,59] This caused a decrease in the retrogradation rate and an increase in the gelatinization temperature.[6]

1.2.4 Starch Modification using Reactive Extrusion

Traditionally starches are modified in aqueous suspensions using a batch process where the reactions are conducted in a vat or vessel.[5] Under batch conditions, the microstructure of starch (pores on the surface of starch and channels within the interior) imposes diffusional control over the reactants that enter the starch macromolecules, thereby slowing the conversion of the chains located in the interior of the starch.[5] Batch reactions can take up to 24 hours to reach complete conversion and are carried out at relatively low temperatures (35-50 °C) to avoid gelatinization, unless gelatinization is desired.[5] The use of a high salt content inhibits gelatinization, which allows for the modification reactions to be performed at higher temperatures.[7] However, the use of high salt content is usually avoided due to the cost of removing the salt from the end product.[7] Some batch reactions require the use of gelatinized starch.[33] This enhances the reaction rate because the swollen starch is more accessible than granular starch.[33] Granular starch is reported to react about 400 times more slowly than gelatinized starch.[33]

Starch modification can also be carried out via reactive extrusion. Twin screw extruders are preferred over single screw extruders because of their greater control over the mixing and residence distributions, which usually generate products of more consistent quality.[7] Moad has reviewed starch modification by reactive extrusion and reported the advantages of reactive extrusion as compared to traditional batch processes.[7] The extruder is capable of mixing highly viscous fluids, hence higher starch concentrations can be used as compared to batch processes.[7] The use of an extruder avoids the expensive costs of organic solvent recovery and disposal, as well as filtering, purifying and drying to obtain the final product.[5] The main benefits of using extruders in industrial applications are high conversion efficiencies and rapid rates of production.[7] Batch reactions are performed on aqueous starch suspensions (30 - 50% solids) over long time periods (2 – 24 h), whereas an extruder can perform the same reactions in much less time (often within 2 – 5 min) and in a homogenous medium at much higher starch concentrations (60 - 80% solids) as well as higher temperatures.[7] For example, Seker and Hanna reported that the crosslinking of starch with sodium trimetaphosphate can be done in under 2 min using a single screw extruder.[33] In contrast, the batch process required 2 h.[33]

The modification of granular starch using reactive extrusion takes less time than the modification of gelatinized starch using a batch process.[33] This is because the extruder physically disrupts the starch granules via shear force, which creates an accessible path for the reagents into the interior of the starch granules.[33] However, most reactions on starch performed in an extruder are done under conditions where the starch is gelatinized.[7] Consequently, the addition point of the reagent(s) along the extruders barrel is critical.[7] It is usually desirable that the reagent(s) be added to the extruder after the starch reaches full gelatinization.[7] High amylose

starch requires higher temperatures for gelatinization and, consequently, higher temperatures for extrusion processing, than low amylose starch does.[7] Moreover, high amylose starch is less prone to shear degradation during extrusion.[7] Since rapid exposure of the interior of the starch to the reagents during reactive extrusion depends upon the gelatinization and/or mechanical shearing of the starch, reactive extrusion is inapplicable for industries where intact starch particles are required.[5]

It is widely accepted that any pre- or post-processing of an extrudate will quickly eliminate any cost advantages of using an extruder.[7] This is mainly because of the costs involved in removing the byproducts and the reagents used during the pre- or post-processing of the extrudate.[7]

When an epoxide is reacted with starch in an aqueous environment the main byproduct is the formation of a glycol, which is formed via hydrolysis of the epoxide.[7,60] The use of extruders minimizes this side reaction because the amount of water present is usually relatively low compared to batch processes, and the residence time of the starch and the reagent(s) in the extruder is relatively short.[7]

Cationic starches have been prepared by reactive extrusion using CHPTMA or GTAC. Higher starch concentrations, higher processing temperatures and higher screw speeds all increase the reaction efficiency.[7] It was reported that when an excess amount of NaOH was used a discoloured product was obtained even though the reaction efficiency was improved.[7] It has also been reported that GTAC is more effective than CHPTMA for cationic modification because the conversion of CHPTMA to GTAC limits the overall reaction efficiency.[7,29] Cationic starches created in extruders are usually prepared in the presence of a plasticizer such as water or

glycerol.[30] The Tara group prepared cationic starches in a twin screw extruder under basic conditions (aqueous NaOH) using CHPTMA and either a 1:1 mixture of glycerol and water or just water as the plasticizer.[30] A slightly higher DS was obtained using the glycerol-water mixture as the plasticizer. This could be explained by the fact that the modified starch prepared using the glycerol-water mixture as the plasticizer was more viscous than the starch plasticized with just water, hence higher screw speeds were required to mix the more viscous material that resulted in higher temperatures, which increased the reaction efficiency.[30]

1.2.5 Starch Modification using Dry Processes

Starch modification reactions employing very small quantities of solvent (usually water) in batch processes, so-called "dry" reaction conditions, have become increasingly popular in industry in recent years. Although high DS are sometimes difficult to achieve in dry processes, this drawback is usually offset by significant cost savings as compared to traditional batch chemistry. Such cost savings are the result of the small amount of solvent used, the decrease in the amount of reagent(s) lost due to decomposition, and the relatively short amount of time that is required to remove the solvent when the reaction is complete. Moreover, purification procedures are sometimes not required.[18] Kavaliauskaite et al. obtained cationic starches with a DS of 0.5 using a dry process at room temperature and a special mixing system called the Powdercat® Process.[31]

1.3 Starch Nanoparticles

Nanoparticles are defined as particles with sizes ranging from 10 - 1000 nm.[34] EcoSynthetix™, a company based in Burlington, Ontario, has developed a proprietary reactive

extrusion process for preparing starch nanoparticles (SNPs) which were given the trade name EcoSphere™ starch nanoparticles (ENPs). In their process, starch, water and/or glycerol are fed into a twin screw extruder at elevated temperatures, followed by the injection of aqueous glyoxal (Figure 1.6). As the product exits the extruder at elevated temperature, the water evaporates and produces agglomerates of solid ENPs (Figure 1.7). The size of the agglomerates is approximately 300 µm, but their dispersion in water breaks up the majority of the aggregates into starch nanoparticles 30-60 nm in diameter. It has been proposed that the ENPs are held together by both intramolecular and intermolecular glyoxal crosslinks. The ENPs exhibit a lower swelling ratio as compared to native starch, and it is has been suggested that this is due to the presence of the crosslinks in the ENPs.[35,36]

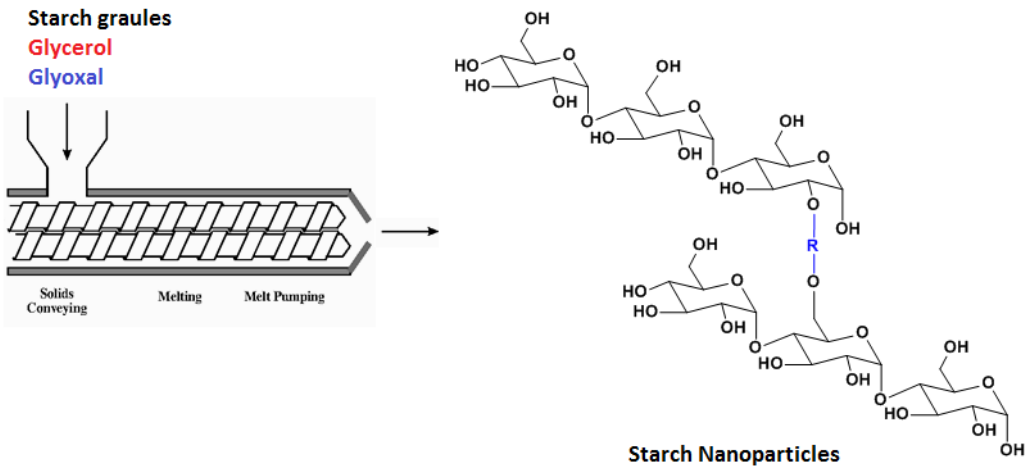

Figure 1.6. Schematic representation of the twin screw extrusion process producing ENPs. A crosslink between the 6-OH and 2-OH group is shown (image taken from ref.[52]).

Figure 1.7. Agglomerates of ENPs obtained after extrusion. (image taken from ref.[35,36])

Aqueous dispersions of the ENPs called Biolatex™ are used in paper mills around the world as a replacement for petroleum-based copolymer latex emulsions in paper coatings.[35,36] Their superior performance in paper coating, as compared to synthetic latexes, has been attributed to the finding that water swollen ENPs are deformed under high shear and high pressure and to their ability to deswell and release water.[35,36] These properties allow the ENPs to act as a lubricant for paper coating, inducing less shear-thickening than what other coating processes would generate.[35,36]

The size of the ENPs dispersed in DMSO and water has been studied by the Gross group using dynamic light scattering (DLS).[37] DLS is a powerful technique to study the dimensions of particles.[38] DLS can provide the hydrodynamic radius (R_h) from the measurement of the diffusion coefficient as well as the size distributions in a population of particles.[38] The particle size distribution of the ENPs had two main peaks in both solvents at around 40 and 300 nm.[11,37] These

were ascribed to isolated ENPs and ENP aggregates.[37] The molecular weight of the ENPs was estimated to be 2.2-2.6 x 10^6 g/mol.[37] Beyond this study, very little else has appeared in the scientific literature on the characterization of ENPs.

The Ma group reported the preparation of SNPs by delivering ethanol into a starch paste solution which resulted in the precipitation of SNPs.[39] They also prepared citric acid crosslinked SNPs (CASN) by subjecting the SNPs to an ethanol solution of citric acid for 12 h followed by removal of the ethanol under vacuum at 50 ^oC for 6 h. The diameter of the CASNs ranged from 50 to 100 nm. The CASNs do not swell or gelatinize at elevated temperatures.[39] Nanocomposites were also prepared by using the CASN as filler in glycerol plasticized-pea starch (GPS) matrix. The introduction of CASN into the matrix improved its tensile strength.

1.4 Thesis Objectives

The ENPs produced by EcoSynthetix™ represent a new material but very little is known about their chemical structure. In order to gain a better understanding of their properties, it is necessary to gain a better understanding of their physical structure. One of the objectives of this thesis was to evaluate the nature of the crosslinks in ENPs using nuclear magnetic resonance spectroscopy (NMR). The characterization of the crosslinks in the ENPs is of fundamental importance as it is believed that the crosslinks are key to the chemical structure and properties of the ENPs when dispersed in aqueous solution. NMR was selected because it has the potential to provide information that cannot be obtained, or is difficult to obtain, using other techniques such as determining the presence or absence of crosslinks in the ENPs and possibly even the chemical structure of the crosslinks, if they are present.

So far the ENPs are being used commercially in their native (unmodified) form and are employed in only one industrial application (paper making). The modification of ENPs is expected to generate new materials with novel properties that can be useful for other commercial purposes. Consequently, a second objective of this thesis was to develop a method for the efficient synthesis of cationically modified ENPs using a dry process. We focused on cationic modification due to the potential of cationically modified ENPs as additives in the paper making industry and other applications as discussed earlier.

Chapter 2

Characterization of ENPs using NMR

2.1 Introduction

ENPs are prepared in the presence of glyoxal (GX). It has been suggested that GX crosslinks the starch chains, and that these crosslinks are partly responsible for the particles' unique physical properties. GX reacts with alcohols in an acid-catalyzed reaction to form hemiacetals and acetals as shown in Figure 2.1. Consequently, the reaction of GX with starch can potentially yield a wide variety of different crosslinks. A small fraction of the crosslinks that are possible in the ENPs are illustrated in Figure 2.2.

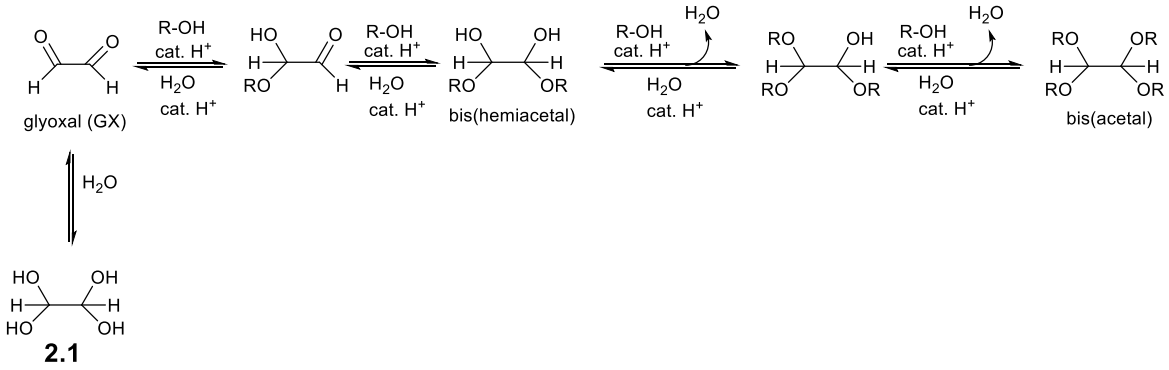

Figure 2.1. Reaction of GX with alcohols to form hemiacetals and acetals.

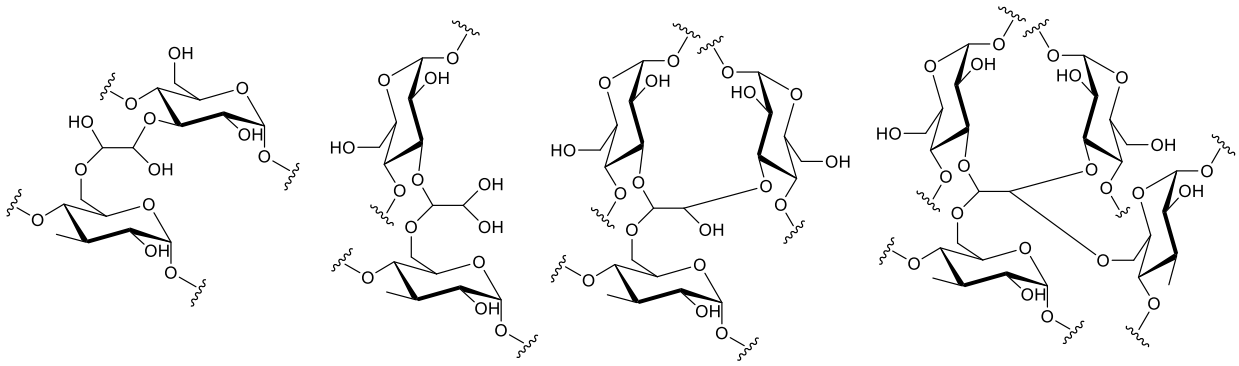

Figure 2.2. A small fraction of the crosslinks that are possible in the ENPs.

An important feature of the GX crosslinks is that they are reversible. In aqueous solution, the equilibrium will shift towards structure **2.1** which is the dominant form of GX in dilute aqueous solution.[40-43] GX can also adopt other forms in aqueous solution including dimeric and trimeric forms of GX.[40-43] This process is also acid-catalyzed. The rate at which the reverse reaction takes place depends upon acid strength, the amount of water present, and the temperature.[40-43]

Before the ENPs are used for paper coating, they are first converted into Biolatex™ by dispersing them in aqueous solution for several hours. Since aqueous solutions of the ENPs are slightly acidic (pH ~ 3-4), it is plausible that none or only part of the GX is involved in the crosslinks present in the dispersion and that most of the crosslinking only occurs after the Biolatex™ is coated onto the paper and the paper is dried.

2.2 Objectives

The objective of the work described in this chapter is to characterize the crosslinks in ENPs using NMR. We are specifically interested in attempting to answer the following questions: How much of GX is involved in crosslinks when the ENPs are dispersed in water? Are the ENPs

crosslinked at all in aqueous solution? If they are not crosslinked or only partially crosslinked, can the unbound GX be quantified by NMR? Does the extent of crosslinking (if any) change when the ENPs are dispersed in an organic solvent? These questions are of fundamental importance as it is believed that the crosslinks are partly responsible for the particles' unique physical properties.

2.3 Result and Discussion

2.3.1 Solubility of ENPs

Prior to any NMR characterization of the ENPs, it was critical to determine the dispersibility of the ENPs in different solvent systems. Such a study provides an understanding of the types of solvents that can be used for the NMR studies. To determine this, the ENPs were added to various solvents (water, DMSO, methanol, ethanol, butanol, isopropyl alcohol, hexane, methylene chloride, ethylene glycol, diethyl ether, acetonitrile and dimethylformamide) and heated to 50 °C for 5 minutes and then examined visually to see if a clear dispersion was formed. Under these conditions, the ENPs were only dispersible in water and DMSO at 20% and 4% weight to volume (g/100 mL) respectively. The ENPs were found to be indispersible in all other solvents under these conditions.

2.3.2 1-D NMR Studies of ENPs in D_2O

The 1-D ^{1}H-NMR spectrum of GX2 ENPs in a 10% dispersion in D_2O is shown in Figure 2.3. Throughout this thesis, the amount of GX used in the preparation of the ENPs is given by a number following the letters GX. For example, GX2 means that the ENPs were prepared with 2 parts GX based on a recipe using 100 parts of starch. As the spectrum in Figure 2.3 is similar to the ^{1}H-NMR spectrum of starch that has been reported in the literature, most of the peaks could

be assigned to the appropriate protons in the ENPs.[14,37,44,45,46] These assignments were later confirmed by 2-D NMR experiments performed on the ENPs. It is important to note that in D_2O, the hydroxyl protons are exchanged with deuterium and hence do not show up in the spectrum. As the ENPs were prepared using glycerol (GY) as a plasticizer, peaks due to GY were also evident in the spectrum. No peaks due to GX are observed. We will later demonstrate that the peak associated with the protons of the hydrated form of GX (structure **2.1**) is masked by the water peak.

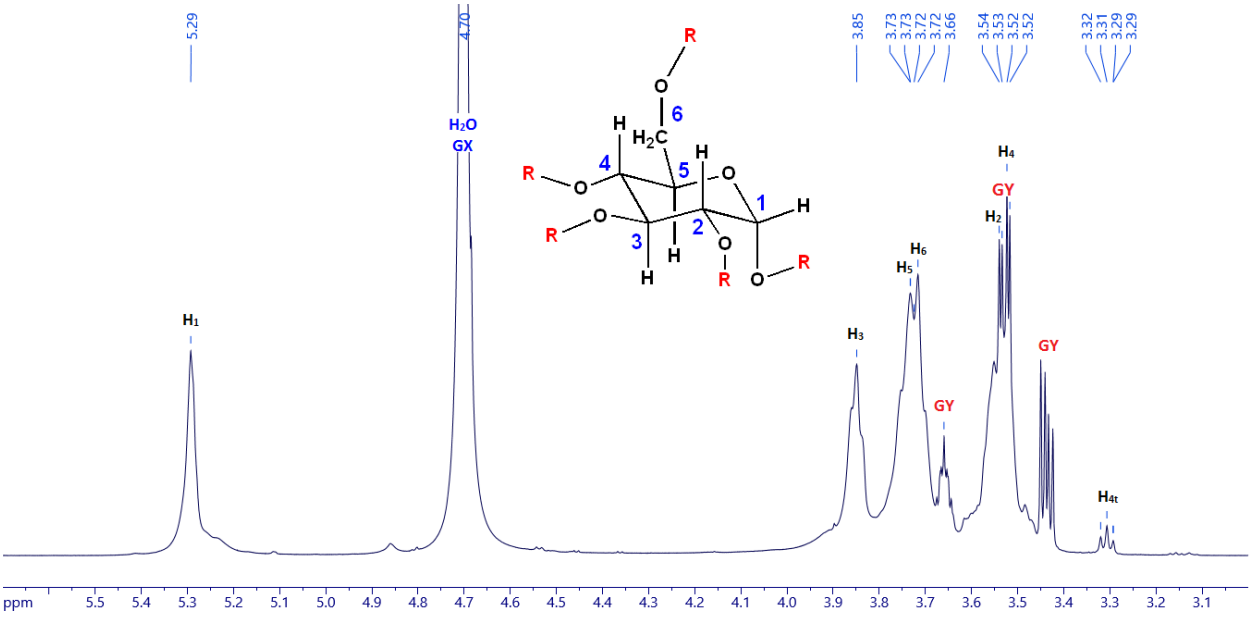

Figure 2.3. ^{1}H-NMR spectrum of a 10% dispersion of GX2 ENPs in D_2O (700 MHz). H_{4t} represents the proton attached to the terminal/non reducing end carbon.

The peaks in the spectrum are fairly broad. One of the reasons for this is that each proton is in its own unique environment. For example, there are many types of H_2 (hydrogens attached to C_2), each of which is in its own unique environment. The shape (sharpness or broadness) of the peaks is also influenced by other factors. One of these factors is the rotation or tumbling rate of the ENPs in solution. A polymer has decreased local mobility because of its large structure

which in turn creates broad peaks in the spectrum. This can help indicate which peaks in the spectrum originate from protons attached to the polymer or to unbound molecules.

The 1-D ^{13}C-NMR spectrum of GX2 ENPs in a 10% dispersion in D_2O is shown in Figure 2.4. Again, as this spectrum is similar to the ^{13}C-NMR spectrum of starch reported in the literature, most of the peaks could be assigned to the appropriate carbons in the ENPs.[14,37,44-46] The validity of these assignments was later reinforced by 2-D NMR experiments on the ENPs. Peaks due to the carbons of GY are also readily evident at 62.4 ppm (CH group) and 72.0 ppm (CH_2 group). We were able to determine that the sharp peak at 90.4 ppm corresponds to the hydrated form of free, unbound GX based on literature spectra of GX[40-43] and by spiking the sample with GX. The peaks due to GX and GY were very sharp which suggested that GX and GY are freely rotating molecules that are not bound to the ENPs. Moreover, if there were GX-GY adducts, one would expect to see more carbon signals arising with slightly different chemical shifts, but this was not seen in this spectrum.

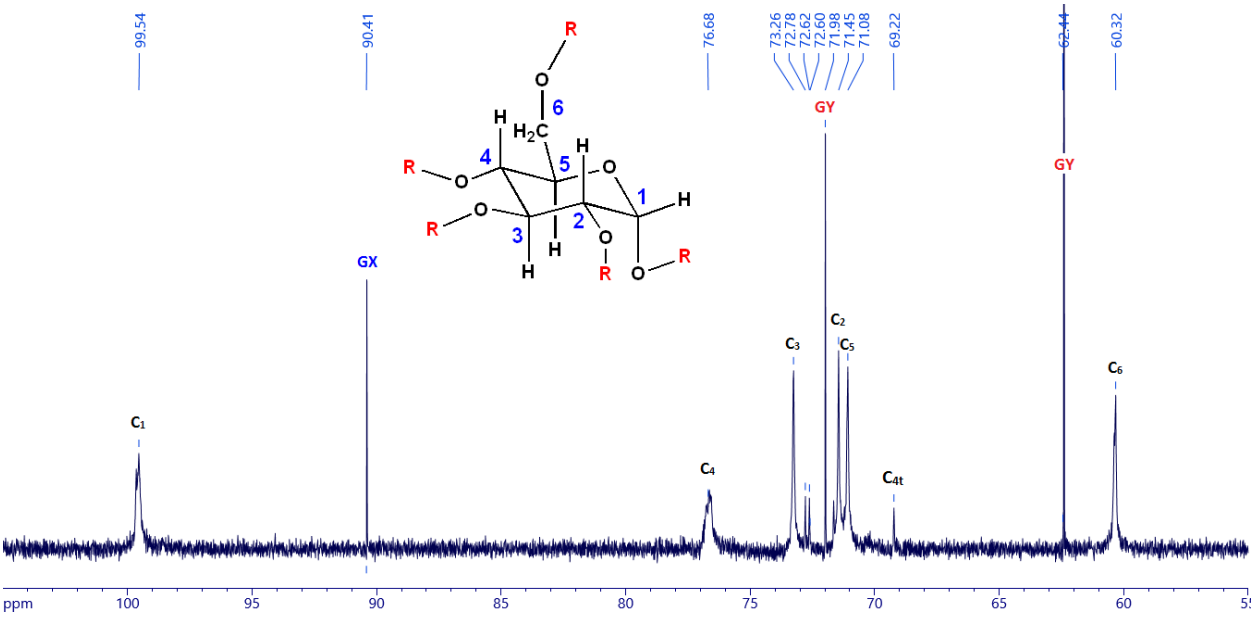

Figure 2.4. ^{13}C-NMR spectrum of a 10 % dispersion of GX2 ENPs in D_2O (176 MHz). The peak labelled C_{4t} corresponds to the carbon at the terminal/non reducing end of the starch chains.

To determine if any other peaks in the NMR spectra were associated with GX, NMR spectra were obtained of ENPs that had been prepared by EcoSynthetix™ with varying amounts of GX. These spectra were analyzed to see which peaks grew larger as the amount of GX was increased. Figure 2.5 shows the stacked ^{1}H-NMR spectra of these ENPs in D_2O. There appears to be very little difference in the spectra as the amount of GX increases.

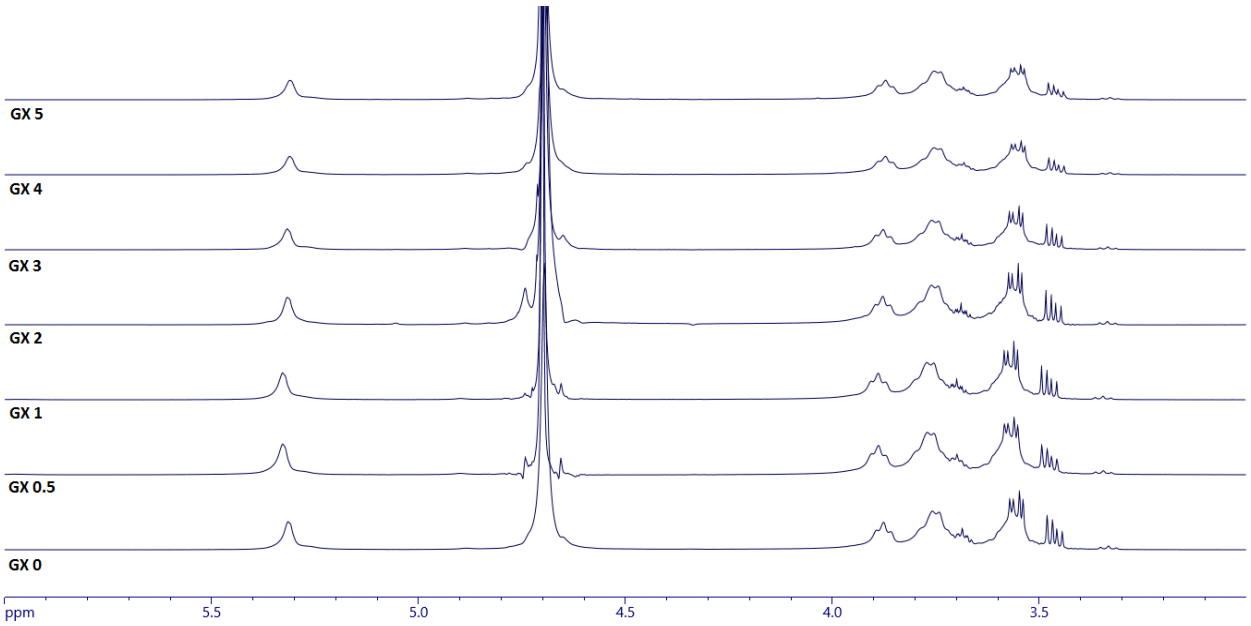

Figure 2.5. ^{1}H-NMR spectra of 10% dispersions of ENPs prepared with varying amounts of GX(0 – 5) in D_2O (500 MHz).

Figure 2.6 shows the stacked ^{13}C-NMR distortionless enhancement by polarization transfer-135 (DEPT-135) spectra of these samples in D_2O. DEPT-135 is a specialized type of ^{13}C-NMR which displays primary and tertiary carbons (CH and CH_3) facing up and secondary carbons (CH_2) facing down. Quaternary carbons are not shown in DEPT-135 experiments, but since there are no quaternary carbons in starch, this does not create a limitation in our application.

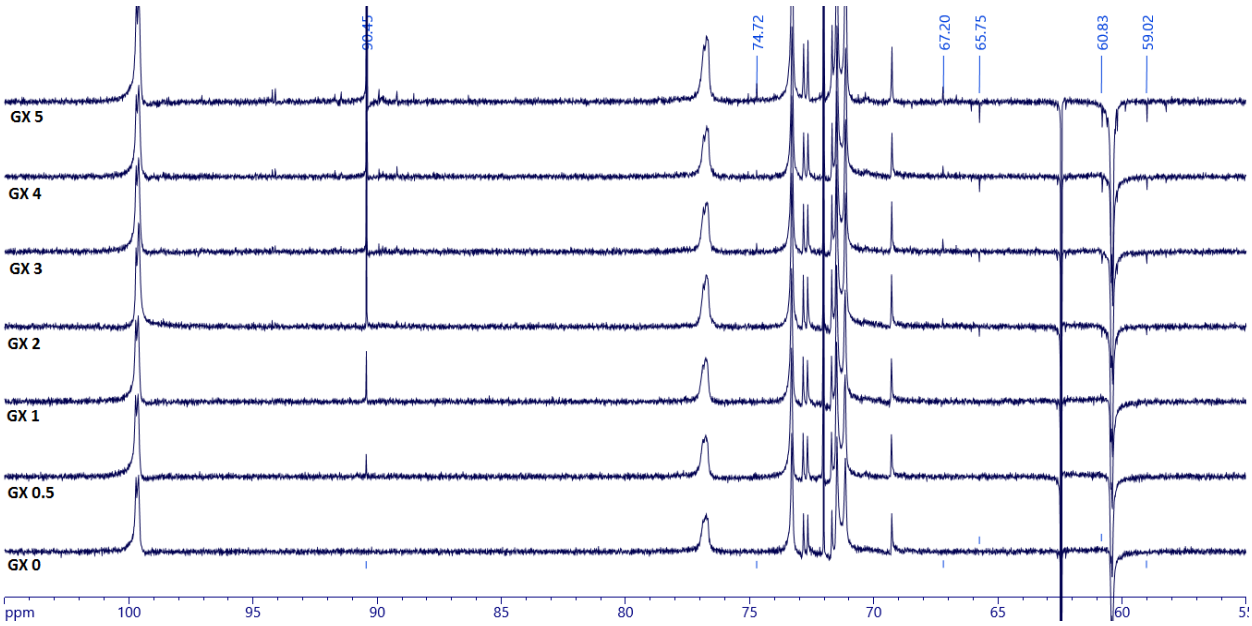

Figure 2.6. DEPT-135 spectra of 10% dispersions of ENPs prepared using varying amounts of GX(0 – 5) in D_2O (125 MHz).

The spectra shown in Figure 2.6 were analyzed to determine which peaks appeared and increased in intensity as the amount of GX that was used to prepare the ENPs was increased. The new and/or growing peaks were found at 59.0, 60.8, 65.7, 67.2, and 74.7 ppm. There were also a variety of small peaks appearing between 86 - 96 ppm. Most of these only begin to appear at the higher GX levels (> GX2). The peaks at 59.0, 60.8 and 65.7 ppm peaks are all facing downwards indicating a CH_2 group. Since only one proton is attached to the carbons in GX and since these new peaks (the new CH_2 peaks) appear between 59 - 66 ppm then these new peaks are not due to GX carbons. It is possible that these new peaks are associated with the methylene carbons of a GX-GY adduct(s). The amount of GX-GY adduct(s) formed during the manufacturing of the ENPs increases as the amount of GX used in the manufacturing of the ENPs increases. Four of the many possible GX-GY adducts that can potentially form are shown in Figure 2.7. The 6-membered ring

formed is structurally very stable and under the conditions found in the extruder, these adducts have a high likelihood of forming. It is also possible that GX is decomposing during the manufacturing process into compounds such as glycolic acid ($HOCH_2COOH$), which is a known decomposition product of GX.[43] More will be said on this later. In any case, it should be pointed out that commercial ENPs are prepared with a quantity of GX similar to that of the GX2 sample and that most of the additional peaks are not seen until the GX level is higher than this.

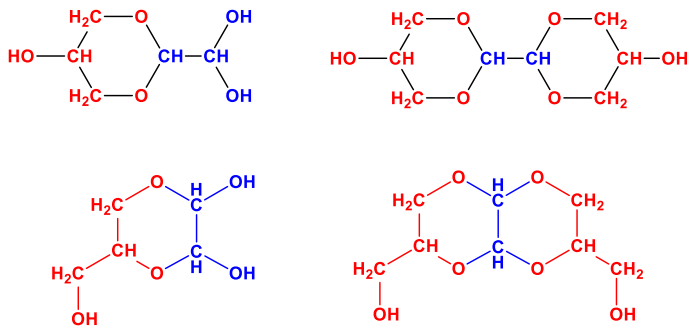

Figure 2.7. Chemical structures of possible GX-GY adducts (GX portion shown in blue and GY portion shown in red).

To determine if GY had an effect on the presence or absence of new peaks in the spectra shown in Figures 2.5 and 2.6, we acquired the ^{1}H- and ^{13}C-NMR spectra in D_2O of a series of ENPs that were prepared by EcoSynthetix™ with varying amounts of GX but in the absence of GY. Figure 2.8 shows the ^{1}H-NMR spectra of the GY-free ENPs in D_2O. Some new, albeit very small peaks appeared at 3.2, 4.1, 4.6, 5.1, and 8.2 ppm as the GX concentration increased. The origin of the compound or compounds related to these peaks is currently unknown. The peak at 8.2 ppm is particularly interesting as it suggests the presence of an aldehyde though it is not as far downfield as where aldehyde protons would normally appear. It could be that some the GX is not hydrated and exists as the aldehyde (or monoaldehyde), though this is not usually seen in a ^{1}H-NMR of a

dilute aqueous solution of GX because only the hydrates (**2.1**) exists. It could also be the carbohydrate in its aldehyde form, though again this would be quite unusual. It is surprising that in the absence of GY, there are more growing peaks observed than in the presence of GY in D_2O. Although the exact origin of the peaks has not yet been identified, two possible explanations can be proposed. As GX is crosslinking the starch, increasing the GX content would slightly change some of the chemical shifts of the protons associated with starch. The second possibility is that various GX species are generated due to high GX concentrations, compared to the one dominant species as observed previously.

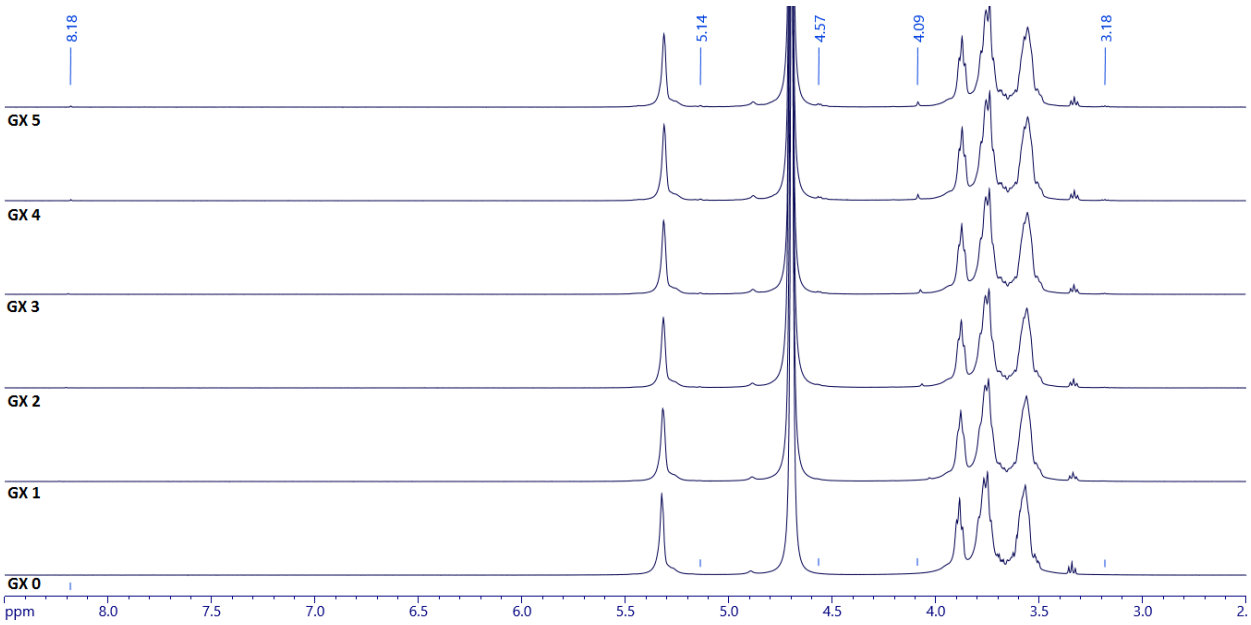

Figure 2.8. ^{1}H-NMR spectra of 10% dispersions of ENPs prepared with varying amounts of GX in D_2O (600 MHz) in the absence of GY.

Figure 2.9 shows the ^{13}C-NMR spectra of 10 % D_2O dispersions of ENPs that were prepared by EcoSynthetix™ with varying amounts of GX but in the absence of GY. The new peaks that appear most prominently as the GX increases are found at 74.5 and 95.7 ppm. Comparing the spectra of the ENPs prepared with GY (Figure 2.6) to those prepared in the absence of GY (Figure

2.9), fewer peaks were found growing in the absence of GY. This suggests that the growing peaks in Figure 2.6 are from GX-GY adducts.

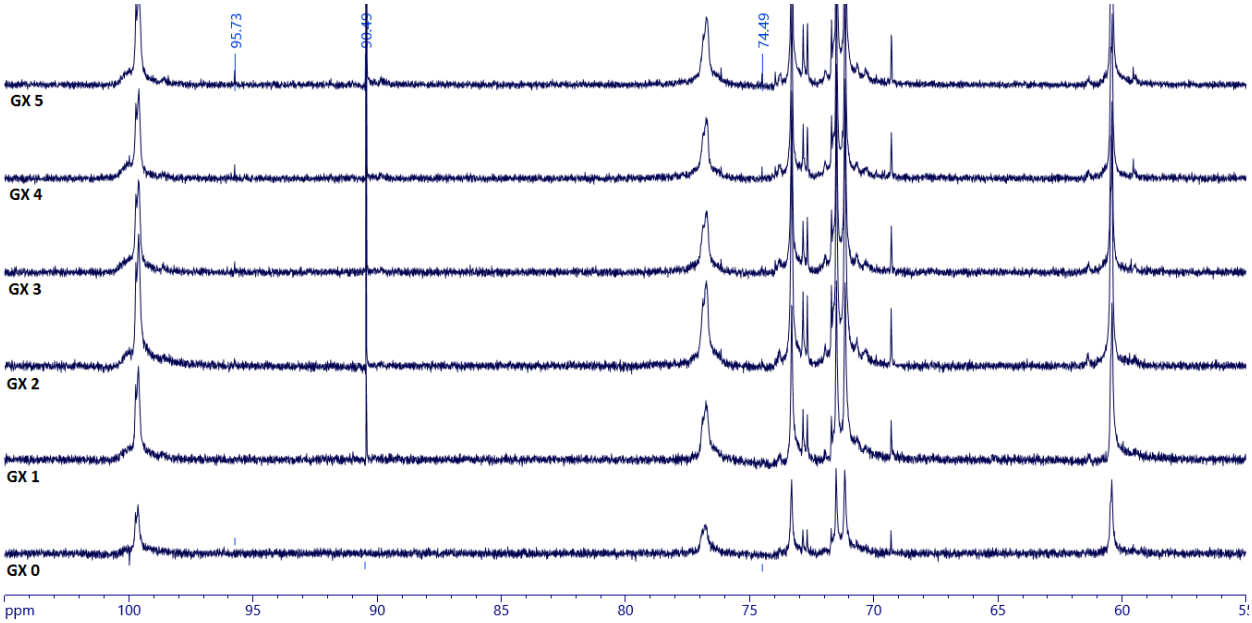

Figure 2.9. ^{13}C-NMR spectra of 10% dispersions of ENPs prepared with varying amounts of GX in D_2O (150 MHz) in the absence of GY.

Figure 2.10 shows the examples of different types of GX species that have been reported to exist in aqueous solution.[40-43,47-49] A ^{1}H- and ^{13}C-NMR study of GX and its acetals in aqueous solution reported that in a 5% aqueous solution of GX, 39% of GX is present in its monomeric form **2.1**, 27% as the dimer **2.2,** and that the rest consists of various trimers and unidentified species.[47-49] In a 40% solution, the monomer species can amount to as little as 11% and the dimer and trimers are the predominant forms.[47-49] The GX used in the synthesis of ENPs originates from a 40% solution (40 g/100 mL). Although the NMR studies described above were done using a 10% dispersion of the ENPs, the concentration of GX in the NMR tube was much less than 10% as the ENPs are prepared with just 0 to 5 parts (in 100 parts of starch) of GX. Consequently, we see predominantly the monomer **2.1** in our spectra. Even the dimer **2.2** is not evident. None of the

dimers and trimers shown in Figure 2.10 exhibit a single peak in the ^{13}C-NMR spectrum at 74.5 ppm.[48] The fact that only one new peak appears between 90 - 105 ppm indicates that only one new GX species is being formed and it must be symmetrical (as we would see more than one new peak in this region if this were not the case). Most (4 of 5 possible isomers) of the isomers of **2.3** are symmetrical and each one would appear as a single peak and each isomer would be expected to have a slightly different chemical shift from the others being diastereomers of one another.[42] However, it has been reported that these isomers exhibit a single chemical shift at 94.2 ppm in the ^{13}C-NMR spectrum in a D_2O/DMSO-d_6 mixture suggesting that they are all rapidly interconverting.[42] So it is possible that the peak observed at 95.7 ppm (Figure 2.9) in pure D_2O is due to the presence of these rapidly interconverting isomers. We are unable to come up with any explanation for the peak at 74.5 ppm.

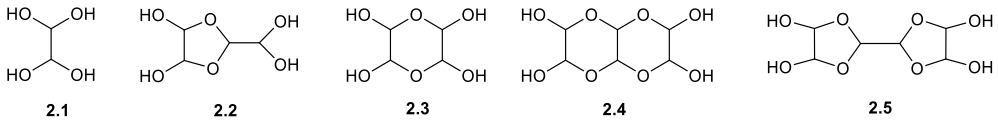

Figure 2.10. Examples of possible GX species that can exist in aqueous solution.

Whether or not the GX in the ENPs are free in solution or crosslinked, it stood to reason that it should be possible to remove the GX and any of its associated low-molecular weight adducts by dialysis or precipitation. To test this, the GX2 ENPs were dialyzed (1 x 10^2 dilution over 24 h) against water using a 1000 Dalton molecular weight cut off membrane (MWCO). After the dialysis, the samples were lyophilized and the resulting white powders were collected and analyzed by NMR.

Precipitation was performed by dispersing 32 g of GX2 ENPs in 1 L of DMSO for 24 h followed by the drop-wise addition of an excess amount of methanol (10x greater than sample volume) using a separatory funnel. The samples were centrifuged at 1000 rpm for 10 minutes. The supernatant was drained and the precipitate re-dispersed in water and lyophilized. The resulting solid particles were examined by NMR.

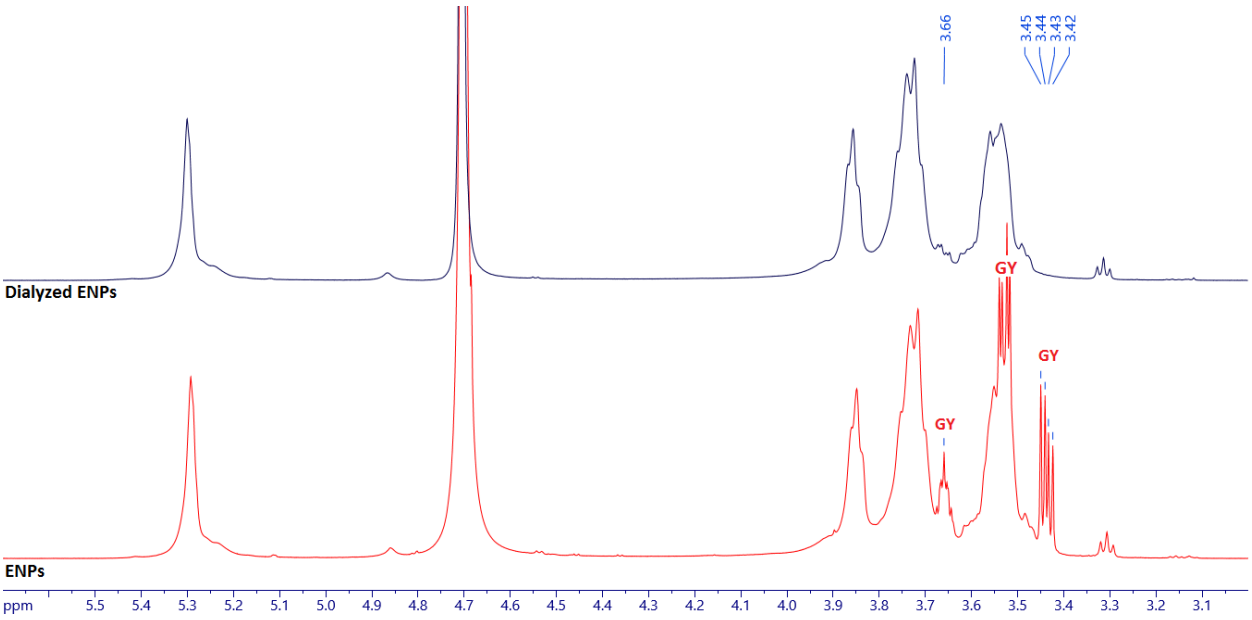

Figure 2.11. ^{1}H-NMR spectra of 10 % dispersions of GX2 ENPs in D_2O (700 MHz).
Top spectrum: Dialyzed ENPs
Bottom spectrum: Undialyzed ENPs

Figure 2.11 shows the ^{1}H-NMR spectra for the dialyzed and undialyzed GX2 ENPs. After dialysis, GY was completely removed indicating that GY was not covalently bound to the polymer. The removal of GX cannot be determined from this ^{1}H-NMR spectrum because the GX protons appear underneath the water peak under the conditions that these NMR spectra were obtained. Figure 2.12 shows the ^{13}C-NMR spectra for the dialyzed and undialyzed GX2 ENPs. GY is removed from the samples and almost all of GX is removed. It is also worthy of note that no peaks other

than those corresponding to GX and GY disappeared after dialysis indicating that all remaining species that have molecular weights greater than 1000 and probably correspond to the ENPs.

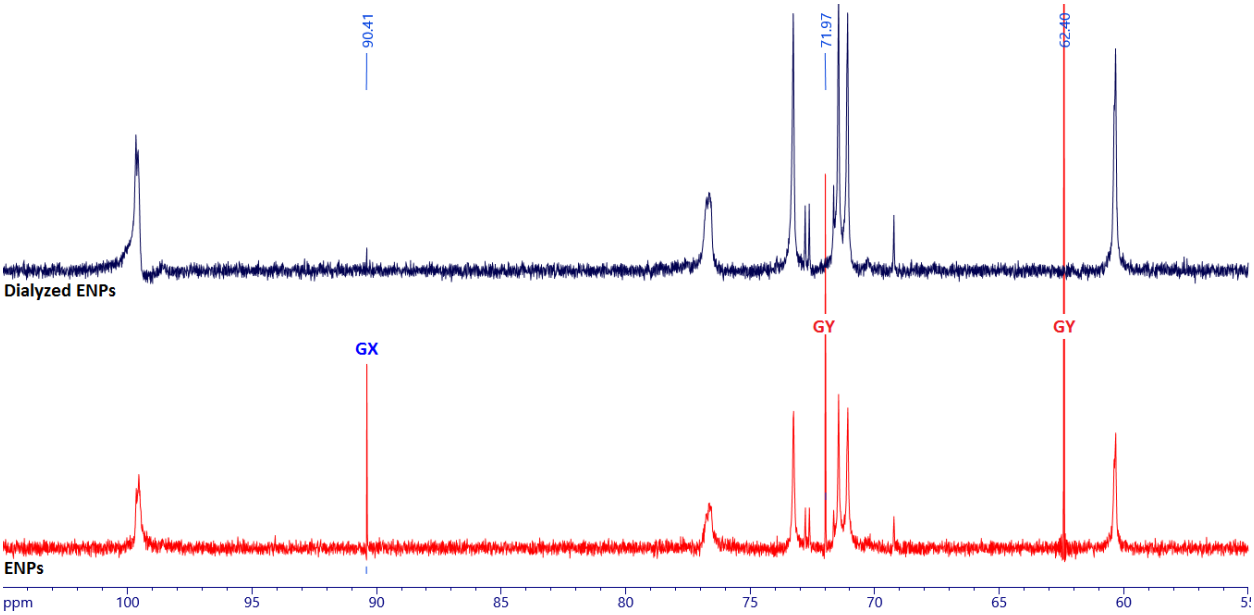

Figure 2.12. ^{13}C-NMR spectra of 10 % dispersions of GX2 ENPs in D_2O (176 MHz).
Top spectrum: Dialyzed ENPs
Bottom spectrum: Undialyzed ENPs

Figure 2.13 shows the ^{1}H-NMR spectra of the GX2 ENPs after 1 and 3 rounds of precipitation. It is clear that not all of the GY is removed after one round of precipitation using our protocol. However after three rounds of precipitation, all of the GY is removed. The removal of the GX cannot be determined from this ^{1}H-NMR spectrum because the GX protons appear underneath the water peak under the conditions that these NMR spectra were obtained.

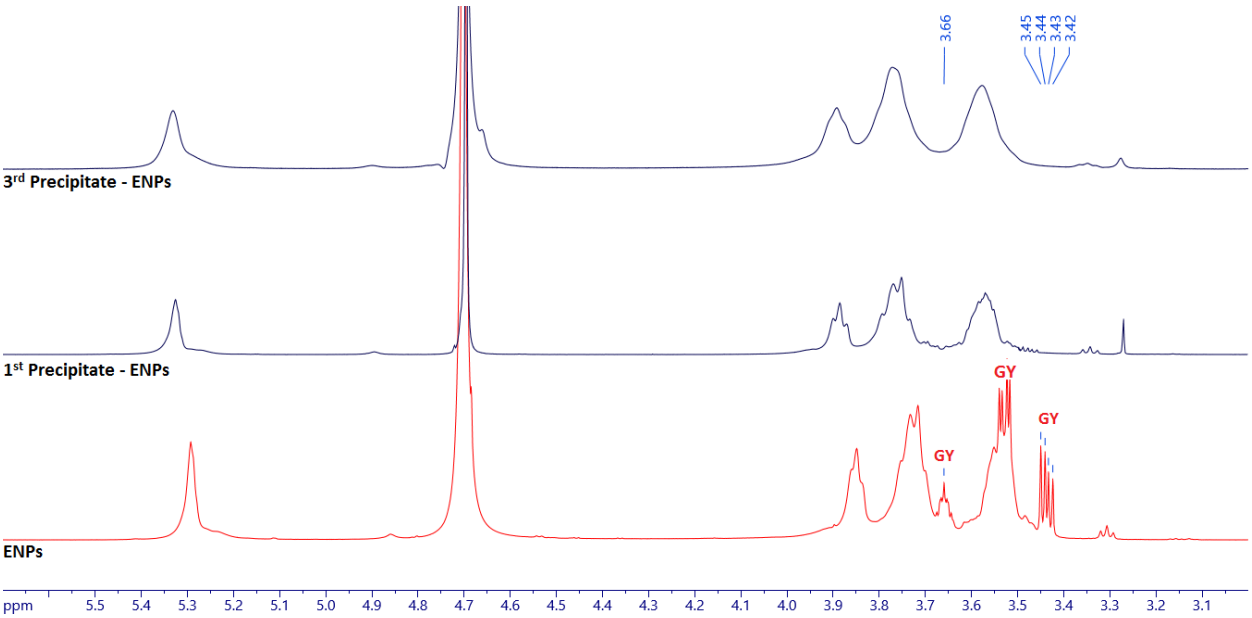

Figure 2.13. ^{1}H-NMR spectra of 10% dispersions of GX2 ENPs in D_2O (700 MHz).
Top spectrum: After 3 rounds of precipitation
Middle spectrum: After one round of precipitation
Bottom spectrum: No precipitation

Figure 2.14 shows the ^{13}C-NMR spectra of the ENPs after 1 and 3 rounds of precipitation. One round of precipitation was insufficient to remove all of the GY which is consistent with the results obtained by ^{1}H-NMR (Figure 2.13). The middle spectrum shown in Figure 2.14 reveals that that the GX was not removed after one round of precipitation. After three rounds of precipitation, both the GX and GY were completely removed from the spectrum.

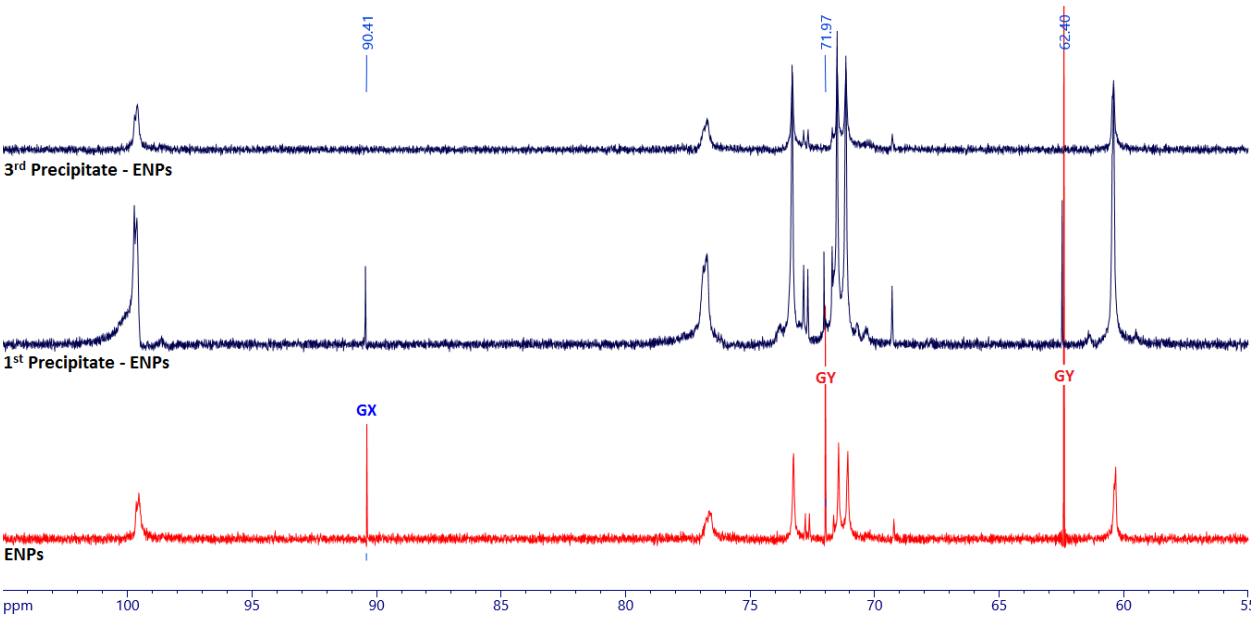

Figure 2.14. ^{13}C-NMR spectra of 10% dispersions of GX2 ENPs in D_2O (176 MHz).
Top spectrum: After 3 rounds of precipitation
Middle spectrum: After one round of precipitation
Bottom spectrum: No precipitation

2.3.3 2-D NMR Studies of ENPs in D_2O

We attributed earlier the peak at 90.4 ppm in the ^{13}C-NMR spectrum to the unbound, hydrated form of GX (compound **2.1**). To provide further evidence that the GX peak seen in the ^{13}C-NMR spectrum is not involved in any crosslinking, we performed 2-D NMR studies on the ENPs. There are many different 2D-NMR experiments that exists but the ones utilized in this thesis are: heteronuclear multiple quantum correlation (HMQC) and heteronuclear multiple bond correlation (HMBC) experiments.

HMQC is a 2D-NMR technique which uses the proton spectrum and carbon spectrum to generate cross-sectional signals between a proton and carbon bond. It is restricted to a one-bond (C-H) coupling. This means that HMQC allows one to determine which protons are bonded to which carbons as illustrated in Figure 2.15.

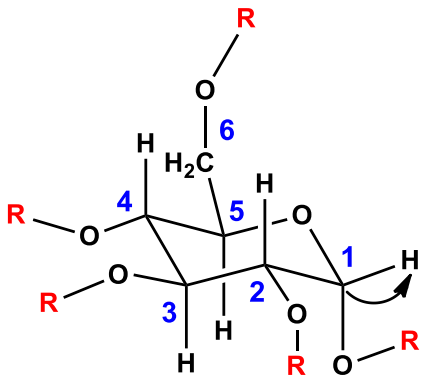

Figure 2.15. An HMQC experiment detects one bond C-H couplings as illustrated above. The arrow represents an example of a coupling that would be detected in an HMQC spectrum in ENPs. Only the C_1 to H_1 coupling is emphasized here but in an HMQC spectrum all the C-H coupling would be evident. Couplings between carbons and hydroxyl protons are never detected in an HMQC experiment regardless of solvent as the hydroxyl protons are not attached to carbons.

HMBC is a 2D-NMR technique which uses a proton spectrum and carbon spectrum to generate cross-sectional signals between a proton and a carbon that are separated by 2, 3 and sometimes 4 bonds (2-, 3- or 4-bond couplings). However, 4-bond couplings are rarely observed. It should be pointed out that sometimes not all of the 2-and 3-bond couplings are detected. The 2, 3 and 4 bond lengths have a wide range of coupling constants and does not necessarily fall in the range of the standard HMBC parameters. Multiple parameters in the HMBC experiment requires optimization to detect all of the couplings in the polymer and this will take a considerable amount of time because HMBC acquisition times are fairly long (~ 8 h) and there are multiple parameters to optimize.

Figure 2.16 illustrates the couplings that are detected in an HMBC experiment for C_2 in ENPs. Based on Figure 2.16, couplings between C_2 and H_1, H_3 and H_4 should be detected. Although it is unlikely, it may be possible to see a signal between C_2 and H_5 which would represent a 4-

bond coupling. HMBC is very useful for determining which hydroxyl protons are coupled to which carbons. Any proton that is not correlating to a carbon in the HMQC experiment would be recognized as a hydroxyl proton. The location of hydroxyl protons can be determined by an HMBC experiment because hydroxyl protons are 2 bonds removed from the carbon to which the hydroxyl groups are attached.

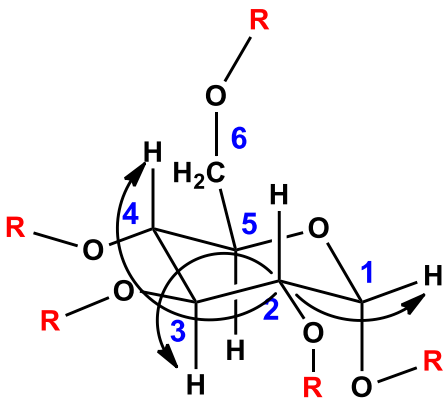

Figure 2.16. An HMBC experiment detects mainly 2- and 3-bond C-H couplings. The arrows illustrate couplings that could be detected in an HMBC spectrum of the ENPs between C_2 and H_1, H_3 and H_4. Only the couplings to C_2 are emphasized here but in an HMBC spectrum all or most 2 and 3 bond C-H couplings would be observed. Couplings between carbons and hydroxyl protons are detected in solvents in which proton exchange does not occur readily such as in DMSO-d_6.

HMBC experiments are less sensitive than HMQC experiments because 2 and 3-bond couplings are usually less intense than single-bond couplings. The reason is that C-H (one-bond) coupling constants cluster over a relatively narrow frequency range so that they can be easily detected by the instrument. By contrast, 2 and 3-bond couplings exhibit a wider range of coupling constants as compared to single bond couplings which makes them more difficult to detect. Consequently, it usually takes longer to complete an HMBC experiment as compared to an HMQC experiment. Sometimes the instrument accidentally captures the single-bond

correlations during an HMBC experiment, producing false-positive signals in the HMBC spectrum. This issue will be discussed in more detail below.

As HMBC can detect 2- and 3-bond couplings, it has the potential to determine whether or not GX is involved in crosslinking. However, prior to 2D-NMR characterization of the ENPs, HMQC and HMBC experiments were performed on a commercially available model glyoxal bis(diallyl acetal) (compound **2.6** in Figure 2.17) to determine whether couplings could be detected between the "alcohol" and the "GX" component of the acetal in an HMBC experiment. If the HMBC experiment was unable to detect these correlations in this simple model system, then it was unlikely that it would the analogous correlations in the ENPs.

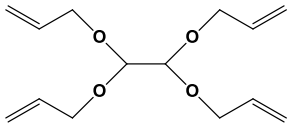

2.6

Figure 2.17. Chemical structure of glyoxal bis (diallyl acetal) (**2.6**).

We first obtained the HMQC spectrum of **2.6** in D_2O as shown in Figure 2.18. The peaks in the 1-D ^{1}H-NMR and ^{13}C-NMR spectra (shown on the axes in Figure 2.18) have been labeled accordingly. The signals have been highlighted for better illustration of where the signals match up. The "GX proton" (H_4) is hidden under the water peak similarly to what was suggested for the ENPs. The correlations between the protons and carbons match those obtained in the HMQC spectrum given in Figure 2.18. They are also in agreement with literature values (for alkene

groups). It should be pointed out that this is a commercial sample of **2.6** which contains some impurities.

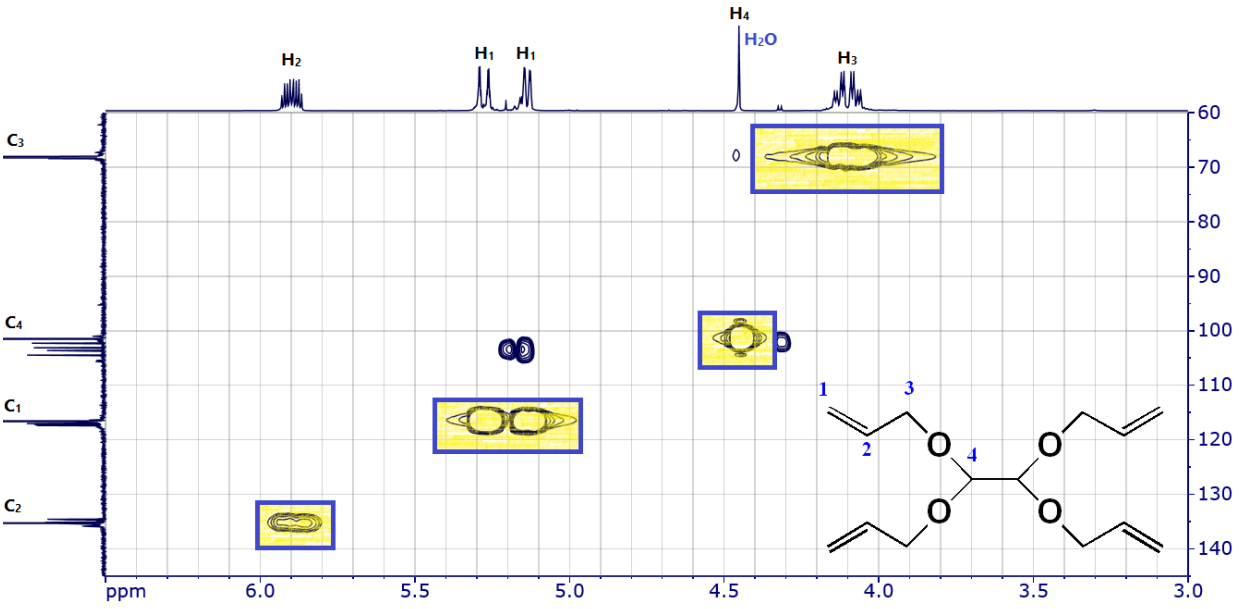

Figure 2.18. The HMQC spectrum of **2.6** in D_2O (600 MHz).

The HMBC spectrum of **2.6** in D_2O is shown in Figure 2.19. Real correlations between the carbons and protons (2 to 3-bond lengths away) are shown in the yellow boxes. Signals in the red boxes indicate false positives. False positive signals often occur in HMBC experiments. These artifacts are one-bond ^{1}H-^{13}C couplings that are not fully suppressed. They are usually easy to identify as they appear as a pair of symmetrical peaks surrounding the corresponding peaks in the 1-D ^{1}H-NMR spectrum (the proton peak is split by ~130 – 180 Hz as a result of a one bond C-H coupling). The correlations (cross-peak signals) between H_4 and C_3 and vice versa in compound **2.6** were readily detected in in the HMBC spectrum of **2.6** indicating that the HMBC experiment was successful in this model system.

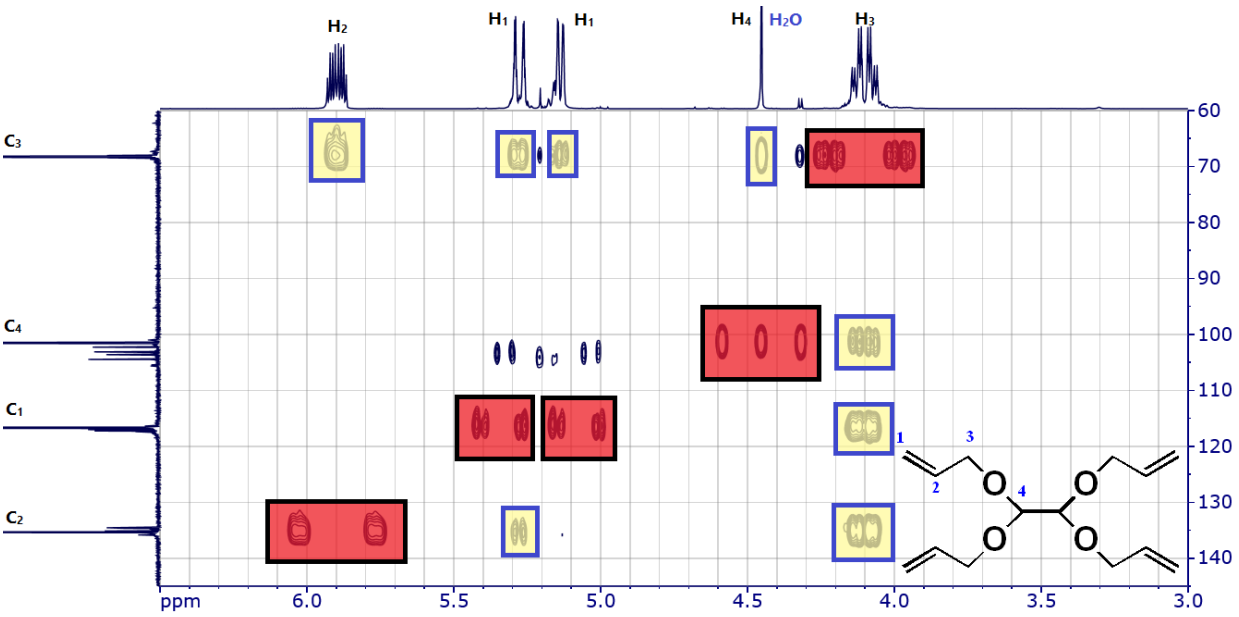

Figure 2.19. The HMBC spectrum of **2.6** in D_2O (600 MHz). Artifacts are highlighted in red.

Figure 2.20 shows the HMQC spectrum of the GX2 ENPs in a 10% mg/mL D_2O dispersion. This spectrum helped us confirm the assignments made in the 1-D spectra shown in Figures 2.3 and 2.4. Moreover, it confirmed that the GX peak in the 1-D ^{1}H-NMR spectrum in Figure 2.3 is indeed hidden under the water peak, as one can readily see the correlation between the peak at 90.3 ppm of GX and the large peak at 4.66 ppm.

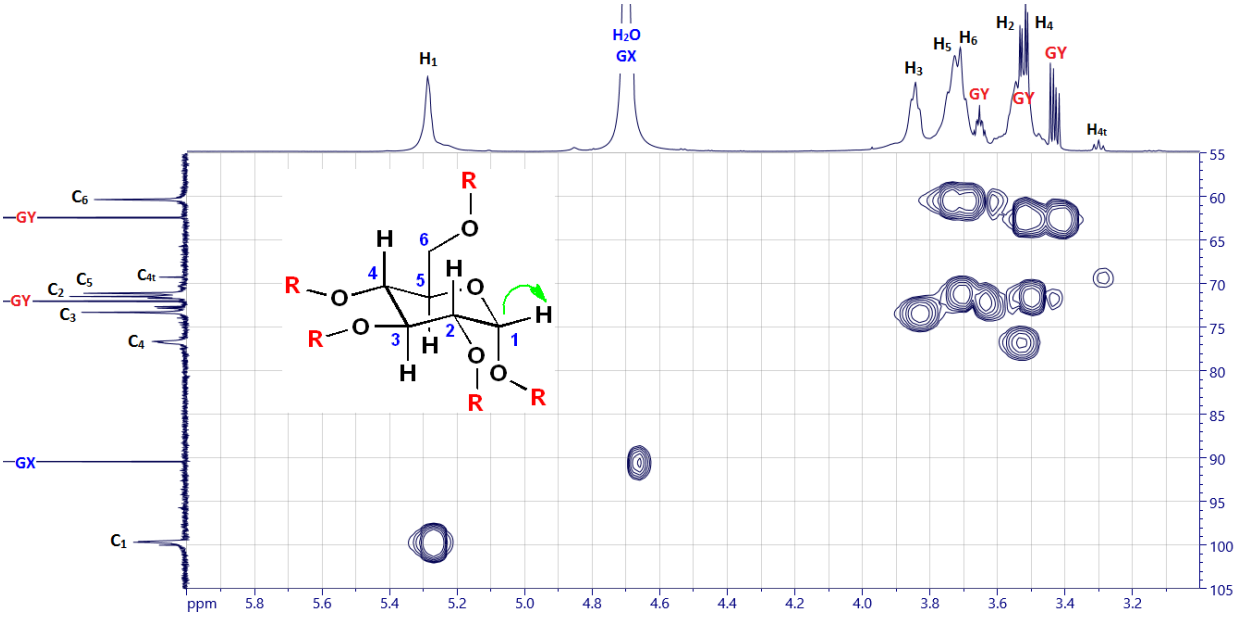

Figure 2.20. The HMQC spectrum of a 10% dispersion of GX2 ENPs in D_2O (700 MHz).

Figure 2.21 shows the HMBC spectrum of the GX2 ENPs in a 10% D_2O dispersion. This spectrum further supported the assignments made in the 1-D spectra shown in Figures 2.3 and 2.4. If the proton and carbon signals of GX observed in the 1-D ^{1}H- and ^{13}C-NMR spectra were involved in crosslinks, then correlations between the GX carbons and the starch protons or the GX protons and the starch carbons should be seen. Unfortunately, there was no observable correlations between the GX protons and the starch carbons or between the GX carbons and any of the starch protons in the HMBC spectrum. Moreover, no GX-GY adducts were detected in this spectrum because no correlations could be found between the GX proton and the GY carbons nor between the GX carbons and the GY protons.

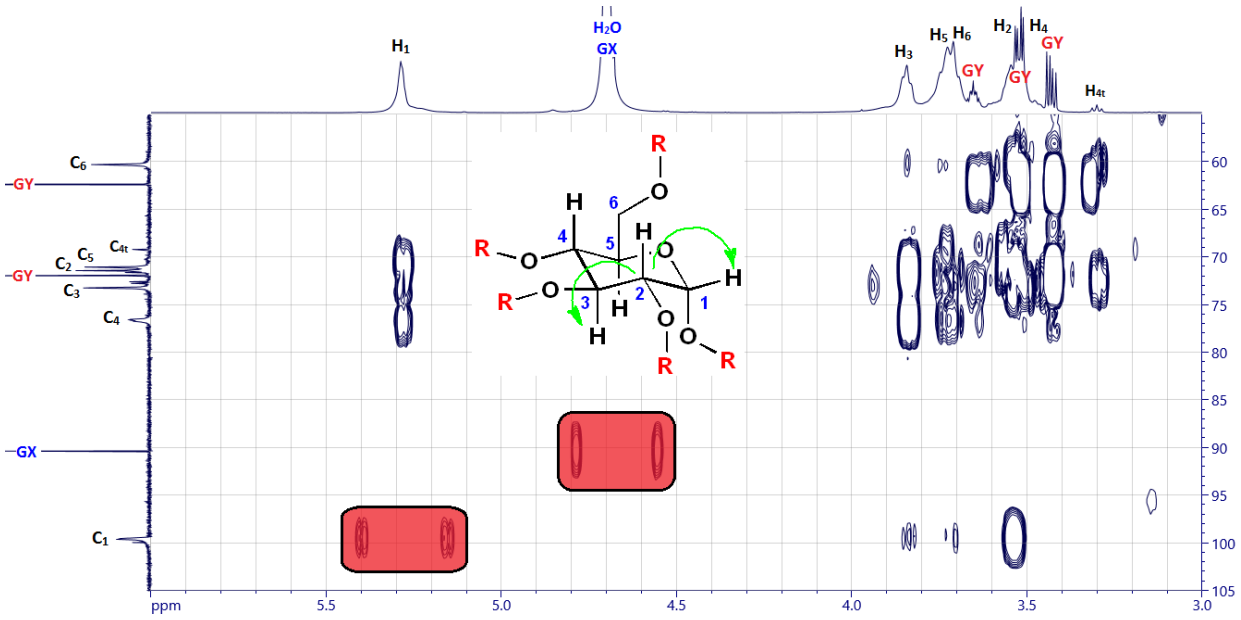

Figure 2.21. The HMBC spectrum of a 10% dispersion of GX2 ENPs in D_2O (700 MHz). Artifacts are highlighted in red.

The HMBC data strongly suggest that the GX signals observed in the 1-D ^{1}H- and ^{13}C-NMR spectra are not correlated with those of starch, thus demonstrating that GX is not involved in crosslinks. However, it is possible that some of the GX is involved in crosslinks but that the crosslinked GX species might not be unobservable in the NMR spectra. There are two main reasons for this. One is that, as pointed out earlier, many different types of crosslinks can potentially exist which would result in many different but weak signals that are difficult to detect. Secondly, if it is crosslinked, the signals might broaden out to the point beyond detection. Nevertheless, we can say with some degree of confidence that some of the GX is not involved in crosslinks when dispersed in water. The next issue we wished to study was the nature of the GX crosslinks when the ENPs were dispersed in an organic solvent such as DMSO.

2.3.4 1-D NMR Studies of ENPs in DMSO-d_6

Since the water content in DMSO is relatively small, the ENPs might remain crosslinked when dispersed in this solvent. Figures 2.22 and 2.23 show the ^{1}H- and ^{13}C-NMR spectra of the GX2 ENPs in a 4% dispersion in DMSO-d_6. The peaks corresponding to the ENPs were assigned according to the studies based on the HMQC and HMBC experiments, and were also supported by literature spectra.[14,37,44-46] Peaks labeled as GX in the spectrum shown in Figure 2.2 indicate that these peaks originate from GX itself and were found to grow with increased GX levels. Several peaks in the NMR spectra remain unidentified. The peaks belonging to the starch polymer are fairly broad as explained earlier. Sharper peaks correspond most likely to molecules that are unbound to the polymer and freely rotating.

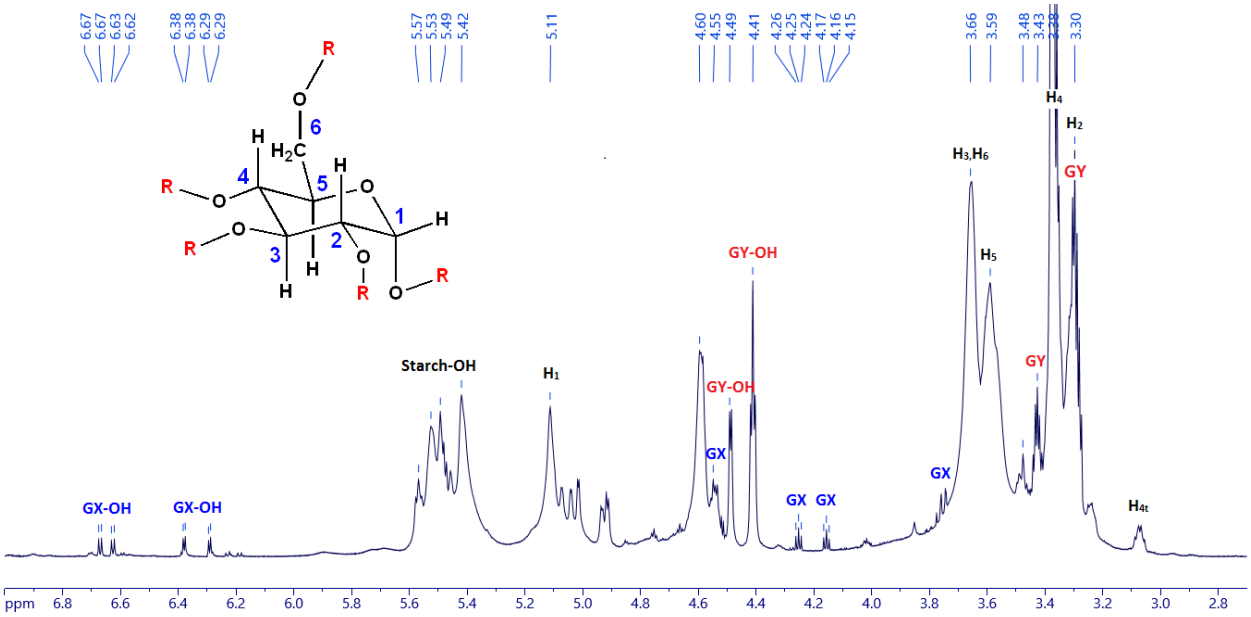

Figure 2.22. ^{1}H-NMR spectrum of a 4% dispersion of GX2 ENPs in DMSO-d_6 (700 MHz).

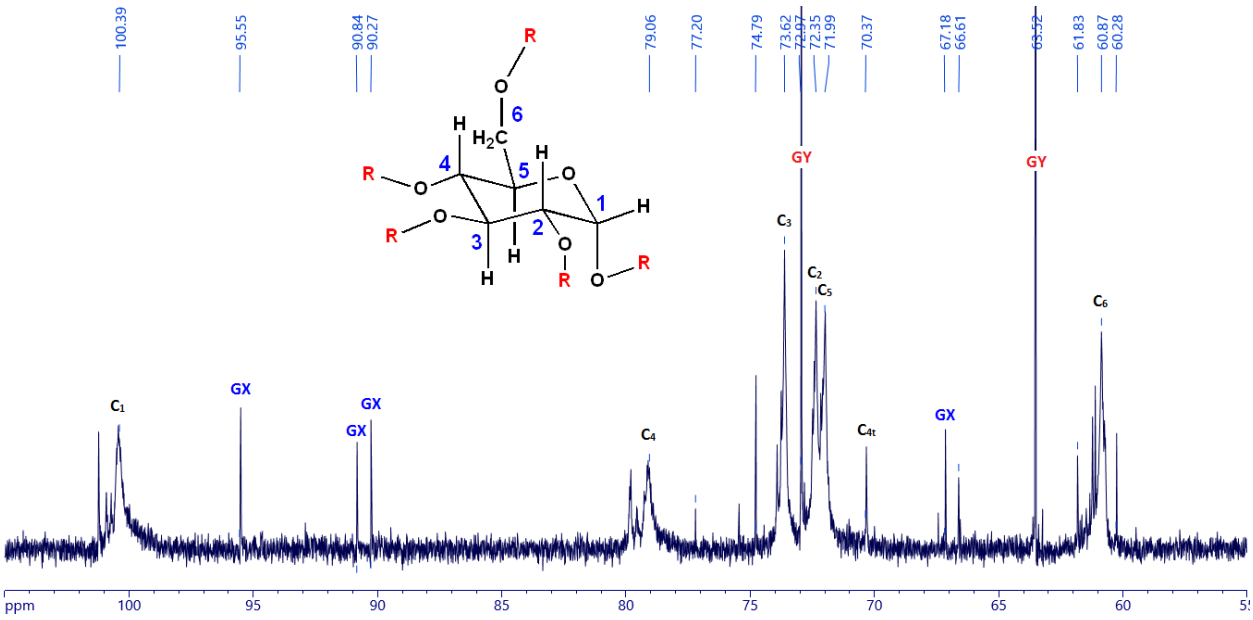

Figure 2.23. ^{13}C-NMR spectrum of a 4% dispersion of GX2 ENPs in DMSO-d_6 (176 MHz).

The NMR spectra of the ENPs in DMSO are considerably more complex in comparison to those obtained in D_2O. One reason for this is because the hydroxyl protons are detected in DMSO. The second reason is that multiple species of GX exist in DMSO whereas in D_2O, only one predominant species exists under the conditions in which our NMR spectra were acquired. The ^{1}H- and ^{13}C-NMR spectra of GX in DMSO shown in Figures 2.24 and 2.25 clearly illustrate this. These peaks are due to the structures shown in Figure 2.10 as well as others. None of the peaks in Figure 2.23 appear to match literature values of ^{13}C-NMR chemical shifts reported for GX in DMSO.[63]

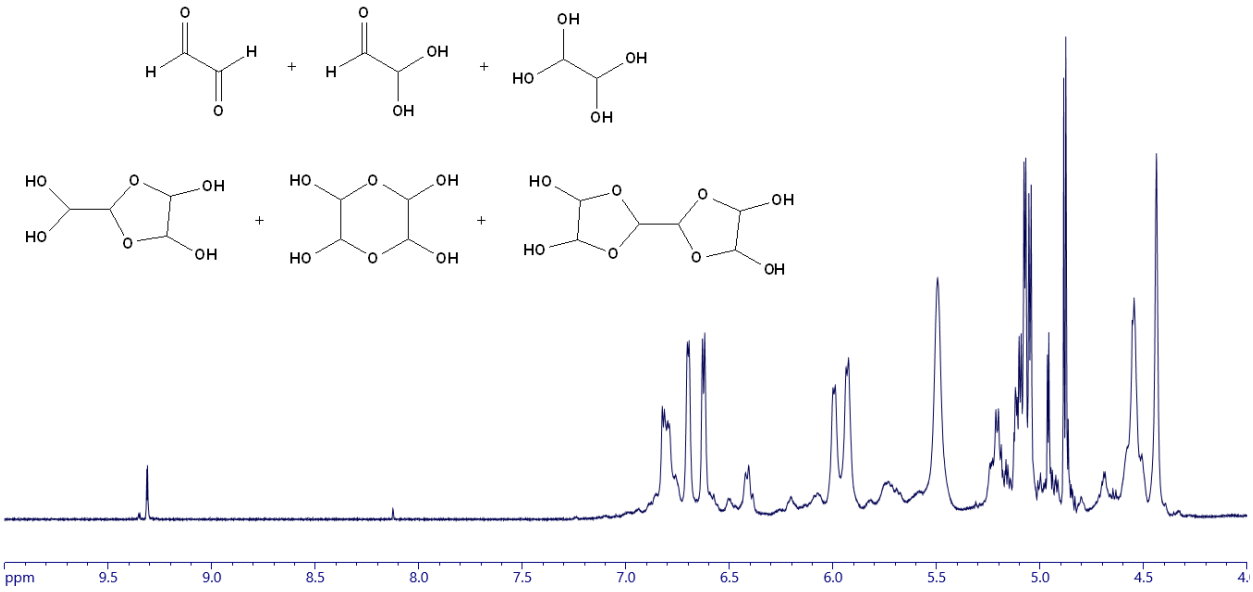

Figure 2.24. ^{1}H-NMR spectrum of GX in a 1% solution in DMSO-d_6 (500 MHz).

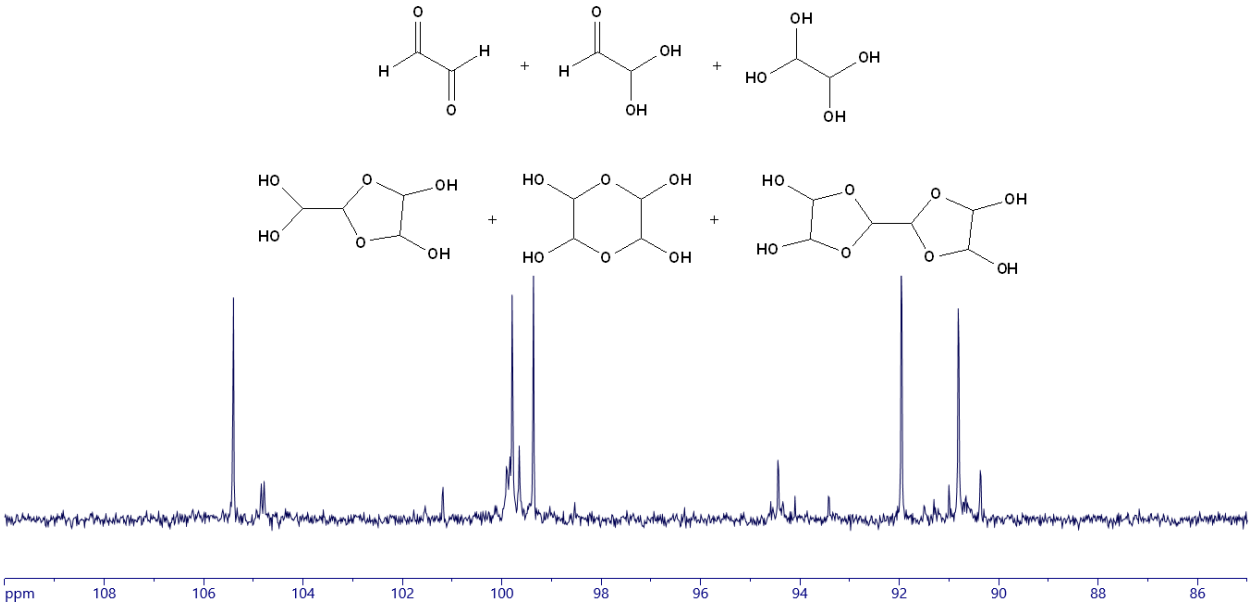

Figure 2.25. ^{13}C-NMR spectrum of GX in a 1% solution in DMSO-d_6 (125 MHz).

The experiments that were used to identify which peaks in the NMR spectra corresponded to GX and GY when the ENPs were dispersed in water were also conducted to identify these peaks when the ENPs were dispersed in DMSO. The results of these experiments

are discussed hereafter. Figure 2.26 compares the ^{1}H-NMR spectra of the dialyzed and undialyzed GX2 ENPs in 4% dispersions in DMSO-d_6. Following dialysis, the GY peaks disappear as well as many of the GX peaks. The only remaining GX peak is found at 4.5 ppm. This observation suggests that the GX peak at 4.5 ppm has the same chemical shift as a starch hydroxyl proton. This leads to complications that are later discussed in the 2D-NMR studies when a hydroxyl proton overlaps with a GX proton.

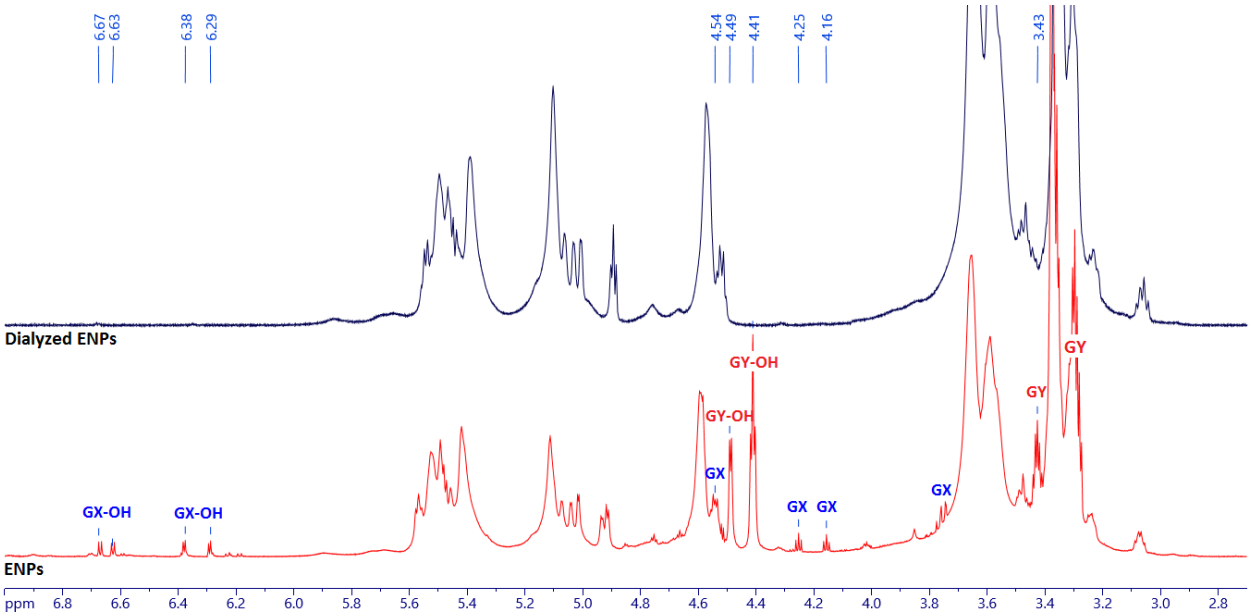

Figure 2.26. ^{1}H-NMR spectra of 4% dispersions of GX2 ENPs in DMSO-d_6 (700 MHz).
Top spectrum: Dialyzed ENPs
Bottom spectrum: Undialyzed ENPs

Figure 2.27 compares the ^{13}C-NMR spectra of the dialyzed and undialyzed GX2 ENPs in 4% dispersions in DMSO-d_6. This comparison provided a substantial amount of information because of the large number of peaks which disappeared after the dialysis treatment. The peaks that were already confidently assigned to GX or a GX adduct of some kind (peaks between 90 - 96 ppm) and GY (63.5 and 73 ppm) disappeared after dialysis. In addition to these, the peaks found at 60.3,

61.8, 67.2, 74.8, 75.4, and 77.2 ppm were also removed after the dialysis. This unmistakably confirms that those peaks arise from molecules unbound to the polymer and belong to either free GY, free GX or GX-GY adducts or GX/GY decomposition products which are also removed by dialysis. Although the exact identity of these adducts are not yet determined, this provides strong support that adducts or decomposition products do exist.

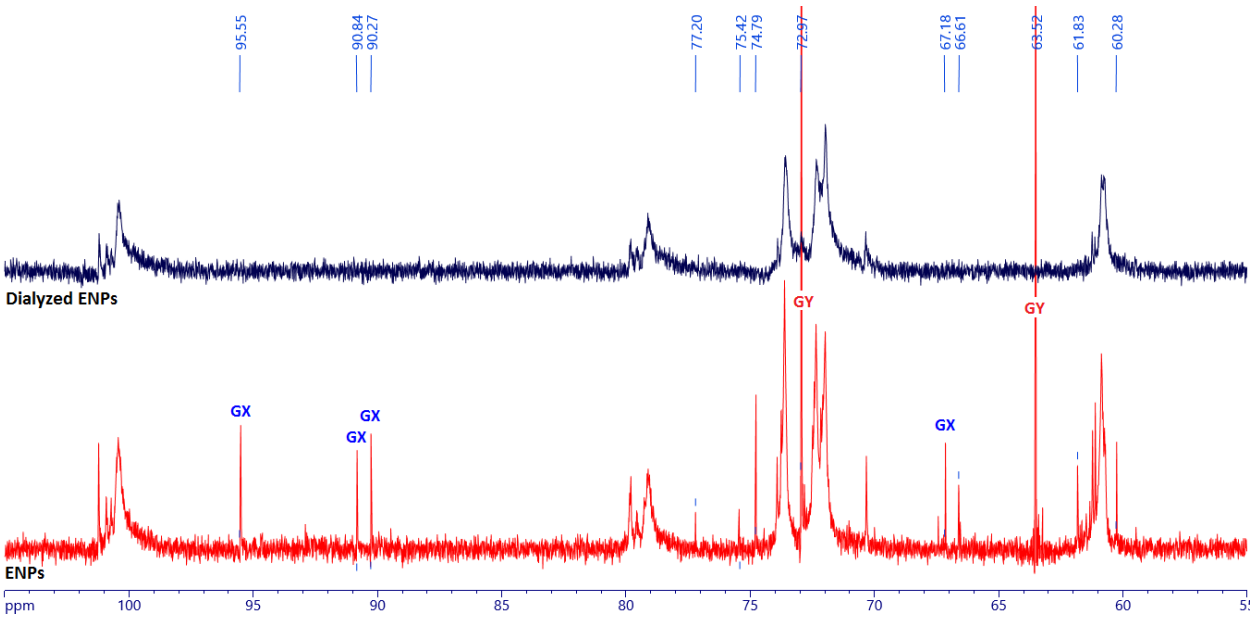

Figure 2.27. ^{13}C-NMR spectra of 4% dispersions of GX2 ENPs in DMSO-d_6 (176 MHz).
Top spectrum: Dialyzed ENPs
Bottom spectrum: Undialyzed ENPs

Figure 2.28 shows the ^{13}C-NMR (DEPT-135) spectra of the ENPs prepared with varying amounts of GX in 4% dispersions in DMSO-d_6. Many new peaks appeared with increasing amount of GX. These peaks were found at: 60.1, 61.1, 61.8, 66.5, 67.1, 74.8, 75.4, 90.3, 90.9, 92.8, and 95.5 ppm. As mentioned previously, DEPT-135 shows the CH and CH_3 carbon signals facing up and the CH_2 carbon signals facing down. Knowing that GX cannot bear a CH_2 group, the increasing amount of GX must lead to either crosslinking at the C_6 position (C_6 is the only CH_2 group on

starch) or the formation of GX-GY adducts or the decomposition of GX. However, not all the growing peaks are CH_2 groups, some are CH groups which would support the claim that GX-GY adducts are forming since these new adducts would have slightly different chemical shifts than unbound GY or GX. The identification of these peaks is very difficult and will require further in-depth study. In any case, these results reinforce our conclusions drawn from the above dialysis experiments in terms of which peaks stem from either GY, GX or GX-GY adducts, or GX or GY decomposition.

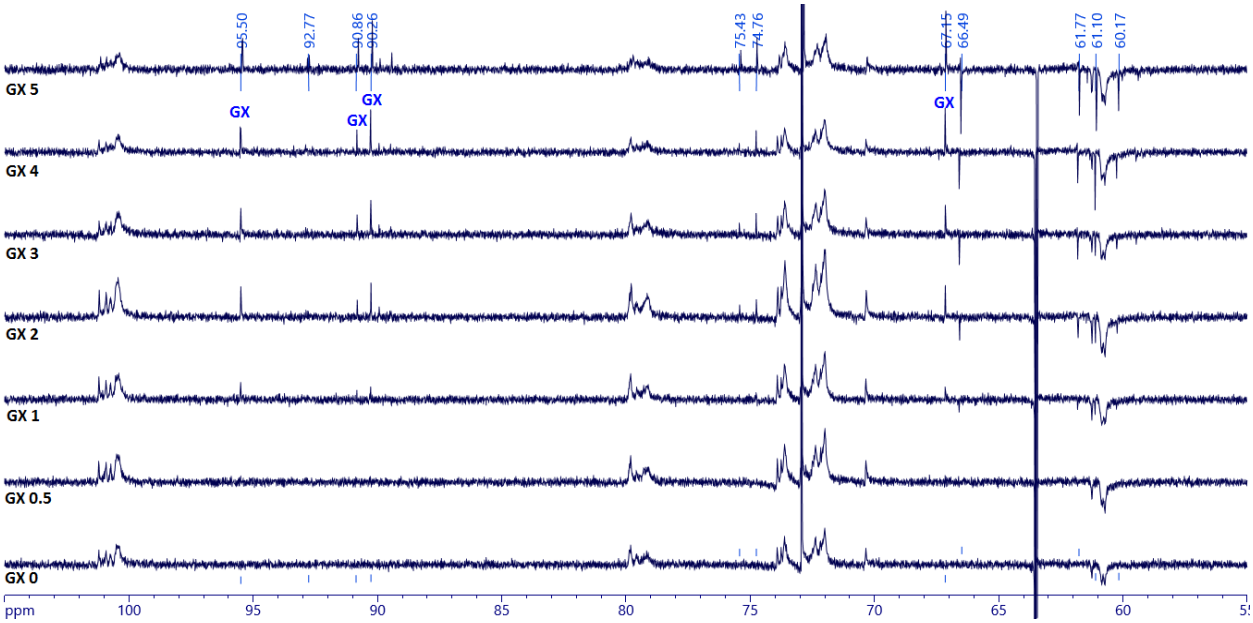

Figure 2.28. ^{13}C-NMR stacked spectra of 4% dispersions of ENPs prepared with varying amounts of GX (0 – 5) in DMSO-d_6 (125 MHz).

Figure 2.29 shows the ^{1}H-NMR spectra of 4% dispersions of the ENPs prepared with varying amounts of GX but in the *absence* of GY in 4% dispersions in DMSO-d_6. Figure 2.30 shows an expanded version of these spectra. Comparing these spectra to the one in Figure 2.22 is very important because the peaks not present in the absence of GY can now be determined. Firstly, the peaks that are observed to grow with increasing amounts of GX had chemical shifts of 2.9,

3.9, 4.3, 6.3, 6.5, 6.6, 6.9, 7.0, and 8.1 ppm. The chemical shift of the peaks appearing between 6.3 and 6.9 ppm suggests that these are hydroxyl protons associated with GX. These peaks are very broad which contrasts with the sharp peaks of the GX hydroxyl protons seen in the ^{1}H-NMR spectrum of the ENPs prepared in the presence of GY in DMSO-d_6 (for example, see the bottom spectrum in Figure 2.26). The broadness of these peaks suggests that GX is involved in a crosslink with starch. We propose that in the absence of GY, all GX molecules are involved in crosslinks. The growing peak at 8.1 ppm suggests the presence of an aldehyde though this chemical shift is somewhat upfield for an aldehyde proton. This peak also appears in the ^{1}H-NMR spectrum of the GY0 ENPs in D_2O (Figure 2.8). It also appears in the ^{1}H-NMR spectrum of just GX alone in DMSO-d_6 (Figure 2.24) indicating that it is not derived from a GX-GY adduct.

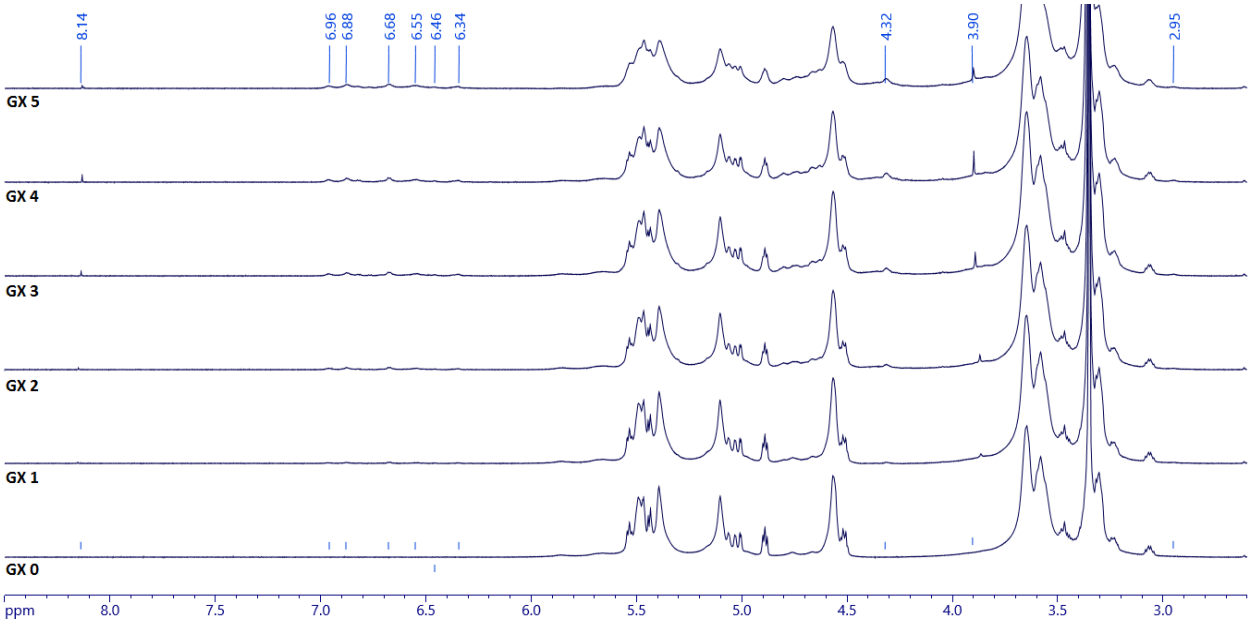

Figure 2.29. ^{1}H-NMR spectra of 4% dispersions of the ENPs prepared with varying amounts of GX (0 – 5) in DMSO-d_6 (600 MHz) in the absence of GY.

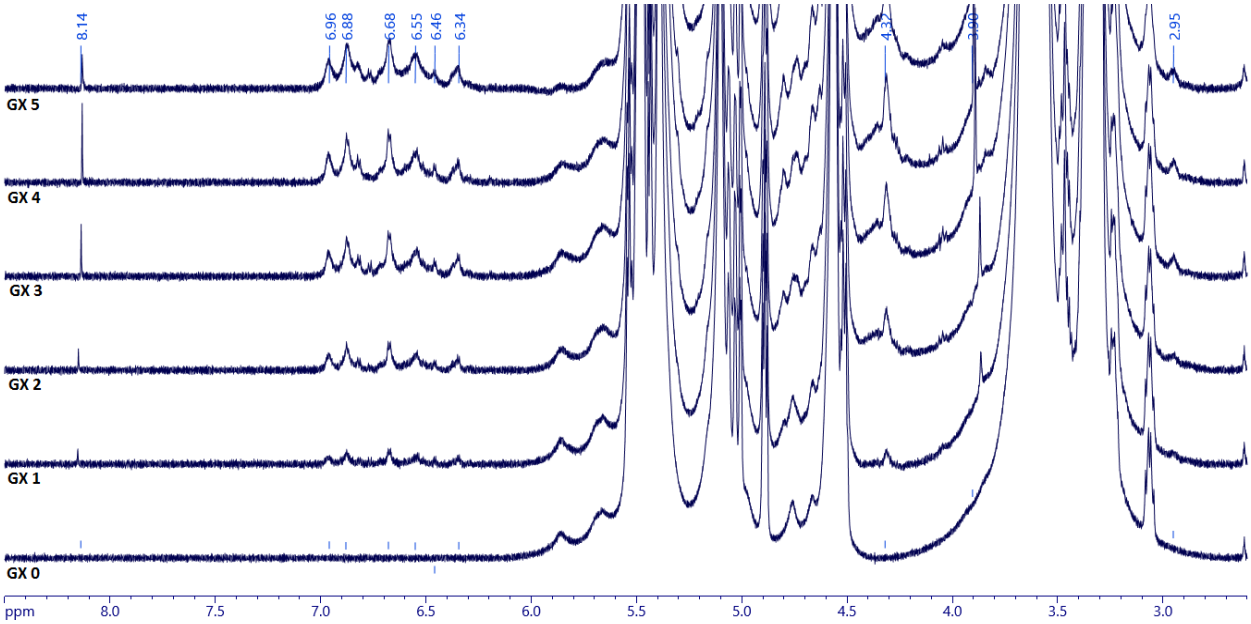

Figure 2.30. Expanded ^{1}H-NMR spectra of 4% dispersions of the ENPs prepared with varying amounts of GX in DMSO-d_6 (600 MHz) in the absence of GY.

Figure 2.31 shows the ^{13}C-NMR spectra of ENPs prepared with varying amounts of GX but in the *absence* of GY in 4% DMSO-d_6 dispersions. The most important observation made here was that no peaks appear between 90 - 105 ppm which is where the GX carbons appear. Compared to the ^{13}C-NMR spectrum of the ENPs prepared in the presence of GY (Figure 2.23), the peaks associated with GX or GX-GY adducts are now completely absent from the spectra shown in Figure 2.31. However, the GX peak is present in the D_2O spectra of these GY-free samples (Figure 2.9). One possible explanation for this is that GX is involved in crosslinks with the starch polymer when dispersed in DMSO but this results in very small and broad peaks which cannot be detected under the conditions of our ^{13}C-NMR experiments. When the samples are dispersed in pure water, some or all of the crosslinking are reversed and unbound GX is detected as a sharp peak in the ^{13}C-NMR spectra (Figure 2.9). We suggest that when GY is *present* during the manufacturing of the ENPs, some or maybe all of the GX is sequestered as adducts with GY and

it is these adducts that we are seeing in the ^{13}C-NMR spectra of ENPs in DMSO (Figures 2.22 and 2.23). If not all GX molecules are sequestered as GX-GY adducts, then the rest is involved in crosslinks but these crosslinks are undetectable by ^{13}C-NMR when the ENPs are dispersed in DMSO.

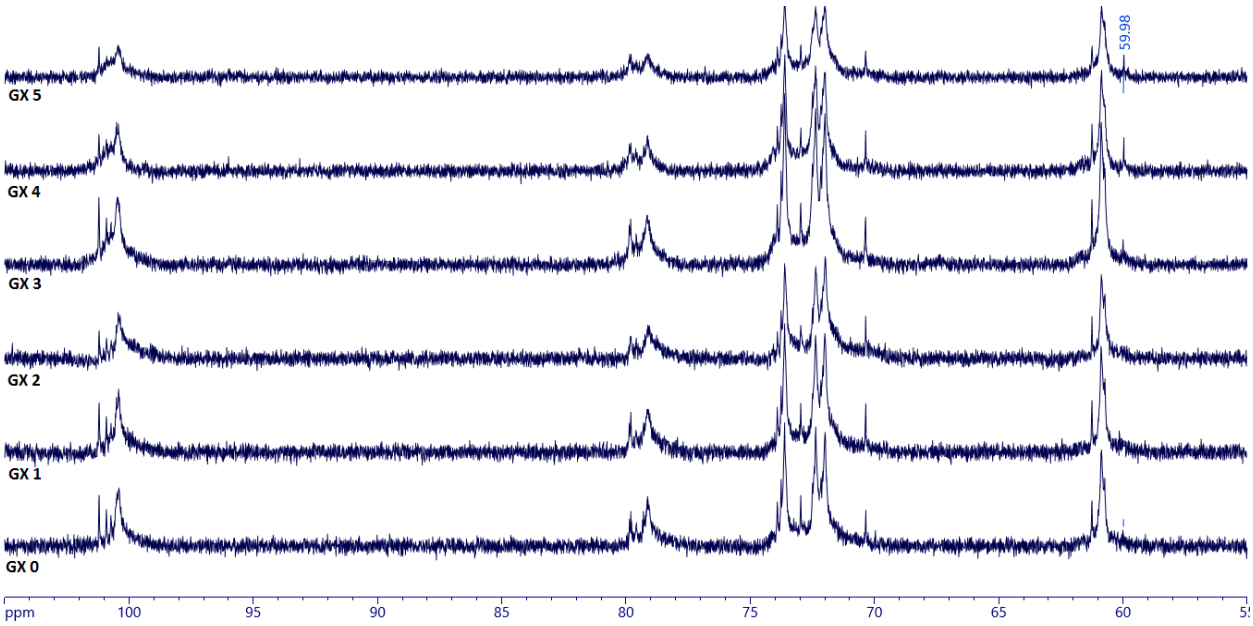

Figure 2.31. ^{13}C-NMR spectra of 4% dispersions of the ENPs prepared with varying amounts of GX (0 – 5) in DMSO-d_6 (150 MHz) in the absence of GY.

A peak is observed to grow in Figure 2.31 at 60.0 ppm. It was also observed in Figure 2.28 and identified as a CH_2 group. This indicates that the 60.0 ppm peak does not belong to a GX-GY adduct. A peak with a similar chemical shift also appears in the ^{13}C-NMR spectra of the ENPs prepared in the presence or absence of GY when dispersed in D_2O (Figures 2.6 and 2.9). This peak could have originated from a C_6 in the ENPs that is involved in a crosslink with GX; however, the fact that it appears in the D_2O spectra (where crosslinking appears to be reversible and favors non-crosslinked species) suggests otherwise. Another possibility is that it is a decomposition product of GX. Glycolic acid ($HOCH_2COOH$) is a common decomposition product of GX. Indeed, it

has been shown that even acetals of GX readily decompose to glycolates at the temperatures used to prepared these ENPs (100-200 °C).[43] The methylene carbon of glycolic acid exhibits a ^{13}C-NMR chemical shift at 60 ppm in DMSO consistent with what is being seen here.[50] The carbonyl carbon of glycolic acid appears at around 175 ppm but was not detected in any of the ^{13}C-NMR spectra described earlier. Carbonyl carbons are often difficult to detect in ^{13}C-NMR spectra. Nevertheless, it will be shown later that when a good signal-to-noise is obtained, by using a 700 MHz NMR spectrometer on the GX5GY0 ENPs (GY0 means that no GY was present during the manufacturing of the ENPs), that this carbonyl carbon can be detected by ^{13}C-NMR. The ^{1}H-NMR spectra of the ENPs run in either DMSO or D_2O also suggest the presence of glycolic acid. All of the ^{1}H-NMR spectra of the GX(1 - 5) GY0 ENPs run in DMSO show a small peak at about 3.9 ppm, which is where the methylene protons of glycolic acid appear in DMSO.[50] The ^{1}H-NMR spectra of the GX(1 - 5) GY0 ENPs run in D_2O show a small peak at 4.09 ppm which is consistent with the methylene protons of glycolic acid in D_2O (Figure 2.8).[50] We also noticed that these glycolic acid peaks are stronger in the ^{1}H-NMR spectra of the GY0 ENPs as compared to ENPs prepared in the presence of GY. This might be due to the reaction of GY with GX so that less GX is available to form glycolic acid.

To determine if the hypothesized crosslinks in the DMSO-dispersed GY-free ENPs could be reversed by the addition of water, ^{1}H-NMR spectra of the GY-free ENPs were obtained in DMSO-d_6-D_2O mixtures. Figure 2.32 shows the ^{1}H-NMR spectrum of GX5GY0 ENPs in an 8:2 DMSO-d_6:D_2O mixture (top spectrum) and in pure DMSO-d_6 (middle spectrum). The ^{1}H-NMR spectrum of GX5 ENPs prepared in the presence of GY in DMSO-d_6 is also shown (bottom spectrum). Peaks originating from hydroxyl protons were no longer visible as the hydroxyl

protons were exchanged with deuterium. In the ^{1}H-NMR spectrum of the GX5GY0 ENPs obtained in the 8:2 DMSO-d_6:D_2O mixture, two sets of doublets appear at 4.58 and 4.91 ppm that were not present or could not be detected (due to overlap with other peaks) in the ^{1}H-NMR spectra of ENPs prepared with or without GY in DMSO-d_6. The sharpness of these peaks suggests that the compound(s) responsible for these peaks is not bound to the ENPs.

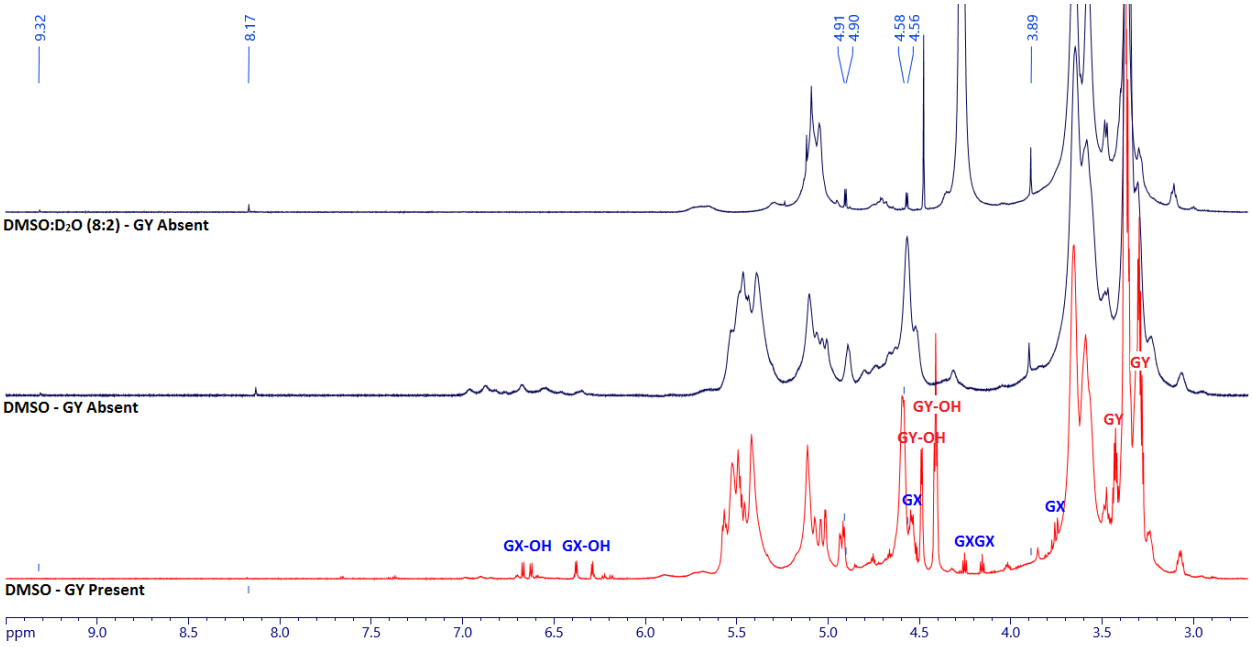

Figure 2.32. ^{1}H-NMR spectra of 4% dispersions of GX5 ENPs in DMSO-d_6:D_2O and DMSO-d_6 (600 MHz).
Top spectrum: GX5GY0 ENPs in DMSO-d_6:D_2O (8:2)
Middle spectrum: GX5GY0 ENPs in DMSO-d_6
Bottom spectrum: GX5 ENPs in DMSO-d_6

Figure 2.33 shows the ^{1}H-NMR spectra of GX0, GX2, and GX5 ENPs prepared in the absence of GY in 4% dispersions in 8:2 DMSO-d_6:D_2O mixtures. New peaks with chemical shifts of 3.89, 4.57 (doublet), 4.91 (doublet), and 8.17 ppm appeared and were found to increase in intensity as the GX content increased. These peaks were also observed in the ^{1}H-NMR spectra of GX5GY0 ENPs in DMSO-d_6:D_2O (8:2) (Figure 2.32, top spectrum). These four peaks are sharp

suggesting that they are unbound molecules and freely rotating. These results suggest that the hypothesized crosslink is reversible.

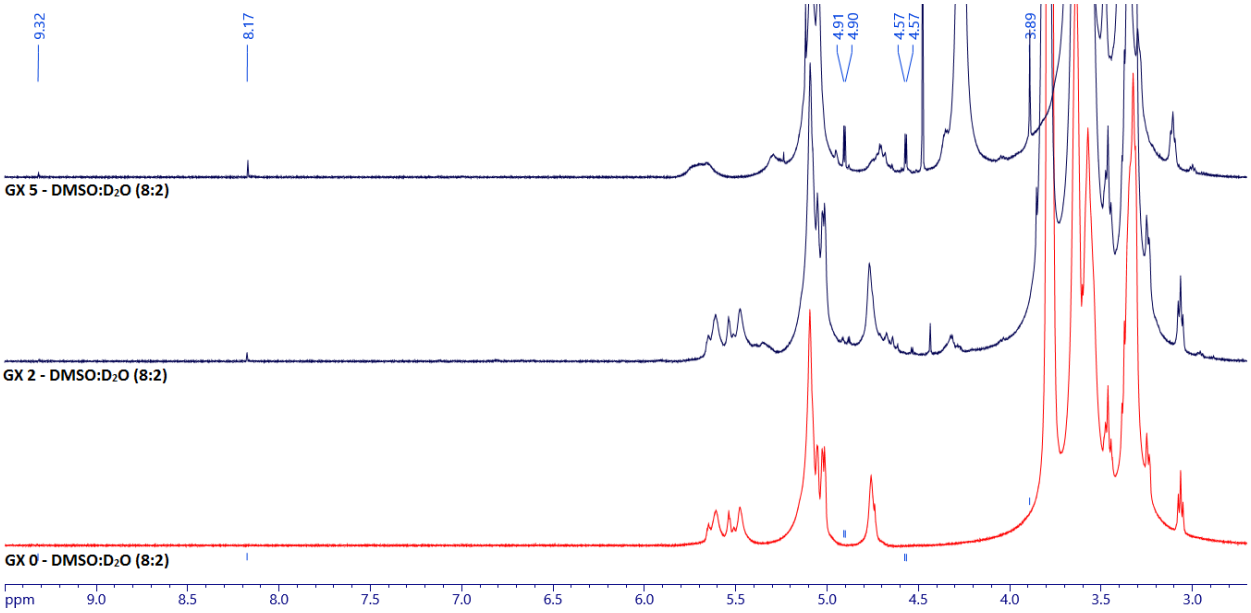

Figure 2.33. ^{1}H-NMR spectra of 4% dispersions of GX0, GX2 and GX5 ENPs prepared in the absence of GY in DMSO-d_6:D_2O (8:2) (700 MHz).
Top spectrum: GX5GY0 ENPs
Middle spectrum: GX2GY0 ENPs
Bottom spectrum: GX0GY0 ENPs

Figure 2.34 shows the ^{1}H-NMR spectra of GX5 ENPs prepared in the absence of GY in various DMSO-d_6/D_2O mixtures. These experiments were done to determine if the intensity of the new peaks observed at approximately 4.6, 4.9, 8.2 and 9.3 ppm in the ^{1}H-NMR spectrum of the GX5GY0 ENPs run in the 8:2 DMSO-d_6:D_2O mixture (Figure 2.32, top spectrum) increased or decreased as the ratio of DMSO-d_6 to D_2O was altered. The doublets at 4.6 and 4.9 ppm did not increase in intensity as the D_2O content was increased. The peak at 8.12 ppm decreased in size (relative to the doublets at 4.6 and 4.9 ppm) upon changing the solvent from a 9:1 DMSO-d_6:D_2O mixture to an 8:2 mixture but then increased when dispersed in the 7:3 mixture. There is no

explanation for the decrease followed by an increase in peak intensity. The ^{1}H-NMR spectrum of the GX5 ENPs in Figure 2.33 shows a very small peak at 9.3 ppm which is probably due to an aldehyde proton. It is also present in all of the spectra shown in Figure 2.34, indicating that for the GX5 ENPs prepared with larger amount of GX, aldehyde species are present when these ENPs are dispersed in DMSO-d_6-D_2O mixtures.

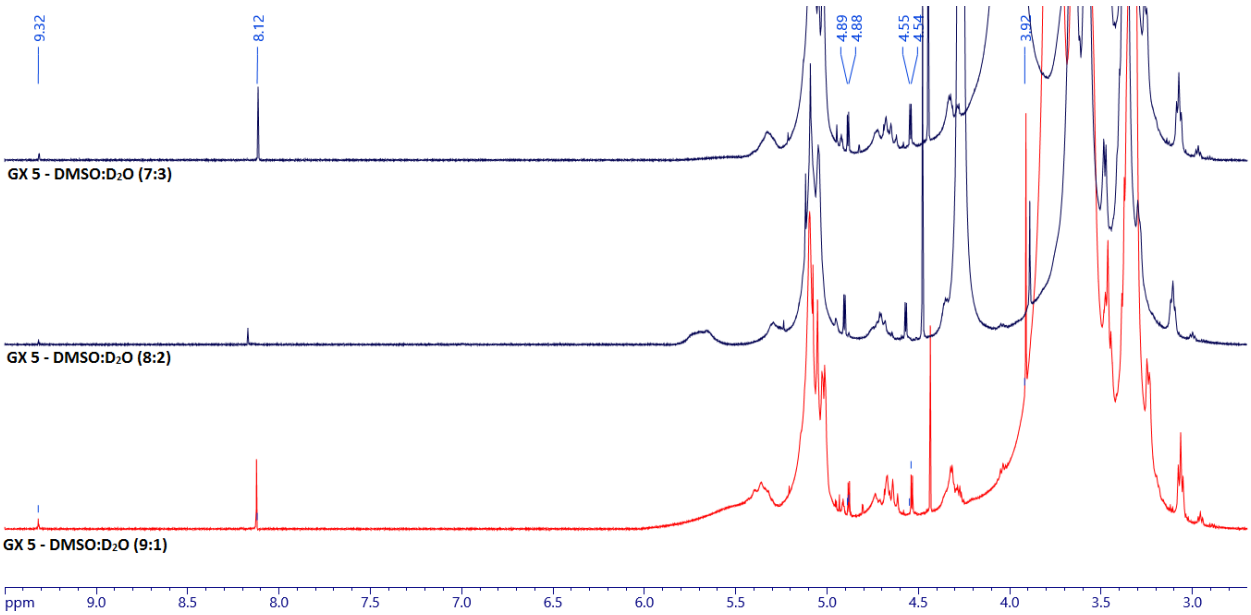

Figure 2.34. ^{1}H-NMR spectra of 4% dispersions of GX5 ENPs prepared in the absence of GY in varying DMSO-d_6:D_2O mixtures (700 MHz).
Top spectrum: DMSO-d_6:D_2O ratio is 7:3
Middle spectrum: DMSO-d_6:D_2O ratio is 8:2
Bottom spectrum: DMSO-d_6:D_2O ratio is 9:1

Figure 2.35 shows the ^{13}C-NMR spectra of GX5 ENPs prepared in the presence or absence of GY in 4% dispersions in either DMSO-d_6 or an 8:2 DMSO-d_6:D_2O mixture. New peaks appeared at: 90.3, 91.3, 94.2, 96.6, 98.8, 99.4, 105.0, and 175.3 ppm when water was added to the GY-free sample (top spectrum in Figure 2.35). This suggests that when water is added to this sample, the crosslinks are reversible and GX dissociates from the polymer. On the basis of literature values

the peaks at: 90.3, 98.8, 99.4, and 105.0 ppm correspond to dimer **2.7** in Figure 2.36 which is the trans isomer of compound **2.2** in Figure 2.10.[40] This assignment is supported by the corresponding ^{1}H-NMR spectrum (top spectrum in Figure 2.33). The two doublets (H_1 and H_2) at 4.55 and 4.89 ppm correspond to protons attached to C_1 and C_2. The protons H_3 and H_4 appear at 5.05 and 5.07 ppm according to the literature.[40] However we do not see peaks corresponding to these protons in our spectra (top spectrum in Figure 2.33) as they are obscured by the starch protons. The small peak at 94.2 ppm corresponds to compound **2.3** in Figure 2.10.[40] We are unable to assign a structure corresponding to the small peak at 96.6 ppm. Lastly, the peak at 175.3 ppm is a carbonyl carbon; most likely originating from a carboxylic acid group such as glycolic acid.

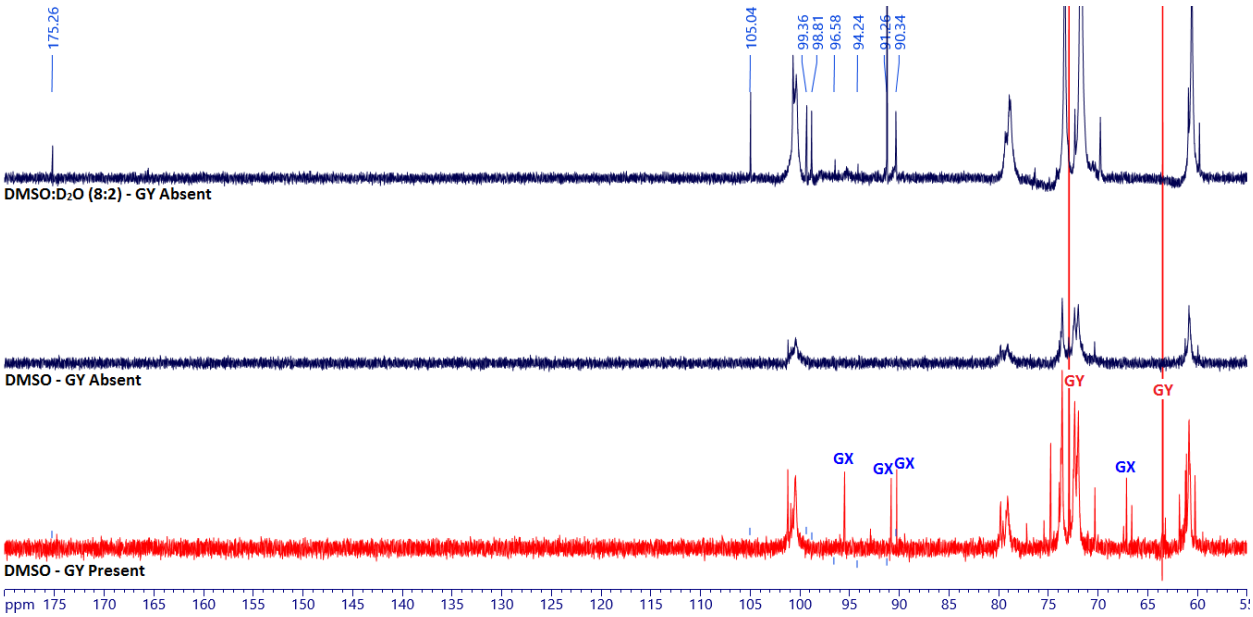

Figure 2.35. ^{13}C-NMR spectra of 4% dispersions of GX5 ENPs in DMSO-d_6:D_2O or DMSO-d_6 (176 MHz).
Top spectrum: ENPs in the absence of GY in DMSO-d_6:D_2O, 8:2
Middle spectrum: ENPs in the absence of GY in DMSO-d_6
Bottom spectrum: ENPs in the presence of GY in DMSO-d_6

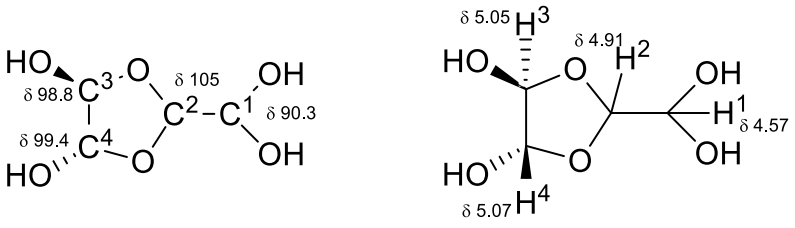

2.7

Figure 2.36. Structure of the trans GX dimer **2.7** showing (**A**) ^{13}C-NMR chemical shifts and (**B**) ^{1}H-NMR chemical shifts.

None of the GX peaks seen in the ^{13}C-NMR spectrum in the GX5GY0 sample run in the 8:2 DMSO-d_6:D_2O mixture (top spectrum in Figure 2.35) matches the GX peaks seen in the ^{13}C-NMR spectrum of the GX5 sample run in DMSO-d_6 (bottom spectrum in Figure 2.35). This suggests that the GX peaks observed in the sample obtained in DMSO-d_6 (bottom spectrum in Figure 2.35) are a result of GX-GY adducts.

There are two other peaks of significant size that appear in the ^{13}C-NMR spectrum of the sample run in the 8:2 mixture (top spectrum in Figure 2.35). One is at 91.3 ppm, which is most likely due to the monomer **2.1**.[40] The top spectrum in Figure 2.37 shows a well-defined peak at 175.3 ppm which corresponds to a carbonyl carbon. This chemical shift does not correspond to the carbonyl carbon of an unhydrated or monohydrated GX which appears further downfield.[40] This chemical shift is more characteristic of a carboxylic acid and most likely due to glycolic acid as discussed above.

Figure 2.37 shows the ^{13}C-NMR spectra of GX0, GX2, and GX5 ENPs prepared in the absence of GY in a 8:2 DMSO-d_6:D_2O mixture. New peaks are only clearly evident at the highest GX level. The following peaks that appear in the GX5 sample (top spectrum of Figure 2.37) are at

59.8, 76.4, 90.3, 91.3, 94.1, 96.6, 98.8, 99.3, 105, and 175 ppm. The origin of these peaks was discussed above. These spectra also prove that the new peaks belong to GX and are not a byproduct from adding water to starch as shown in the GX0 spectrum (bottom spectrum in Figure 2.37).

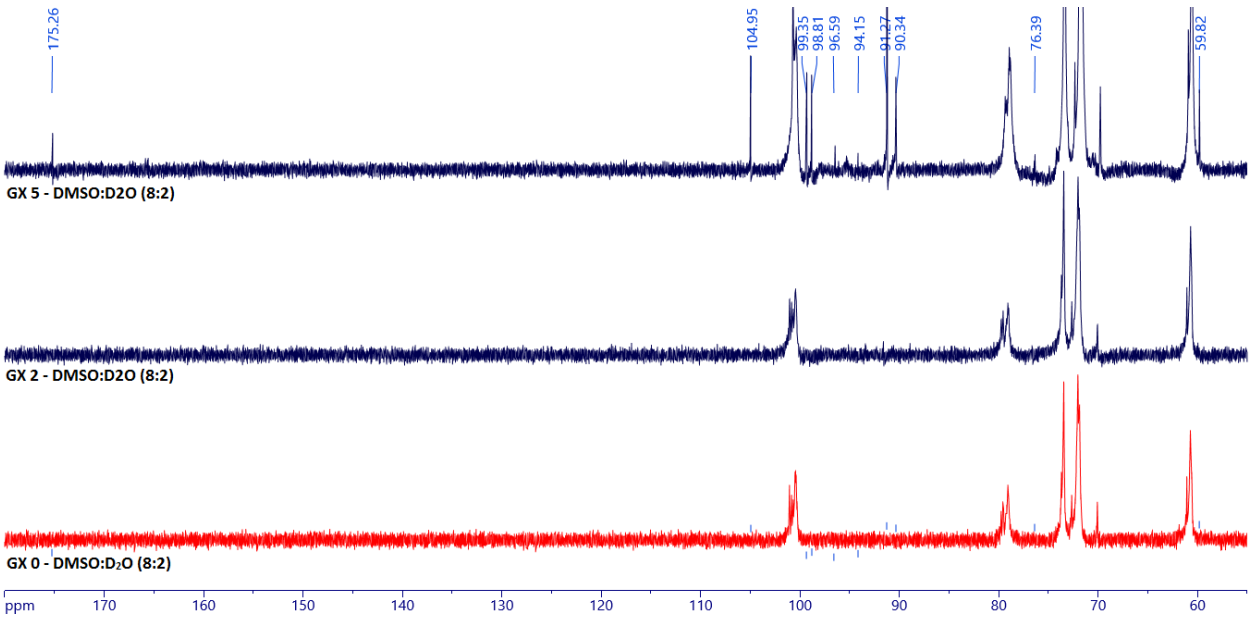

Figure 2.37. ^{13}C-NMR spectra of 4% dispersions of GX0, GX2 and GX5 ENPs prepared in the absence of GY in DMSO-d_6:D_2O mixtures (8:2) (176 MHz).
Top spectrum: GX5GY0 ENPs
Middle spectrum: GX2GY0 ENPs
Bottom spectrum: GX0GY0 ENPs

2.3.5 2-D NMR Studies of ENPs in DMSO-d_6

Are the ENPs prepared in the presence of GY crosslinked when dispersed in DMSO? 2-D NMR studies may shed some light on this issue since such crosslinks might be detectable in an HMBC spectrum. Figures 2.38 and 2.39 show the HMQC and HMBC spectra of the GX2 ENPs in a 4% dispersion in DMSO-d_6. There is a considerable amount of complexity in these spectra, hence

a detailed analysis will be conducted. To reiterate, an HMBC experiment is capable of detecting 2 to 3 bond coupling between a proton and a carbon. Thus if crosslinks exist, a correlation between the GX proton and a starch carbon or a GX carbon and a starch proton, should be observed.

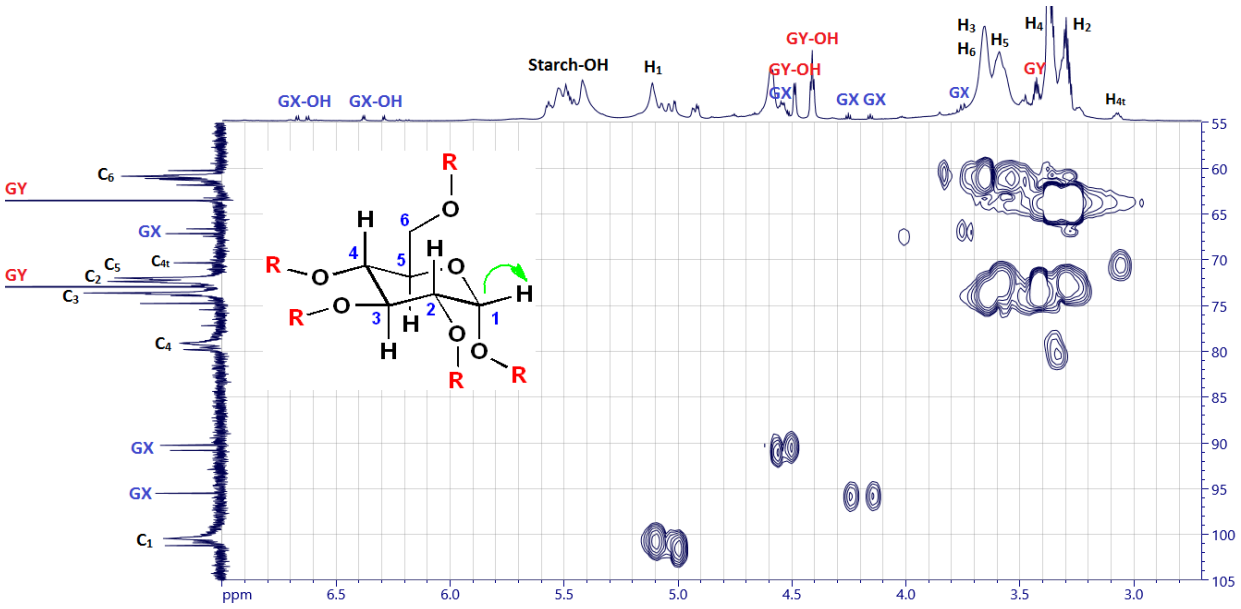

Figure 2.38. HMQC spectrum of a 4% dispersion of GX2 ENPs in DMSO-d_6 (700 MHz).

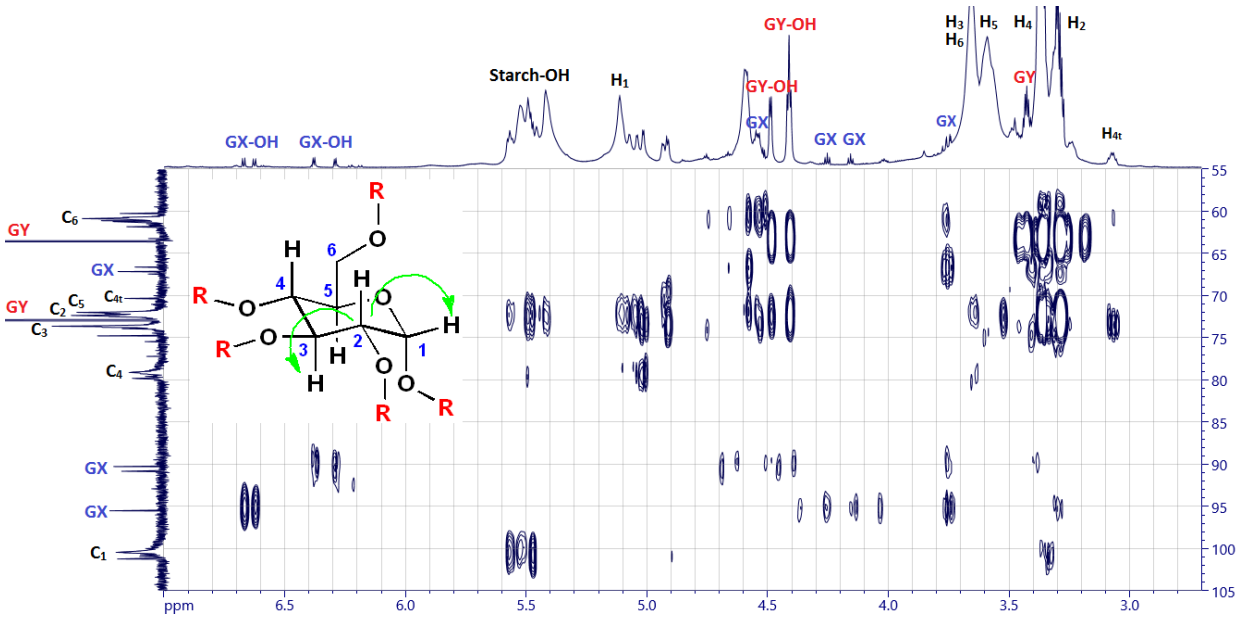

Figure 2.39. HMBC spectrum of a 4% dispersion of GX2 ENPs in DMSO-d_6 (700 MHz).

The peaks that were confidently assigned to the GX carbons appeared at 90.3, 90.8, 95.51, and 95.54 ppm (the peak at 95.5 ppm is actually two peaks). The chemical shift of the carbon at 90.3 ppm suggests that it is not part of a dioxolane (five-membered) ring, whose carbons tend to have slightly higher chemical shifts (100 - 105 ppm).[40] The HMQC spectrum reveals that the protons that appear at 4.48 ppm are bonded to this carbon. These protons do not appear as singlets and are obscured by other peaks. The chemical shift of these protons suggests that these are methine (CH) protons with two oxygens attached to the methine carbon. No other protons are directly attached to this carbon.

The HMBC spectrum shows that the carbon at 90.3 ppm correlates to a proton at 6.36 ppm that appears as a doublet. The fact that this correlation did not appear in the HMQC spectrum and its chemical shift both indicate that this proton is a hydroxyl proton attached to this carbon. This carbon also correlates to protons that appear at 3.75 ppm (multiplet) and 3.37 ppm (obscured by other peaks). A chemical shift of 3.37 ppm suggests that these are methylene protons with one oxygen attached to the methylene carbon. The protons at 3.37 ppm could be associated with GY or the C_4 or C_2 atoms of starch, though it is not possible to tell with absolute certainty. A chemical shift at 3.75 ppm also suggests that these are the protons of a methylene group bound to an oxygen, though a methine proton (CH) cannot be ruled out. The peaks at 3.37 ppm and 3.75 ppm could be diastereotopic methylene protons. We propose that the carbon a 90.3 ppm is part of a general structure shown in Figure 2.40. GX could be involved in crosslinks or forming a GX-GY adduct or glycolic acid, however there is no clear evidence supporting any of these possibilities.

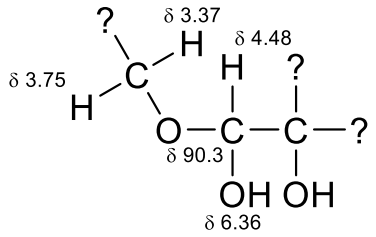

Figure 2.40. Possible partial structure of GX crosslinks or adducts derived from the GX carbon appearing at 90.3 ppm.

It is impossible to tell if the proton(s) at 3.37 ppm correlate to any other carbons due to overlapping peaks. On the other hand, the peak(s) at 3.75 ppm corresponds to proton(s) that appear(s) to correlate to several other carbons, though assigning correlations to this/these proton(s) should be done with caution as there are other small peaks in very close proximity. The HMQC spectrum suggests that that this/these proton(s) may be directly bound to a carbon corresponding to one of the two peaks at 67 ppm. However, the HMBC spectrum suggests a 2-3 bond correlation with one or both carbons having a chemical shift around 67 ppm. One of these carbons is a methylene carbon as determined by the DEPT-135 experiments. It also correlates to one or more of the carbon peaks clustered around 61 ppm, which are all methylene protons and are associated with C_6 of starch or possibly a glycolic acid derivative. Finally this/these proton(s) correlate(s) to one or both of the GX peaks at around 95.5 ppm.

The chemical shift of the carbon at 90.8 ppm suggests that it is not part of a dioxolane (five-membered) ring. The HMQC spectrum reveals that the protons with a chemical shift at 4.54 ppm are bonded to this carbon. These protons appear as a multiplet although the multiplicity cannot be determined with certainty due its proximity to other peaks. Their chemical shift

suggests that this is a methine (CH) proton and not methylene (CH_2) protons, and that they are in close proximity to one or two oxygens. No other protons are directly attached to this carbon.

The HMBC spectrum reveals that the carbon peak at 90.8 ppm correlates to proton peaks at 6.28 ppm that appear as a doublet. The fact that this correlation did not appear in the HMQC spectrum and their chemical shift both indicate that these are hydroxyl protons attached to this carbon. This carbon does not appear to correlate to any other protons in the HMBC spectrum, which is unexpected. If it is part of the GX skeleton, there should be an adjacent carbon with a proton attached to it, which should couple to this carbon unless the protons attached to the two GX carbons/hydrogens are equivalent. This suggests a symmetrical molecule as shown in Figure 2.41.

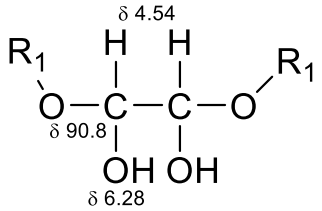

Figure 2.41. Possible partial structure of a GX crosslink or adduct derived from the GX carbon appearing at 90.8 ppm.

The peak at 95.5 ppm is actually two peaks with chemical shifts of 95.52 ppm and 95.54 ppm. The chemical shift of these carbons suggests that they are part or five- (dioxolane) or six-membered (dioxane) ring acetals, as these carbons usually appear further down field (beyond 94 ppm) compared to their acyclic counterparts, though this cannot be said with certainty. They could be diastereomers.

The HMQC spectrum reveals that the protons that appear as triplets at 4.12 ppm and 4.24 ppm are directly bound to one or both of the carbons that appear at 95.52 and 95.54 ppm. These triplets cannot be a result of this carbon being bonded to a methylene group because the adjacent carbon must be a GX carbon which can be bonded to only one proton (each GX carbon can only have one proton directly bound to it). It is more likely that these are overlapping doublets of doublets and so appear as triplets.

The HMBC spectrum reveals that one or both of the carbons at 95.52 and 95.54 ppm correlate to protons at 6.61 ppm (doublet) and 6.67 (doublet) ppm. Their chemical shifts and the fact that these correlations do not appear in the HMQC spectrum indicate that these are hydroxyl protons that are attached to the carbons. It is not possible to determine with certainty if each one of these two carbons has one hydroxyl group attached or if one has two nonequivalent hydroxyl groups attached and the other has no hydroxyl group attached. However the fact that these exhibit almost identical chemical shifts suggests that they both bear hydroxyl groups and that the doublet at 6.61 ppm is associated with one of these carbons and the doublet at 6.67 ppm is associated with the other carbon.

It is particularly interesting to note that the protons at 4.12 ppm and 4.24 ppm do not correlate to any other carbons in the HMBC spectrum. This would suggest that there are no carbons that are 2-3 bond lengths away from these protons, which is difficult to reconcile since at least one of the carbons to which these protons are directly attached correlates to the methylene protons at 3.28 and 3.75 ppm. So one would expect to see a correlation between one or both of the protons at 4.12 and 4.24 ppm and a methylene carbon. This was not observed. It

is possible that HMBC did not pick up this correlation as it is quite common for an HMBC experiment to miss some correlations.

The doublets between 6.25 and 6.65 ppm and the triplets at 4.12 and 4.24 ppm all integrate to the same value indicating that they all correspond to the same number of protons. In order for either one of the protons at 4.12 ppm and 4.22 ppm to appear as a triplet the two doublets that would arise from one of these protons being split by the hydroxyl proton and adjacent C-H proton would have to partially overlap. The most we can tell so far about substituents on the carbons at 95.52 and 95.54 ppm is shown in Figure 2.42.

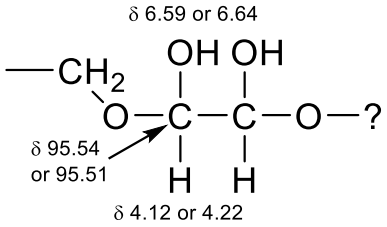

Figure 2.42. Possible partial structure of a GX crosslink or adduct derived from the GX carbon appearing at 90.51 and or 90.54 ppm.

Does any of the above data suggest the presence of GX crosslinks in the ENPs? This is difficult to determine because of the overlapping signals in the spectra. The protons with chemical shifts at 4.12 and 4.24 ppm, which are known to be directly attached to GX carbons (95.52 and 95.54 ppm) do not correlate to any carbons associated with the ENPs, which suggest that these GX carbons are not involved in crosslinks. On the contrary, the protons with chemical shifts at 4.48 and 4.54 ppm, that are directly attached to GX carbons (90.3 and 90.8 ppm) appear to correlate with carbons associated with the ENPs (C_3 and C_6). This means that the protons attached to C_3 and C_6 should correlate to the GX carbon peaks at 90.3 ppm and 90.8 ppm. This

does not appear to be the case. The proton peak at 3.75 ppm, which were associated with GX, correlates to several GX carbons as well as some unidentified carbons with chemical shift around 67 ppm. This proton appears to correlate with the carbon peak C_6 of the ENPs.

It appears that it is not possible to determine from the 2-D NMR studies discussed above whether or not crosslinks exist in ENPs prepared in the presence of GY when dispersed in DMSO. The 1-D ^{13}C-NMR spectra of the GY-free ENPs in pure DMSO-d_6 suggest that if crosslinks exist, they are not detectable by ^{13}C-NMR as no GX peaks are detected in these spectra. If this is indeed the case, then the GX peaks seen in the ^{1}H- and ^{13}C-NMR spectrum of the ENPs prepared with GY in DMSO-d_6 must be due to non-crosslinked GX (monomers, dimers, oligomers, GX-GY adducts or glycolic acid). The sharpness of the peaks that are associated with the GX peaks in these spectra supports this conclusion.

In Section 2.3.4, it was found that the GX could not be detected in the ^{13}C-NMR spectrum of the ENPs that had been prepared in the absence of GY. These results suggest that GX was involved in crosslinks with the ENPs. However, when water was added to these samples, peaks associated with GX appeared indicating that the crosslinks were reversible. We assigned the structure of these GX species based on the chemical shifts found in the literature for GX species in DMSO/D_2O mixtures. To confirm that these assignments were correct, we analyzed a DMSO-d_6/D_2O mixture of the GY-free ENPs by 2-D NMR. The HMQC and HMBC spectra of this mixture are shown in Figures 2.43 and 2.44.

In the ^{13}C-NMR spectra of the ENPs run in DMSO-d_6/D_2O mixtures (for example see Figure 2.35 and 2.37, top spectra), the peaks at 90.3, 98.8, 99.4, and 105.0 ppm were assigned to the

C_1, C_3, C_4 and C_2 carbons of dimer **2.7** (Figure 2.36) respectively**.** These assignments were based on chemical shift values found in the literature.[40] In the ^{1}H-NMR spectra of the ENPs run in DMSO-d_6/D_2O mixtures (for example see Figures 2.33 and 2.34, top spectra), the two doublets at 4.57 and 4.91 ppm were assigned to the H_1 and H_2 protons in dimer **2.7** respectively**.** The peaks of protons H_3 and H_4 in dimer **2.7** appear at 5.05 and 5.07 ppm according to the literature.[40] However, the peaks corresponding to these protons were not observed in the ^{1}H-NMR spectrum as they were obscured by the starch protons. To obtain further support for these assignments, the HMQC and HMBC spectra for a 4% dispersion of GX5GY0 ENPs in a 7:3 DMSO-d_6:D_2O mixture were obtained. These spectra are shown in Figures 2.43 and 2.44.

The HMQC spectrum (Figure 2.43) clearly supports the above assignments for compound **2.7**. The proton appearing as a doublet at 4.57 ppm correlated to the carbon peak at 90.3 ppm. Therefore, this proton is definitely bonded to C_1. The proton appearing as a doublet at 4.91 ppm correlated to the carbon peak at 105 ppm. Therefore, this proton must be bonded to C_2. The two carbon peaks at 98.8 and 99.4 ppm correlated to proton peaks at 5.05 and 5.08 ppm. Therefore, these protons are attached to C_3 and C_4. The large carbon peak at 91.3 ppm correlated to protons that appeared as a singlet at 4.44 ppm, which supports our previous assumption that these protons and carbons are due to monomer **2.1**. There is a strong correlation between the carbon peak at 59 ppm and the proton singlet at 3.93 ppm. This supports our previous identification of these atoms belonging to glycolic acid (GC_{acid}).

The HMBC spectrum (Figure 2.44) illustrates the limitations of HMBC experiments. A correlation should exist between H_1 and C_2 but this was not seen. However, H_2 correlates with C_1 as it should. H_2 should also correlate with C_3 and C_4 but this was not seen. On the other hand, H_3

and H_4 correlate with C_2 as they should. This illustrates very clearly that not all the correlations are always detected in HMBC experiments. In order for these correlations to be detected, the HMBC pulse sequence would have to be adjusted (by trial and error) and this is a lengthy procedure. No correlations exist in the HMBC spectrum between the GX peaks and the starch peaks, suggesting that the crosslinks do not exist or that they cannot be detected by NMR.

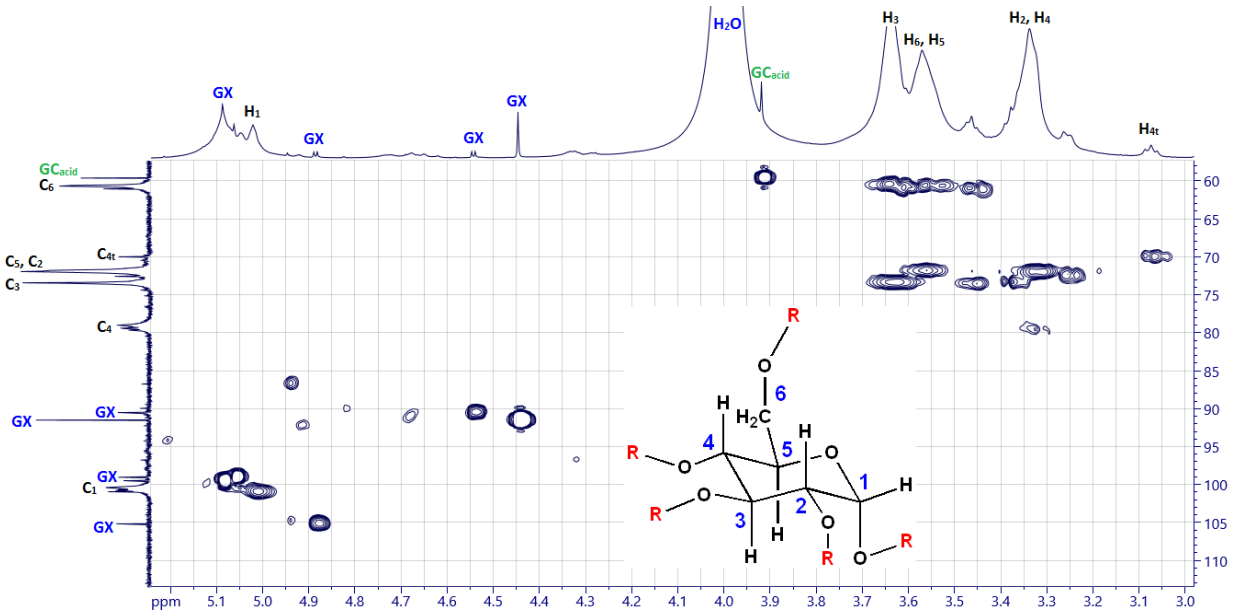

Figure 2.43. The HMQC spectrum of a 4% dispersion of GX5GY0 ENPs in a 7:3 DMSO-d_6:D_2O mixture (700 MHz). GC_{acid} stands for glycolic acid.

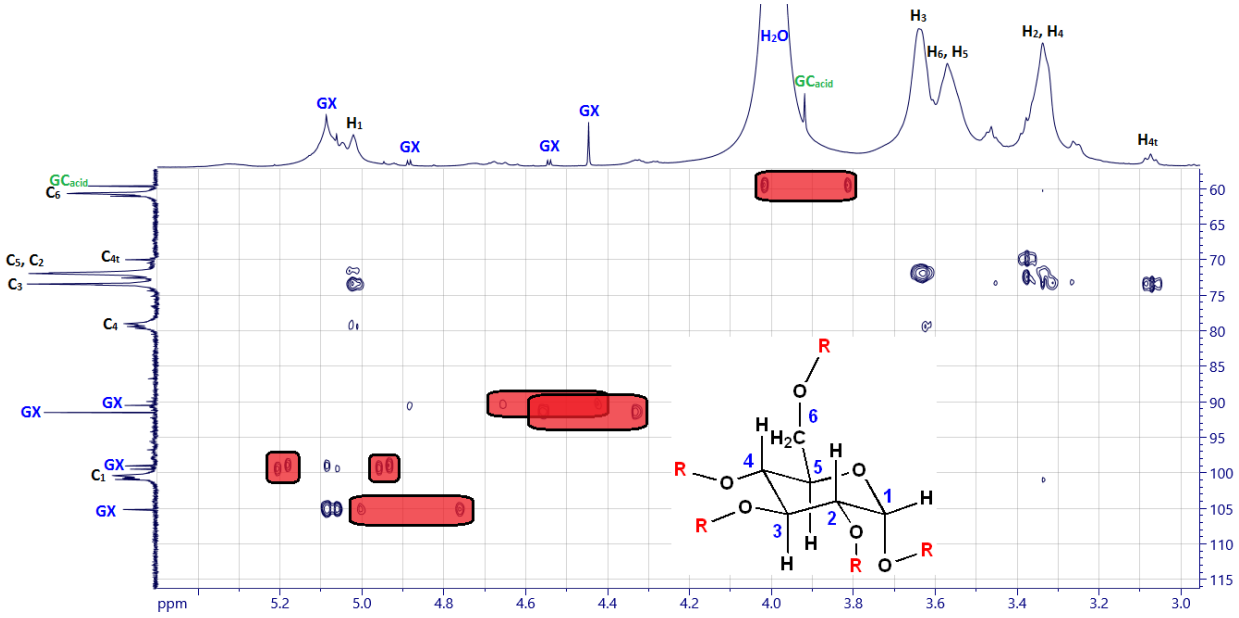

Figure 2.44. The HMBC spectrum of a 4% dispersion of GX5GY0 ENPs in 7:3 DMSO-d_6:D_2O mixture (700 MHz). Artifacts are highlighted in red. GC_{acid} stands for glycolic acid.

2.3.6 Quantification of GX and GY in ENPs Dispersed in Water by ^{1}H-NMR

Our NMR studies of the ENPs dispersed in water suggest that only some or possibly none of the GX is involved in crosslinks when the ENPs are dispersed in water. Since the amount of GX used in the manufacturing of the ENPs was known, we wished to determine if all GX species identified in the ^{1}H-NMR spectra of the ENPs in water was equal to the amount of GX used in the manufacturing of the ENPs. If this was the case, it would be possible to conclude that the ENPs are not crosslinked when they are dispersed in water since all of the GX is unbound. To answer this question, the amount of GX present in the water-dispersed ENPs needed to be quantified by ^{1}H-NMR.

We initially thought that because the GX proton is hidden under the water peak in the ^{1}H-NMR, GX quantification would be impossible. The alternative approach was to use ^{13}C-NMR for

quantification. However, the signal-to-noise ratio in ^{13}C-NMR is significantly lower compared to ^{1}H-NMR experiments and the required relaxation times are longer making quantification by ^{13}C-NMR imprecise and time consuming. Nevertheless, the problem of the GX proton being hidden under the water peak was overcome by heating the samples to 60 °C during the ^{1}H-NMR experiments. This idea was inspired by a study by Zhang et al. who demonstrated that the GX peak in the ^{1}H-NMR spectrum of aqueous solutions of GX-crosslinked poly(vinyl alcohol) could be observed if the NMR spectra were obtained at 60 ^{o}C.[51] The elevated temperature shifted the GX peak downfield making it visible and accessible for integration. Figure 2.45 shows the ^{1}H-NMR spectra for the ENPs containing varying amounts of GX at 60 °C. The growth of the GX peak at 5.07 ppm is clearly visible.

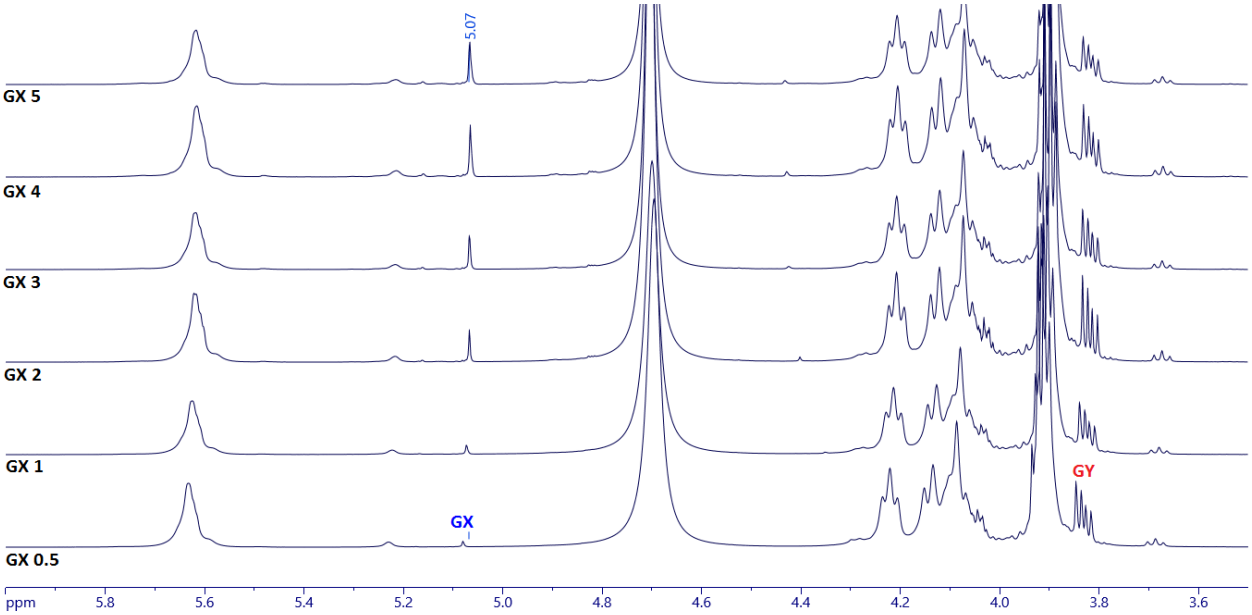

Figure 2.45. ^{1}H-NMR spectra of 10% dispersions of GX(0.5 – 5) ENPs in D_2O at 60 °C (600 MHz).

An internal standard needed to be added to the NMR tube for quantification. The internal standard needed to meet the following criteria: it has to be soluble in the same solution (i.e. have

similar solubility properties as the ENPs), have an NMR signal that does not interfere with any of the starch peaks (otherwise integration would be inaccurate), have a high boiling point to avoid any volatility issues, and lastly be unreactive with starch. Ethanol was chosen as internal standard because the CH_3 peak would not overlap any of the starch peaks. Ethanol has a boiling point of 78 °C, high enough to prevent its evaporation during the NMR experiment. Lastly, the solubility of ethanol in water is comparable to that of the ENPs.

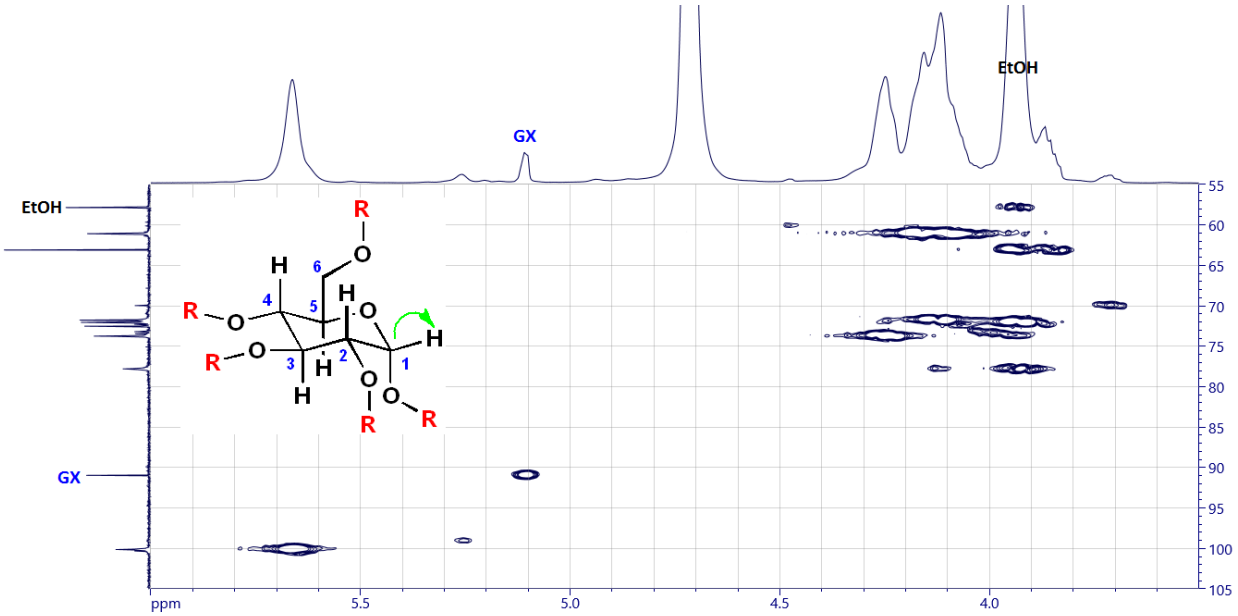

Figure 2.46. The HMQC spectrum of a 10% dispersion of GX5GY0 ENPs in D_2O at 60 °C containing EtOH (600 MHz).

Figures 2.46 and 2.47 show the HMQC and HMBC spectra for GX5 ENPs containing EtOH at 60 °C. The HMQC spectrum provided further evidence that the peak at 5.07 ppm in the ^{1}H-NMR spectrum is indeed due to the GX protons because these GX protons correlate with the GX carbon peak at 91 ppm. The overlap between the CH_2 group of ethanol and the starch peaks was not an issue because the only peak used for integration was the methyl protons of ethanol and the GX proton. The HMBC spectrum provided evidence that the internal standard (ethanol) is not

reacting with the ENPs. It also showed that GX was not correlating with any of the starch carbons, which further supports our claim that in water, GX observed in the 1-D ^{1}H- and ^{13}C- NMR spectra of the ENPs is not involved in crosslinks.

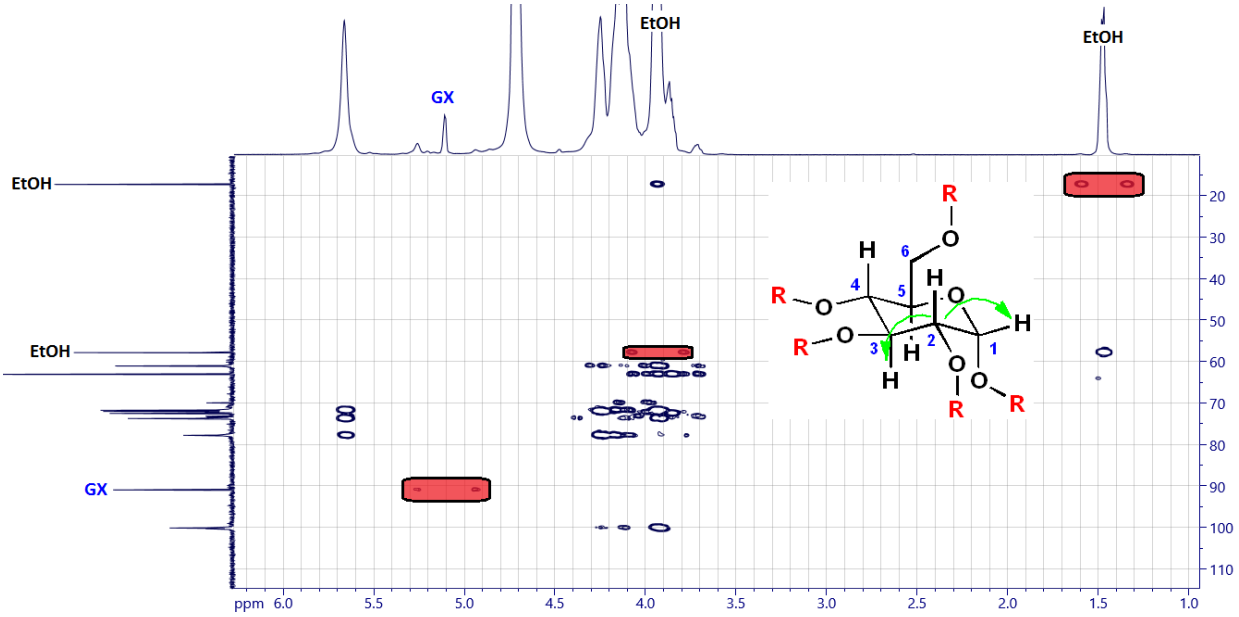

Figure 2.47. The HMBC spectrum of a 10% dispersion of GX5GY0 ENPs in D_2O at 60 °C containing EtOH (600 MHz). Artifacts are highlighted in red.

GX quantification was performed on three sets of samples: GX(0.5 – 5) ENPs prepared in the presence of GY, GX(0.5 – 5) ENPs prepared in the absence of GY, and a set of blind samples supplied by EcoSynthetix™ to validate and test the reliability of the method. The samples were prepared by dispersing a known quantity of the ENPs in D_2O, followed by the addition of a known amount of EtOH via a glass syringe. The samples were placed in a heating block set to 60 °C for a minimum of 30 minutes and then placed in a 600 MHz NMR spectrometer equipped with a probe that was pre-equilibrated to 60 °C. The sample was left to equilibrate in the probe for 25 minutes before a spectrum was acquired. Quantification of GX was accomplished by comparing the integration of the GX peak to the integration of the peak corresponding to the CH_3 group of

ethanol. Since the exact molar amount of ethanol added to the sample was known, the amount of GX could be calculated using these integration values.

Figure 2.48 shows that there is a linear relationship between the calculated amount of GX versus the mass of ENPs. Surprisingly, the lines do not go through the origin. One explanation for this is that some of the ethanol evaporated onto the sides and cap of the NMR tubes, which would be difficult to detect due to the small quantity of ethanol used. The samples were not incubated in the heating block for the same amount of time. If the lower GX samples were left in the heating block for longer than the higher GX samples, then an overestimation of the amount of GX would occur for the low GX samples. Unfortunately, we did not record how long each sample was left in the heating block. The lines are expected to cross the origin, because at 0 g of ENPs, there should be 0 g of GX, as demonstrated in Figure 2.51. It is highly recommended that this experiment be repeated because the lines are expected to cross the origin and there is no plausible explanation for it not to cross the origin.

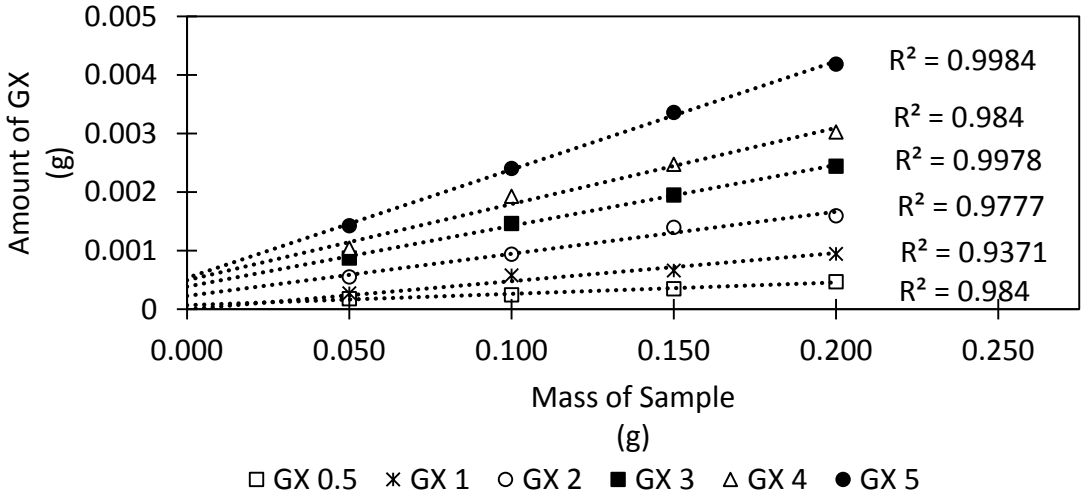

Figure 2.48. Amount of GX in GX(0 – 5) ENPs (GY-present) as determined by ^{1}H-NMR versus the mass of the GX(0 – 5) ENPs (GY-present).

Figure 2.49 compares the amount of GX calculated from the NMR studies mentioned above to the amount of GX that was used in the manufacturing of the ENPs. In these calculations, the amount of GX put into the extruder was converted into a mass amount (expected amount) and compared to the amount that was determined by NMR (calculated amount). It was observed that the calculated amount is approximately 40% less than what was used for their manufacturing. Some of this difference can be accounted for by the moisture content of the ENPs. EcoSynthetix™ has determined that the ENPs contain approximately 8-12% water (by weight). All following graphs have the moisture in the starch corrected for, however there would still be a significant amount of GX that could not be accounted for. The fact that the amount of GX determined by NMR cannot account for all of the GX that was used in the manufacturing of the ENPs process raises concerns. The "missing" GX may be due to any or a combination of the following causes: (1) some of the GX molecules crosslink the polymer and the crosslinks are undetectable by NMR due to broad peaks; (2) some of the GX is reacting with the GY to form GX-GY adducts or, (3) the remainder of the GX is decomposing into compounds such as glycolic acid. The first possibility– that some of the crosslinks might not be reversible is entirely plausible. Perhaps only hemiacetal crosslinks are rapidly reversible while full acetal crosslinks reverse much more slowly. The second option is likely because it was shown that with higher GX amounts, new species of GY are introduced, leading us to believe that GX-GY adducts are formed. However, if such large amounts of GX-GY adducts were formed in water, these adducts should be readily detected in our ^{1}H-NMR spectra in D_2O but they were not observed. The third possibility is definitely occurring though to what extent has not been determined.

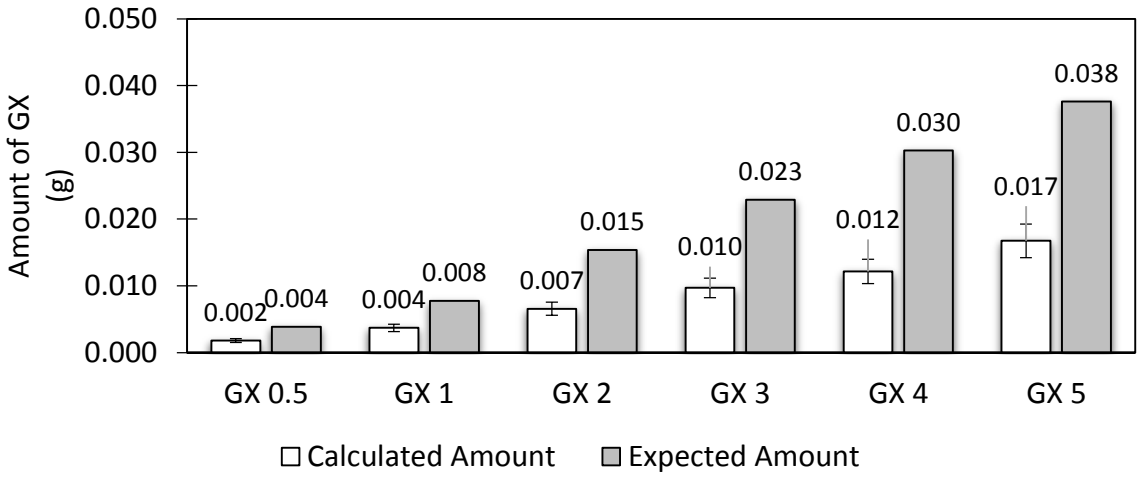

Figure 2.49. A comparison of the amount of GX in GX(0.5 – 5) ENPs, as determined by ^{1}H-NMR in 10% dispersions in D_2O, to the amount of GX used for manufacturing the GX(0.5 – 5) ENPs.

To provide further evidence that the missing GX is not due to the formation of GX-GY adducts, we also determined the amount of GX in D_2O-dispersed GX(0 – 5), GY-free ENPs by ^{1}H-NMR. The results are shown in Figure 2.50. Similarly to the samples prepared with GY, approximately 40% of the GX is missing which means that the missing GX is not due to the formation of GX-GY adducts. The only two options remaining to explain the missing GX are: (1) crosslinking of the polymer and/or (2) GX decomposition.

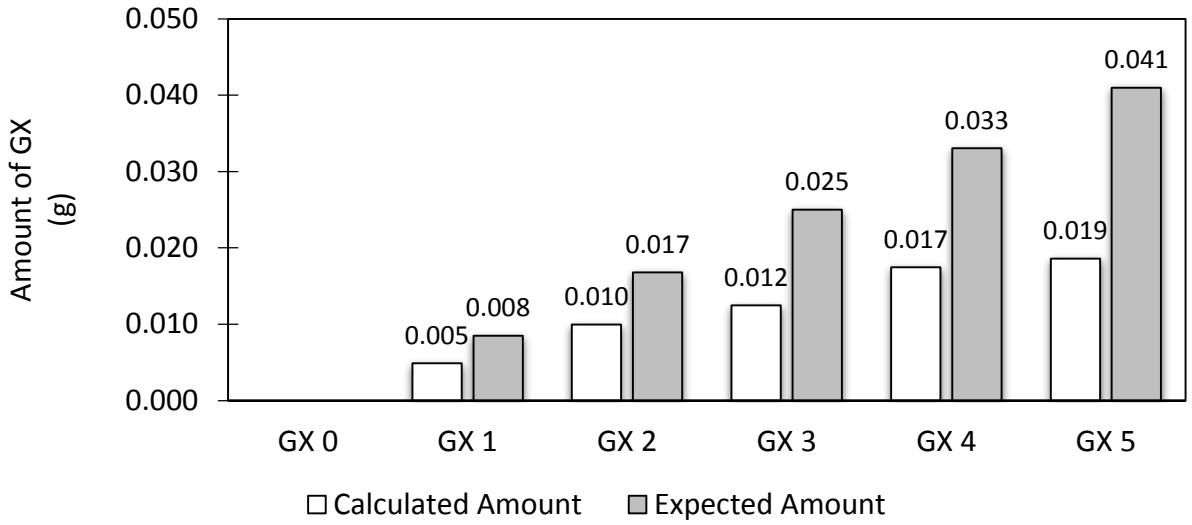

Figure 2.50. A comparison of the amount of GX in GX(0 – 5) GY-absent ENPs, as determined by ^{1}H-NMR in 10 % dispersions in D_2O, to the amount of GX used for manufacturing the GX(0 – 5) ENPs

To determine that no personal bias was affecting the outcome of these experiments, EcoSynthetix™ provided blind ENP samples to test the precision of our method. We had no prior knowledge of the amount of GX or GY used in the preparation of these samples. Figure 2.51 shows the plot of the calculated amount of GX in 10% dispersions in D_2O versus the amount of GX used in the manufacturing of the blind ENP samples. Each experiment was performed in triplicate. The precision was good as evidenced by the good R^2 values obtained. However, these studies do not test for the accuracy of the method. In contrast to the data shown in Figure 2.48, the lines in Figure 2.52 do pass through the origin as expected. We do not have an explanation for this difference.

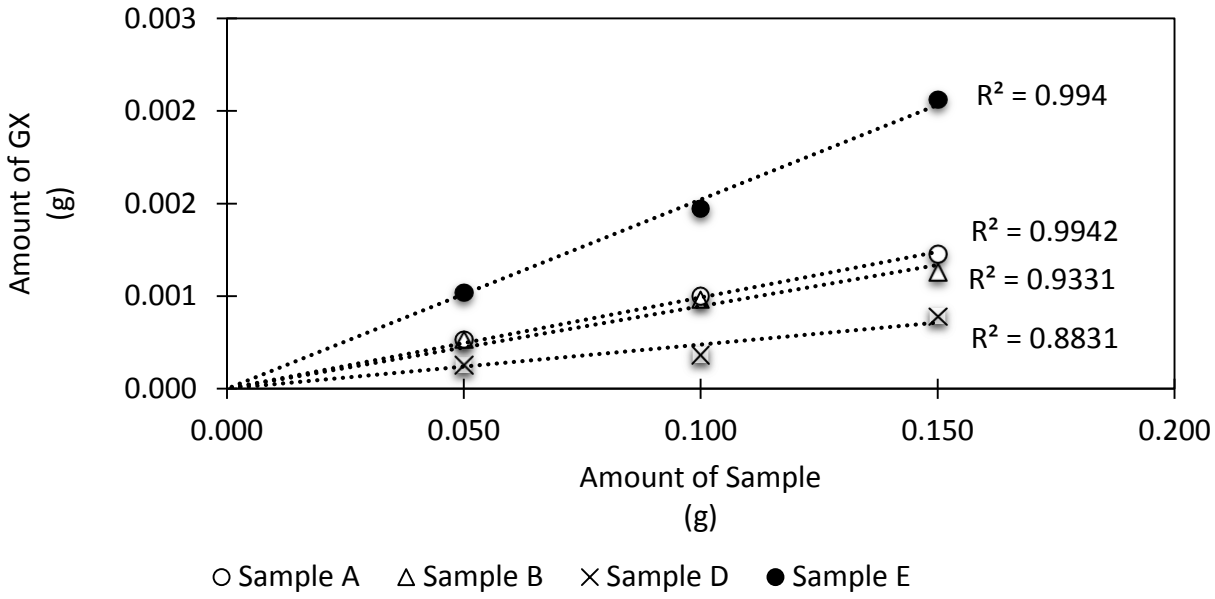

Figure 2.51. The amount of GX in blind ENP samples as determined by ^{1}H-NMR in 10 % dispersions in D_2O, versus the mass of the blind ENP samples.

Figure 2.52 compares the amount of GX in D_2O-dispersed blind ENP samples as determined by ^{1}H-NMR, to the amount of GX that was used in the preparation of the blind ENP samples. It was observed that the calculated amount is approximately 40% less than what was used for their manufacturing. The exception to this was sample D, for which 80% of the GX was accounted for. This anomaly is probably due to inaccuracies that are inherent when integrating small peaks. In this sample only a very small amount of GX had been used in its manufacture and so the GX peak was very small. Some, but certainly not all, of the difference between the calculated amount of GX in the ENPs and the amount of GX used in the manufacturing of the ENPs can be accounted for if the water content in the ENPs was taken into account during our calculations.

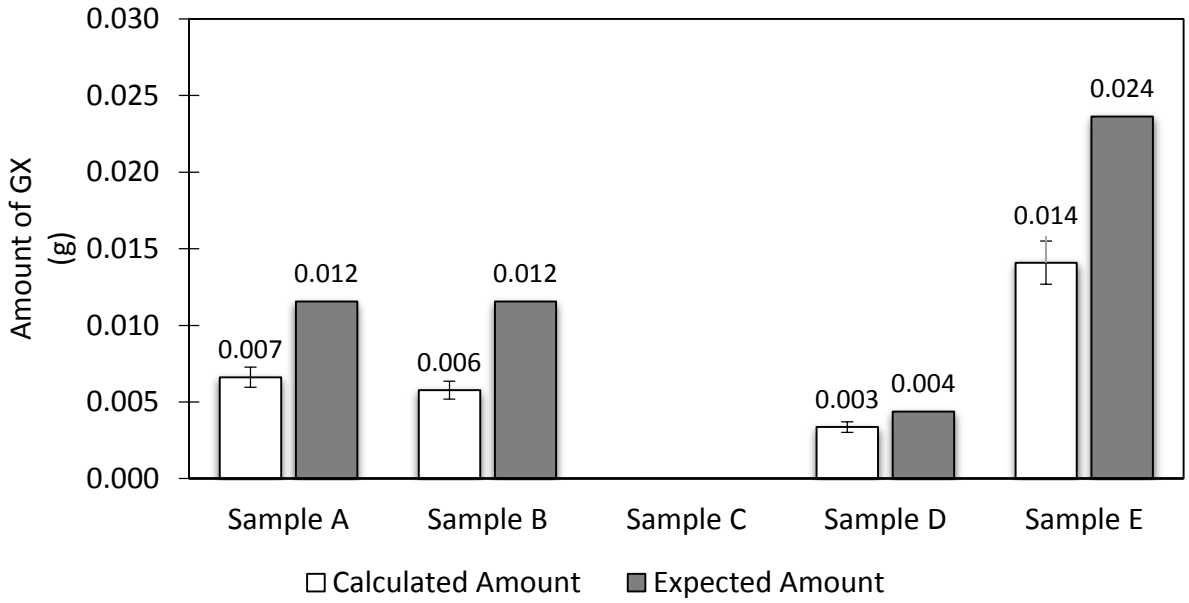

Figure 2.52. A comparison of the amount of GX in blind ENP samples as determined by ^{1}H-NMR in 10 % dispersion in D_2O, to the amount of GX used for manufacturing of the blind samples.

The amount of GY in D_2O-dispersed GX(0 – 5) ENPs was also determined using the same ^{1}H-NMR technique described above for the GX quantifications. These calculated amounts of GY were compared to the amount of GY that was used in the preparation of the ENPs. It was found that all of the GY can be accounted for, suggesting that the missing GX is not due to GX-GY adducts. The calculated amount of GY was higher than the expected amount for two reasons. Firstly, the GY peaks that were integrated (the doublet of doublets that appears between 3.4 - 3.45 ppm – see Figure 2.3 – which correspond to two protons) overlaps with some of the ENP peaks. As a result, these peaks integrated to more than what they should have. Due to the overlapping peaks with the ENPs, NMR is not a good method for accurately determining the amount of GY present. Secondly, the water content of the ENPs was not corrected for when the amount of GX or GY was calculated. If the water content of the ENPs were corrected in our

calculations, then the amounts of GY calculated would be closer to the amounts of GY used in the manufacturing of the ENPs.

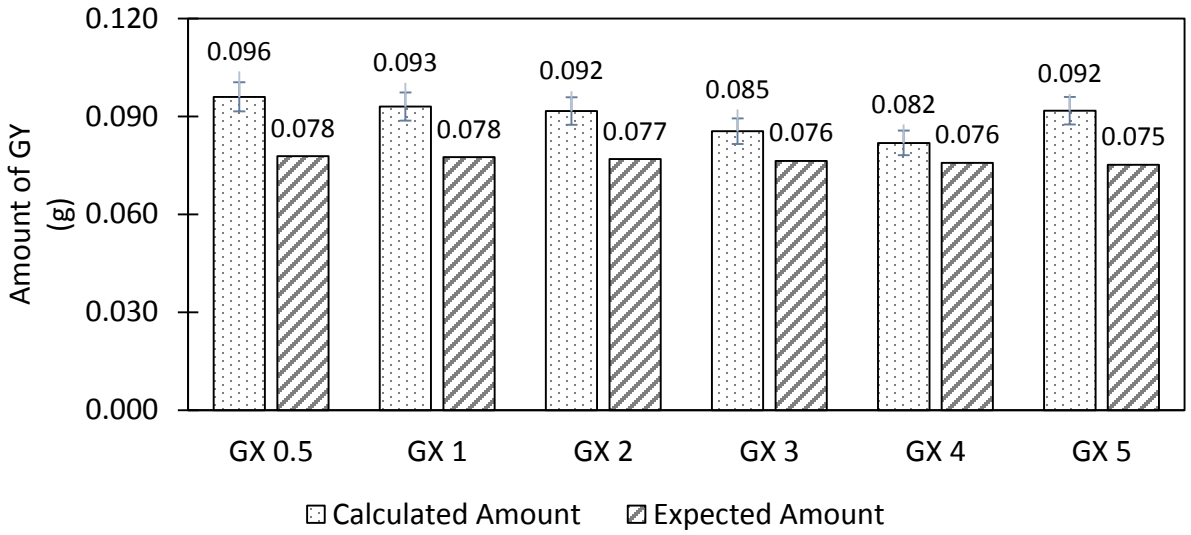

Figure 2.53. A comparison of the amount of GY calculated by ^{1}H-NMR in GX(0.5 – 5) ENPs to the amount of GY used for manufacturing of the GX(0.5 – 5) ENPs.

Figure 2.54 compares the amount of GY in the D_2O-dispersed blind ENP samples as determined by ^{1}H-NMR to the amount of GY that was used in the preparation of the blind ENP samples. The calculated amount of GY in samples A and B was 29-36% higher than the amount that used in their preparation. The amount of GY used in the preparation of these two samples was substantially lower than the amount of GY used in the manufacture of all the other ENPs studied in this chapter. Consequently, the GY peaks that were integrated (the doublet of doublets that appear between 3.4 - 3.45 ppm) to determine the GY content were substantially smaller in samples A and B as compared to the GY peaks in the other ENPs studied in this chapter. It was mentioned previously that the GY peaks between 3.4 and 3.45 ppm overlap slightly with some of the ENP peaks. Hence, due to their relatively small size, the integration of the GY peaks

in samples A and B was less accurate in comparison to the other (higher GY) samples due to the overlap with some of the ENP peaks. In other words, the GY peaks in samples A and B integrated to significantly more than what they should have as a result of the overlap with the ENP peaks.

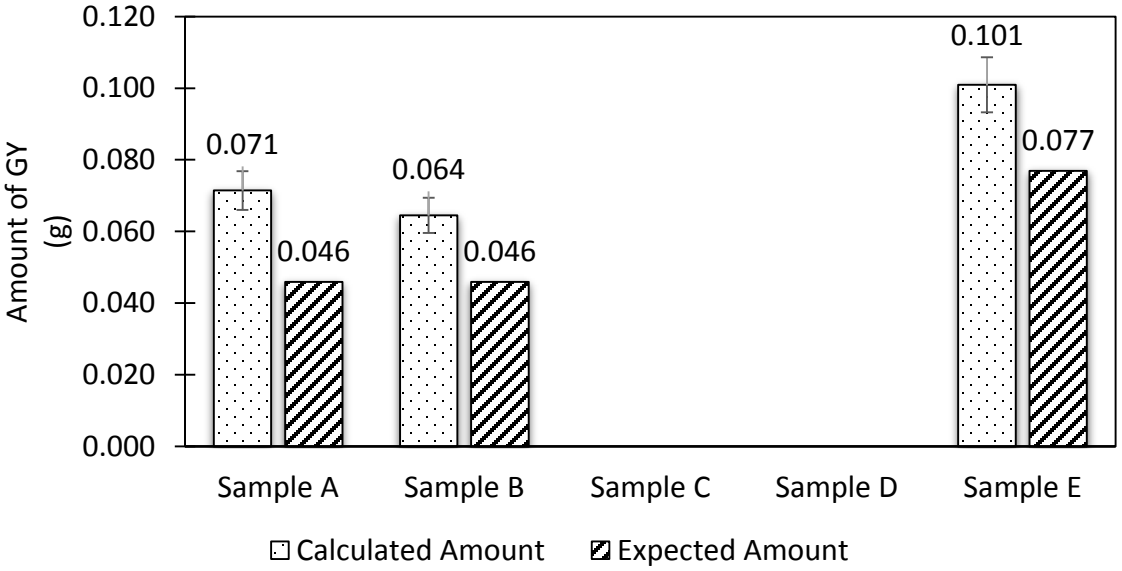

Figure 2.54. A comparison of the amount of GY in blind ENP samples as determined by ^{1}H-NMR in 10 % dispersions in D_2O to the amount used for manufacturing the blind samples.

2.3.7 Degradation of the ENPs using α-Amylase

As already stated above, one possible explanation for the "missing" GX in aqueous dispersions of the ENPs is that some of the GX is still involved in crosslinks with the ENPs. We reasoned that if the ENPs could be broken down using amylase, then any crosslinked GX would be released into the surrounding medium and be detectable by ^{1}H-NMR or ^{13}C-NMR as free GX. If the GX was released into the medium after amylase treatment then the GX peak should increase in intensity/area in the ^{1}H- and ^{13}C-NMR spectra.

The ENPs were prepared as a 10% dispersion in water containing 10% amylase by weight. The ENPs were digested by the enzyme for 24 h at room temperature and then lyophilized to retrieve a solid powder. The solid powder was then dispersed in D_2O for NMR analysis. Unfortunately, GX strongly inhibits amylase activity. The ^{1}H- and ^{13}C-NMR spectra of GX0 ENPs treated with amylase (Figures 2.55 and 2.56, second spectra from bottom) were significantly different from the ^{1}H- and ^{13}C-NMR spectra of GX2 ENPs (bottom spectra in Figures 2.55 and 2.56) that were not treated with amylase which indicated that the GX0 ENPs were broken down by amylase. The ^{1}H- and ^{13}C-NMR spectra of the GX1-5 ENPs after being subjected to amylase were almost identical to the ^{1}H- and ^{13}C-NMR spectra of the GX2 ENPs that had not been subjected to amylase indicating that GX inhibits the enzyme.

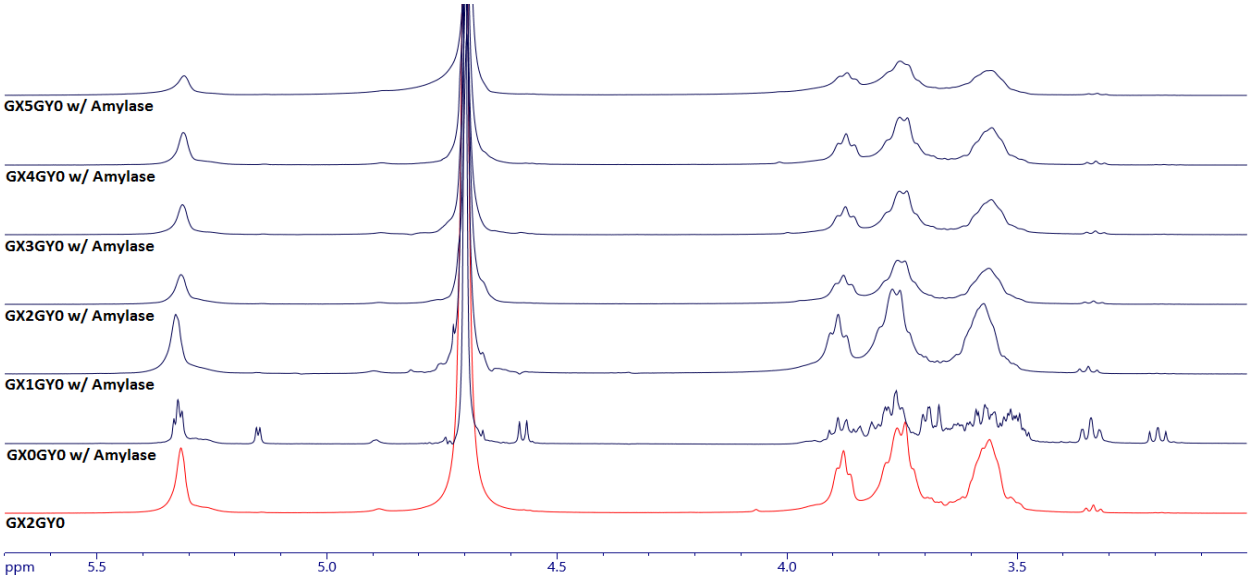

Figure 2.55. ^{1}H-NMR spectra of 10% dispersions of GX(0 - 5)GY0 ENPs in D_2O (600 MHz) after treatment with α-amylase. The ENPs in the bottom spectrum were not treated with amylase.

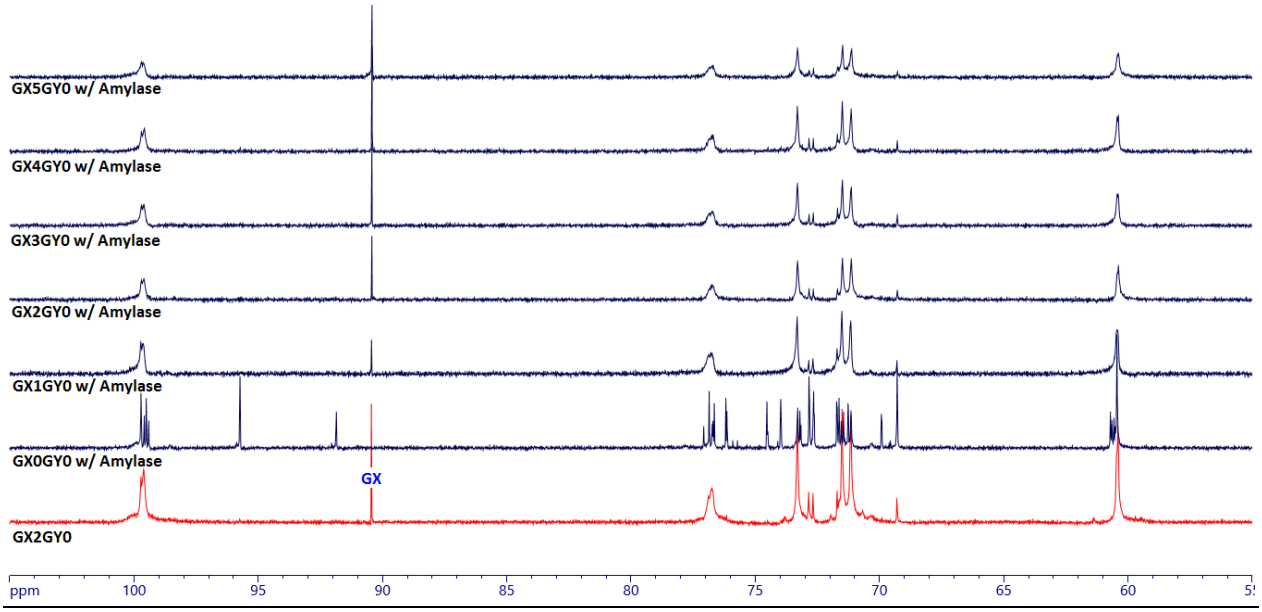

Figure 2.56. ^{13}C-NMR spectra of 10% dispersions of GX(0 – 5)GY0 ENPs in D_2O (150 MHz) after treatment with α-amylase. The ENPs in the bottom spectrum were not treated with amylase.

2.4 Summary and Future Work

A combination of NMR techniques were utilized to evaluate the nature of the crosslinks in ENPs. Free GX was readily detected by NMR when the ENPs were dispersed in water. This suggests that the crosslinks in the ENPs are reversible in water. The GX content of the ENPs dispersed in D_2O was quantified using ^{1}H-NMR. Only approximately half of the GX that was used in the manufacture of the ENPs could be accounted for by ^{1}H-NMR. It is possible that only some of the GX was released when dispersed in water and that the rest was involved in crosslinks. Future studies will focus on developing a method for determining how much GX, if any, is still involved in crosslinks when the ENPs are dispersed in water. Performing the amylase studies in the presence of an excess amount of bisulfite might enable us to do this. Bisulfite rapidly forms a stable adduct with GX in water and this adduct appears as a singlet at 4.9 ppm in the ^{1}H-NMR

spectrum and will not be masked by the water peak. From our studies, we know that GX inhibits amylase. However, if the bisulfite sequesters the GX before it inhibits the amylase then any GX released upon amylase degradation would be detected by an increase in area of the peak at 4.9 ppm. Such studies are currently in progress in the Taylor group. The GX quantification studies will be repeated using a different internal standard such as sodium acetate, since ethanol gave inconsistent results in that the lines in Figure 2.48 did not pass through the origin while the lines in Figure 2.15 did pass through the origin as expected. This difference may have been due to the loss of ethanol by evaporation during the experiment.

We provided evidence that when the ENPs are prepared in the presence of GY and are dispersed in DMSO, some or possibly all of the GX is sequestered as GX-GY adducts. Our studies indicated that for ENPs that were prepared in the absence of GY, most or all of the GX is involved in crosslinks but these crosslinks can be completely or partially reversed when water is added to the dispersion.

2.5 Experimental

2.5.1 NMR

All the ENP samples were donated by EcoSynthetix Inc. (Burlington, Ontario). Deuterium oxide (D_2O) and deuterated dimethylsulfoxide (DMSO-d_6) were purchased from Sigma Aldrich Chemical Co. (Milwaukee, Wisc., USA). ^{1}H- and ^{13}C-NMR spectra were recorded on Bruker 500, 600 or 700 MHz NMR machines. The 700 MHz instrument utilized a CryoProbe™, the 600 MHz instrument utilized a Quattro Resonance X1+X2+X3 Decoupling Inverse probe (QNP) and the 500 MHz instrument utilized a Triple Resonance X1+X2 Nucleus Decoupling Inverse Probe (TXI). ^{1}H-

and ^{13}C-NMR chemical shifts of spectra run in DMSO-d_6 or DMSO-d_6/D_2O were referenced to the DMSO solvent residual peak at 2.50 ppm and 39.5 ppm respectively. ^{1}H-NMR chemical shifts of spectra run in D_2O were referenced to the solvent residual peak at 4.80 ppm. ^{13}C-NMR chemical shifts of spectra run in D_2O were referenced to 4,4-dimethyl-4-silapentane-1-sulfonic acid (DSS) peak at 0.0 ppm. α-Amylase from porcine pancreas was provided by Dr. Liu in dry powder and was purchased from Sigma Aldrich (Milwaukee, Wisc., USA).

2.5.2 Dialysis and Precipitation of ENPs

All the dialyzes were performed by dispersing the approximately 1.5 g of sample in 15.0 mL of water (10% concentration) and dialyzed against deionized and distilled water (1500 mL) using a Spectra/Por® 1000 MWCO membrane. The water was changed three times every 3 hours (3×10^2 fold dilution). The dialyzed dispersion was lyophilized to give the ENPs as a dry powder.

Precipitation of the ENPs was performed by dispersing 32 g of ENPs in 1 L of DMSO (4% concentration). The dispersion was allowed to stir under gentle heating ($\leq$ 50 °C) for 24 h. The dispersion was added drop-wise to methanol (1 L) over 60 min. The precipitate was collected by suction filtration and dried under vacuum in a round bottom flask for 24 h.

2.5.3 Quantification of GX using ^{1}H-NMR

Quantification studies using ^{1}H-NMR were performed on the Bruker Advance 600 MHz instrument at 60 °C (333.15 K) equipped with a TXI probe. D_1 was set to 5 s and number of scans to 64. Ethanol was added as an internal standard via a glass syringe to an NMR tube containing a precisely known amount of ENP dispersed in D_2O. The samples were allowed 20 minutes to equilibrate with the heated probe before acquisition.

2.5.4 α-Amylase Degradation of ENPs

A solution comprised of 1 g of α-amylase in 1 mL of water was made. Then 1 g of ENPs were dispersed in 1 mL of the amylase solution. The samples were allowed to stand at room temperature for 24 hours and then lyophilized. The resulting dry powder was collected and dispersed in D_2O for NMR analysis using the Bruker Advance 500 MHz instrument.

Chapter 3

Dry Cationic Modification of ENPs

3.1 Introduction

As stated in Chapter 1, cationic starches have been used extensively in the papermaking industry and have been examined as potential candidates to replace synthetic flocculants or sorbents in industrial applications. Reagents such as GTAC or CHPTMA have been widely used for preparing cationic starches.[21,31] Traditionally these modifications have been done in aqueous solution. For economic reasons given in Section 1.2.5, it is now common in the industry to perform this reaction under dry conditions (using a minimal amount of solvent). Although the DS obtained using the dry process are lower than the DS obtained when the reactions are performed in solution, the DS obtained in dry reactions are sufficient for the needs of the paper making industry where cationic starches with DS in the range of 0.02 - 0.15 are used.

3.2 Objectives

The objective of the work described in this chapter is to develop dry reaction conditions for the cationic modification of ENPs. Cationically modified ENPs may prove to be superior to cationic starches as additives in the paper making industry by acting as stronger flocculants for calcium carbonate fillers.[51] In wastewater treatment, cationic starch flocculants cannot withstand the high mechanical forces encountered during the flocculation process as compared to synthetic flocculants. If cationically modified ENPs exhibit stronger flocculation behaviour and

physical strength as compared to cationic starch, then they could be used by the flocculant industry.

3.3 Results and Discussion

3.3.1 Determination of Anhydroglucose units (AGUs)

Before attempting any modifications to the ENPs, the number of anhydroglucose units (AGUs) in the ENPs was determined using ^{1}H-NMR. More specifically, the integration of the peak corresponding to the anomeric protons in the ^{1}H-NMR spectrum of the ENPs was compared to the integration of the methyl peak of ethanol which was used as an internal standard. The anomeric proton was used because it is free from any interference from other peaks and because each AGU unit contains one anomeric proton. Figure 3.1 shows the calculated amount of AGUs and the expected amount of AGUs in GX2GY0 ENPs. The slight differences in the calculated amount and expected amount can be attributed to the fact that the starch samples absorb moisture which leads to the 8-10% difference observed in Figure 3.1.

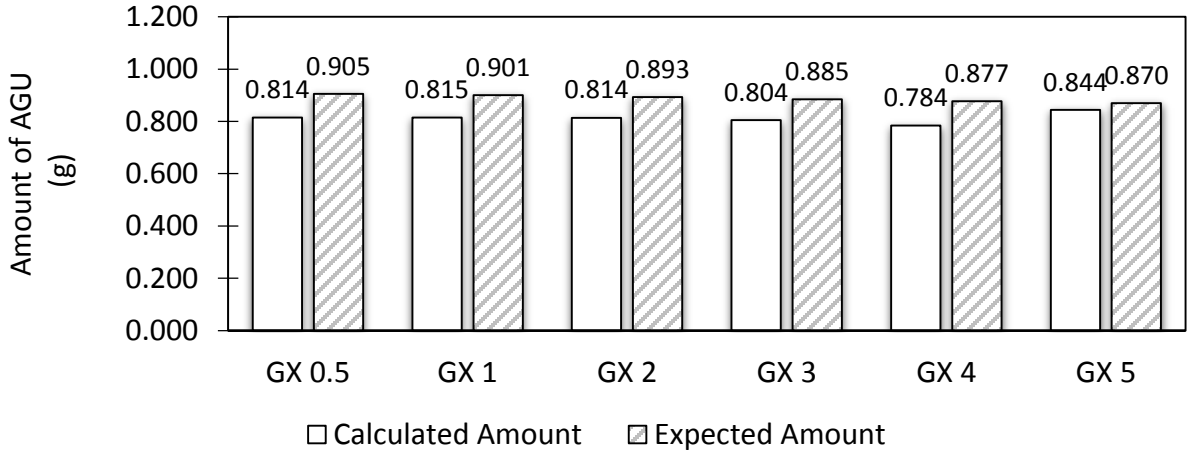

Figure 3.1. The calculated and expected amount of AGUs in ENPs that were prepared with varying amounts of GX.

3.3.2 NMR Spectra of Cationically Modified ENPs and Calculating DS

The DS for all the reactions performed in this study was determined by ^{1}H-NMR.[55] The ^{1}H-NMR spectrum of a D_2O solution of cationically modified GX2GY0 ENPs prepared in our lab is shown in Figure 3.2. The DS was calculated from the integration ratios of the methyl protons (H_{10}) and anomeric proton (H_1). Because there are nine methyl protons and one anomeric proton, the DS was calculated by dividing the integrated of the methyl group peak by 9. For example in the spectrum shown in Figure 3.2, setting the integration of the anomeric proton equal to one yields an integral for the methyl groups equal to 0.55. Hence the DS would equal 0.55/9 = 0.061. The protons on C_7, C_8, and C_9 are hidden under the starch protons and are not visible in the spectrum.

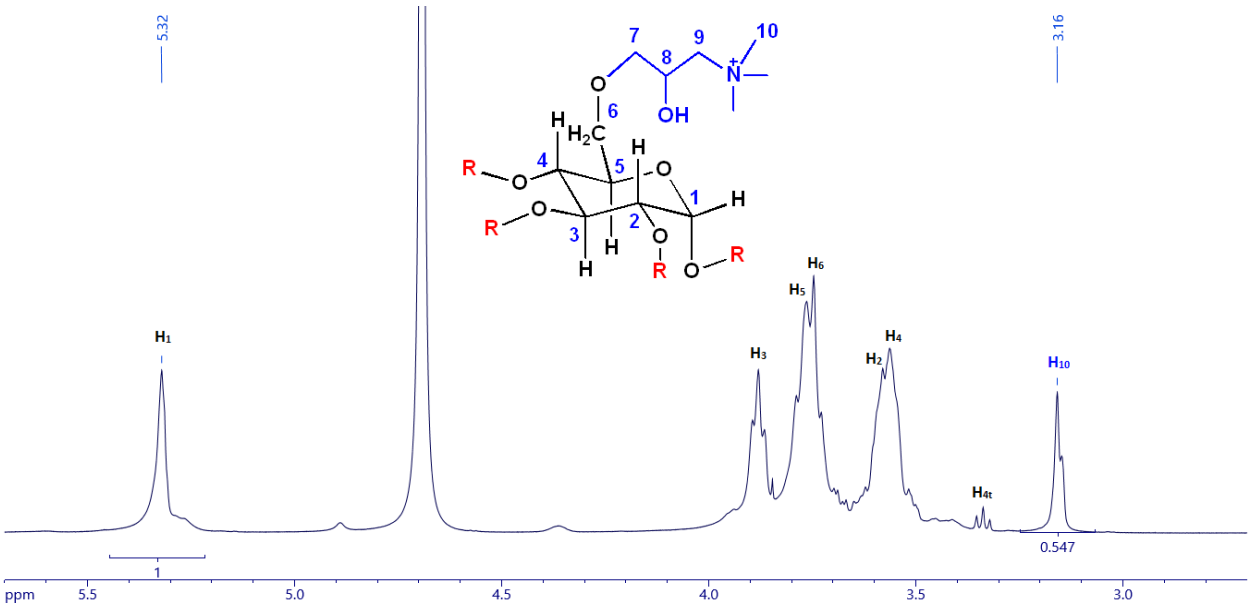

Figure 3.2. ^{1}H-NMR spectrum of a 10% dispersion of cationically modified GX2GY0 ENPs in D_2O (600 MHz).

Figure 3.3 shows the ^{13}C-NMR spectrum of cationically modified GX2GY0 ENPs in a 10% dispersion in D_2O. Figure 3.4 compares the ^{13}C-NMR spectrum of unmodified GX2GY0 ENPs in a

10% dispersion in D_2O to the ^{13}C-NMR spectrum of cationically modified ENPs in a 10% dispersion in D_2O. The differences between these spectra can be attributed to the introduction of the cationic group and the fact that the modified ENPs were subjected to dialysis after the reaction to remove unreacted or decomposed reagent. The peaks due to GX are absent from the spectrum of the cationically modified ENPs as the GX was removed in the dialysis step. The peak corresponding to the methyl groups (C_{10}) appears at 54.2 ppm. Peaks corresponding to the other carbons of the glycidyltrimethylammonium moiety (carbons 7, 8, and 9) are more difficult to identify because these peaks are small and broad (peaks appearing at 65 and 67 ppm corresponding to C_8 and C_9 respectively) or because they overlap with peaks from the ENPs.

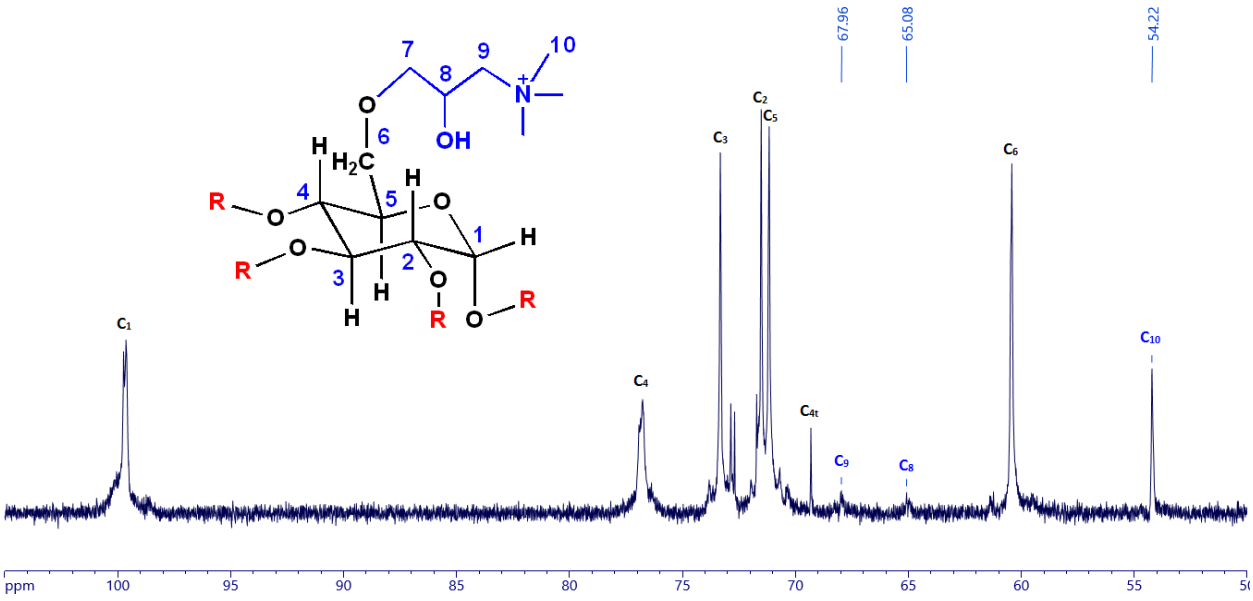

Figure 3.3. ^{13}C-NMR spectrum of a 10% dispersion of cationically modified GX2GY0 ENPs in D_2O (150 MHz).

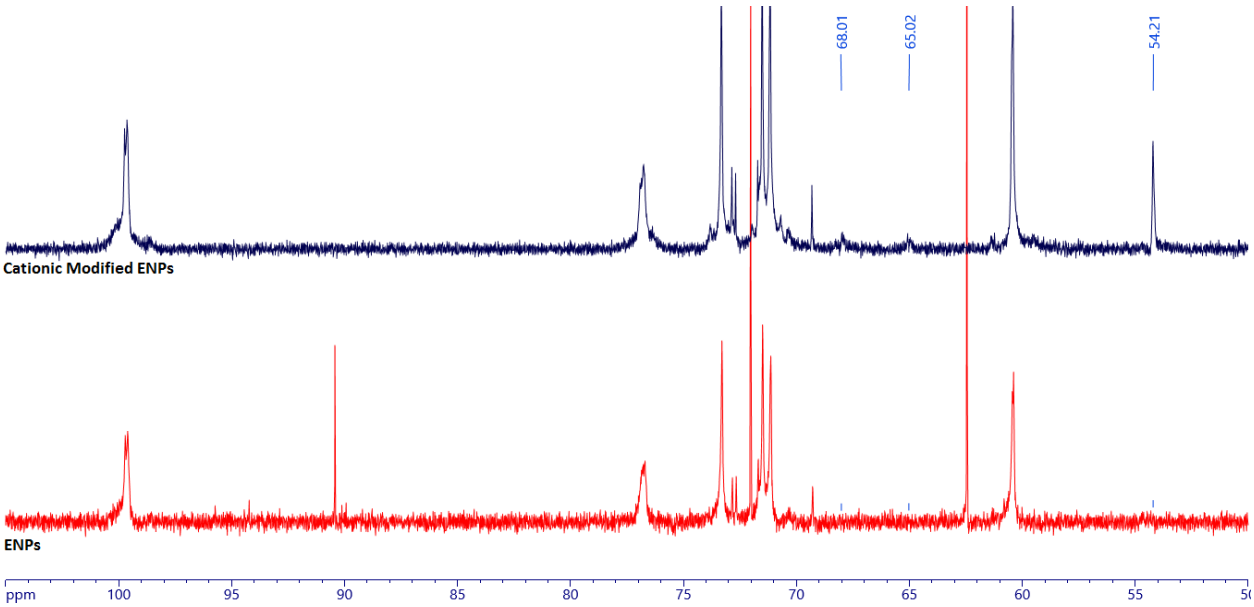

Figure 3.4. ^{13}C-NMR spectra of 10% dispersions of cationically modified GX2GY0 ENPs compared to unmodified ENPs in D_2O (150 MHz).
Top spectrum: Cationically modified ENPs
Bottom spectrum: Unmodified ENPs

Figure 3.5 shows the HMQC spectrum of the cationically modified ENPs. The correlation between C_{10} and H_{10} is clear. C_9/H_9, C_8/H_8 and C_7/H_7 correlations cannot be seen or determined probably because of the low intensity of these peaks or because they overlap with the ENP peaks.

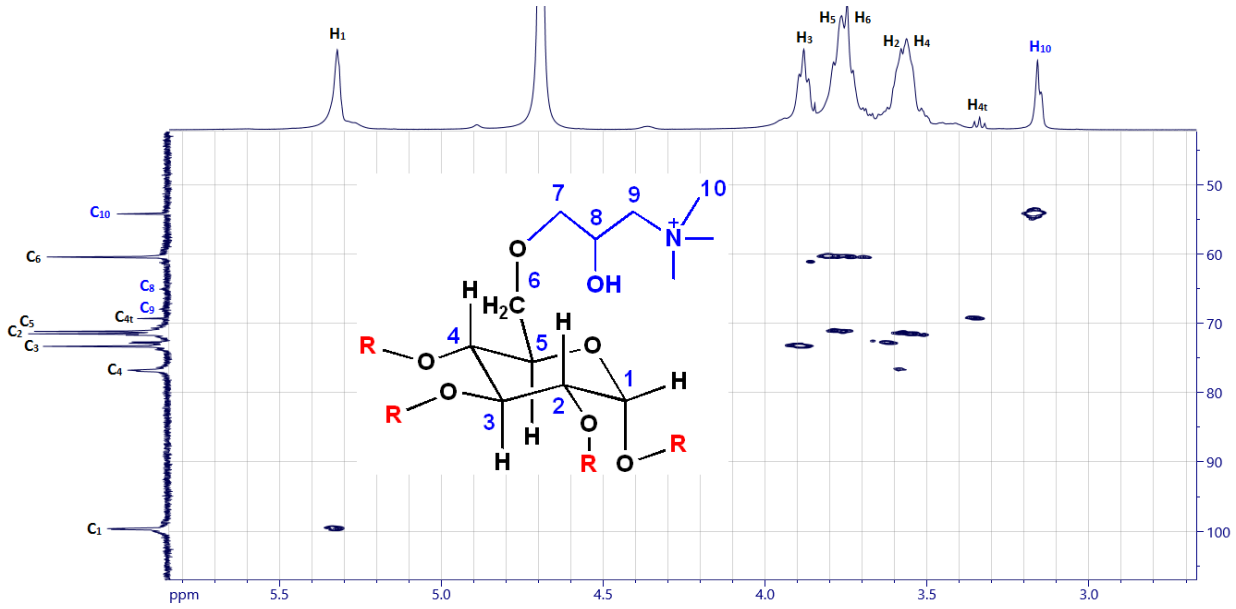

Figure 3.5. HMQC spectrum of a 10% dispersion of cationically modified GX2GY0 ENPs in D_2O (600 MHz)

Figure 3.6 shows the HMBC spectrum of the cationically modified ENPs. The objective here was to determine where the modification takes place. Unfortunately, since the protons of the cationic group are buried under the starch protons and the carbon of interest (C_7) is buried under the starch carbons, it is almost impossible to draw conclusions as to where the modification is taking place. Although C_8 and C_9 are observed, they are not the carbons that would correlate with the starch protons. However the signal between C_9 and H_{10} is present, which confirms the ^{13}C-NMR assignment for C_9.

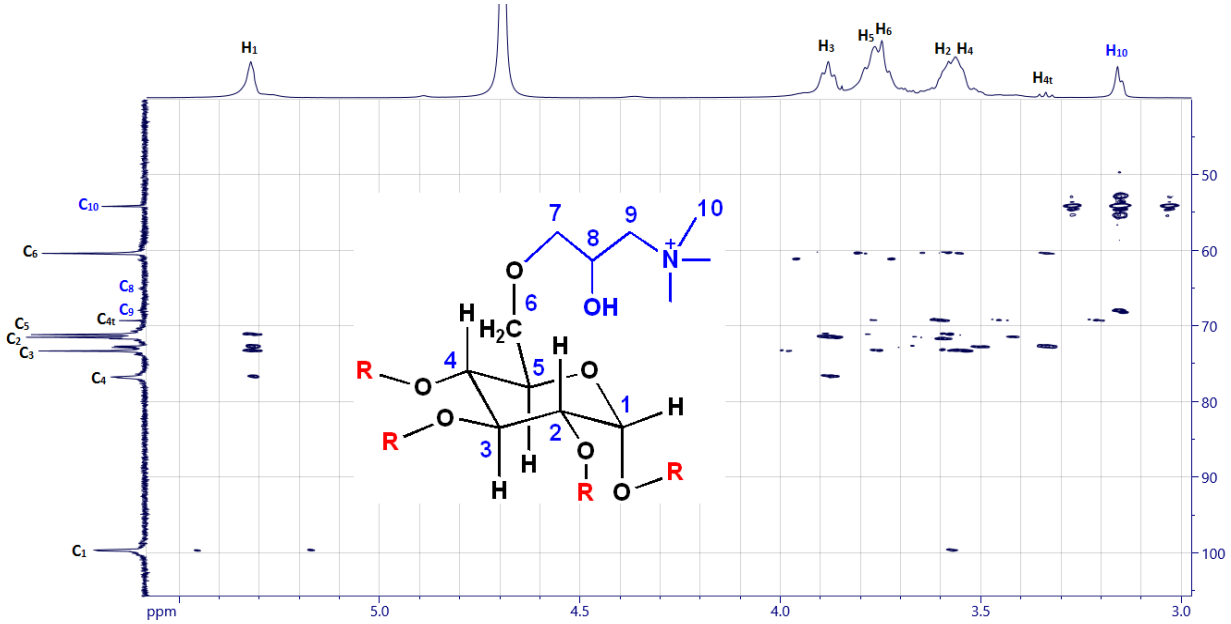

Figure 3.6. HMBC spectrum of a 10% dispersion of cationically modified GX2GY0 ENPs in D_2O (600 MHz).

3.3.3 Modifications with GTAC

GX2GY0 ENPs were used in all of the reactions described in this chapter and these reactions were carried out as follows. The ENPs were added to a blender, along with a calculated amount of reagent (GTAC or CHPTMA) and base. The mixture was blended at high speed for 3 minutes. A considerable amount of heat was generated during this process. The resulting homogeneous powder was transferred to a vial which was put into an oven that was equilibrated to the desired temperature. After a specific period of time, the vial was removed from the oven. The sample was completely dispersed in water, and then dialyzed against water. After the dialysis was completed, the solution was lyophilized and the resulting powder was analyzed by NMR. The dialysis step was essential as it was found that unreacted cationizing reagent adsorbed strongly

onto the polymer, which would result in an incorrect DS if it were not removed by dialysis. We are defining the reaction time as the amount of time the vial spent in the oven (oven duration).

Cationic modification of the ENPs was initially examined using a 75% aqueous solution of GTAC (Figure 3.7) as the cationizing reagent. For all of the GTAC reactions, 1 mol equivalent of GTAC was used per mole of AGU. Although the reaction is base-catalyzed, we first attempted the reaction in the absence of base. The mixture was allowed to react in an oven at 30, 60, 90, 120, and 150 °C for 0.5, 1, 2, 3, or 5 h.

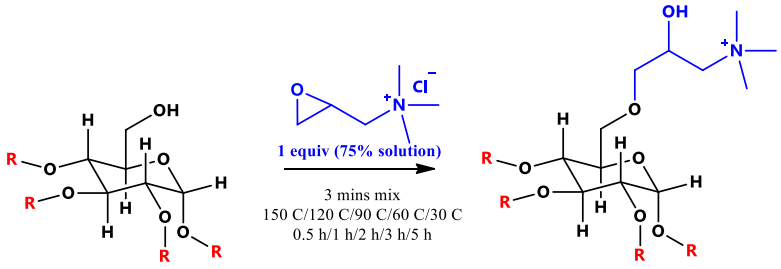

Figure 3.7. Reaction of GX2GY0 ENPs with GTAC in the absence of base.

Figure 3.8 shows the plot of the DS vs. oven temperature for the reaction described in Figure 3.7. The lowest DS was obtained at the lowest oven temperature (30 °C) regardless of the reaction time. The DS increased as the oven temperature increased to 90 °C. The DS decreased or did not change significantly at oven temperatures greater than 90 °C. When the reactions were performed at oven temperatures above 90 °C, the products were black and had a scent of burnt starch. This suggested to us that the ENPs were decomposing at these temperatures. At 90 °C and lower oven temperatures, the product was still beige in colour and had no scent of burnt starch. The highest obtained DS was 0.12 for reaction times of 3 and 5 h at 90 °C.

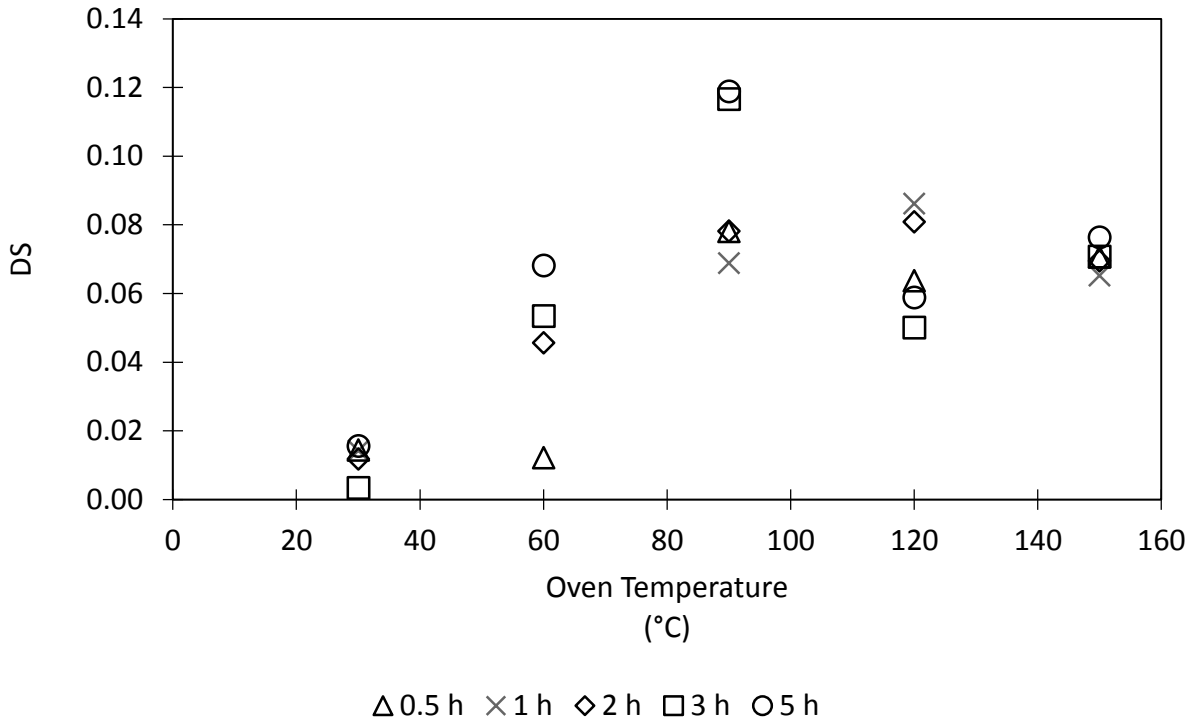

Figure 3.8. Plot of the DS vs. oven temperature for the reaction of the ENPs with GTAC in the absence of base.

Figure 3.9 shows the plots of the DS vs. reaction time for the same reaction. This representation provided an alternative perspective of the data presented in Figure 3.8. Figure 3.9 shows that at 90 °C, the highest DS was obtained. Although there was evidence of ENP degradation at the elevated temperatures, the lowest DS obtained for all reaction times was at the lowest oven temperature (30 °C).

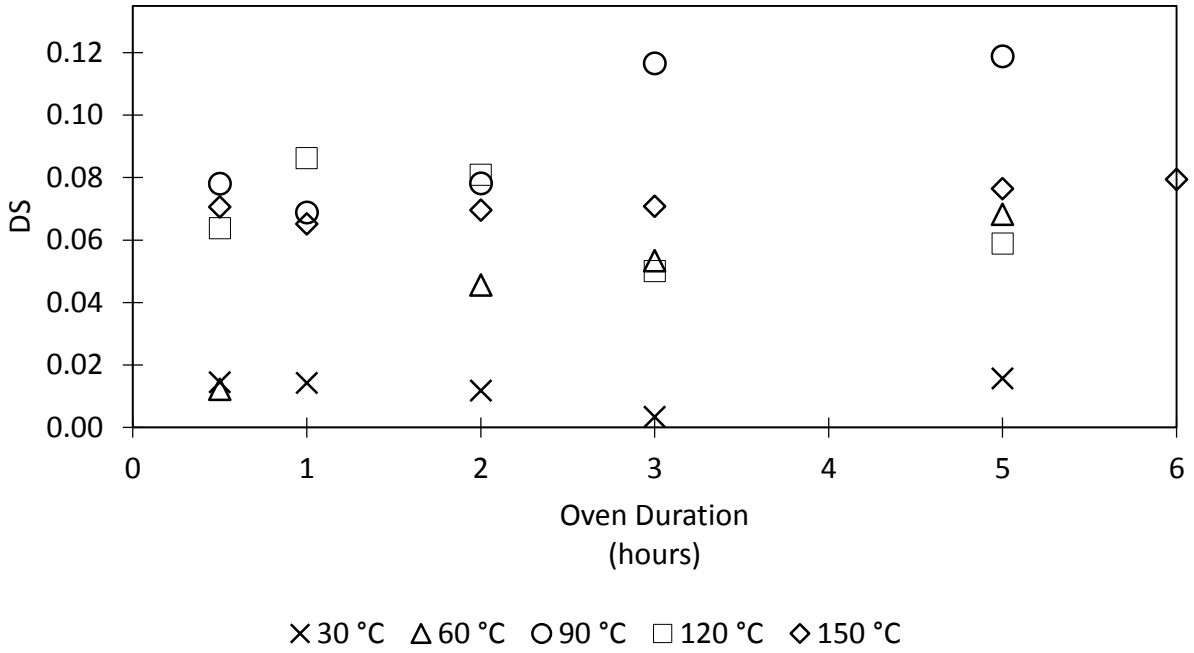

Figure 3.9. Plot of the DS vs. reaction time for the reaction of ENPs with GTAC in the absence of base.

The effect of base on the DS for the reaction shown in Figure 3.7 was initially examined by performing the reaction in the presence of 1.4 molar equivalents of CaO per mol of GTAC at an oven temperature of 150 °C for various reaction times. The CaO was added as a solid during the mixing process. The DS of these reactions and the DS of the reactions performed in the absence of base are compared in Figure 3.10. The reactions performed in the presence of CaO yielded higher DS at all reaction times as compared to the reactions performed in the absence of CaO. The most significant difference is seen at the lower reaction times (30 - 120 min). It is evident that at 150 °C, the longer reaction times led to reagent, ENP, or product decomposition because a black, burnt product was obtained. Hence, the base had a smaller effect on the DS at the longer reaction times. The highest DS obtained, 0.27, was achieved for an oven temperature of 150 °C and reaction time of 1 h.

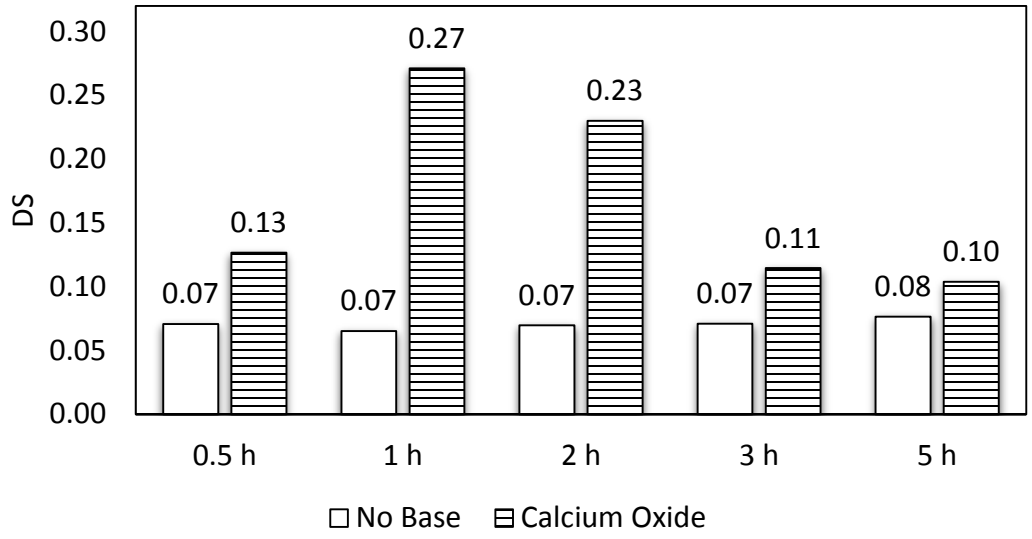

Figure 3.10. The DS for ENPs modified using GTAC in the presence and absence of CaO (1.4 mol equivalents per mol of CHPTMA) at an oven temperature of 150 °C.

The reaction shown in Figure 3.7 was also performed in the presence of a catalytic amount of NaOH. NaOH was also examined as a base because it is a more suitable base for reactions performed in an extruder. In the presence of water, CaO is converted to $Ca(OH)_2$. which is relatively insoluble in water and forms a residue on glass and metal surfaces. This residue is difficult to remove from the extruder. The modification reaction using GTAC and a catalytic NaOH amount was performed in the presence of 0.1 mol equivalents of NaOH per mol of GTAC at oven temperatures of 60 and 150 °C for 15 - 60 min. The NaOH was added as a solid during mixing. The DS was considerably higher at 150 °C as compared to 60 °C as shown in Figure 3.11. At 150 °C, a DS of 0.06 was obtained after 15 min and the DS did not change significantly as reaction times increased. This may indicate that the reagent decomposed at this temperature and increased reaction times did not affect the DS. At 60 °C, the DS increased with time indicating that the reagent was not decomposed. Although there seems to be a significant difference in the DS for

the reactions conducted at 60 °C as compared to 150 °C, the DS for both temperatures are actually comparable or lower than for the analogous reactions performed in the absence of base, as shown in Figure 3.12.

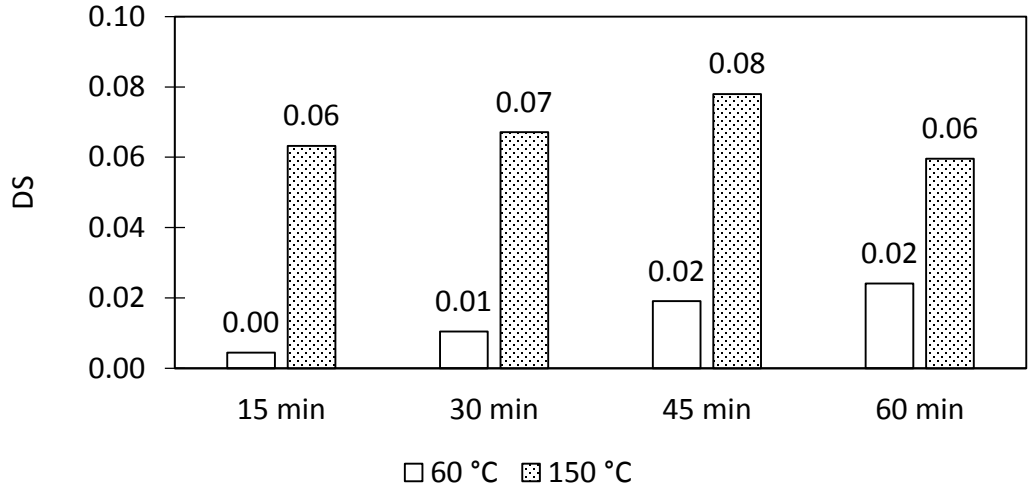

Figure 3.11. The DS for ENPs modified using GTAC in the presence of a catalytic quantity of NaOH (0.1 mol equivalents per mol of GTAC) at oven temperatures of 60 and 150 °C.

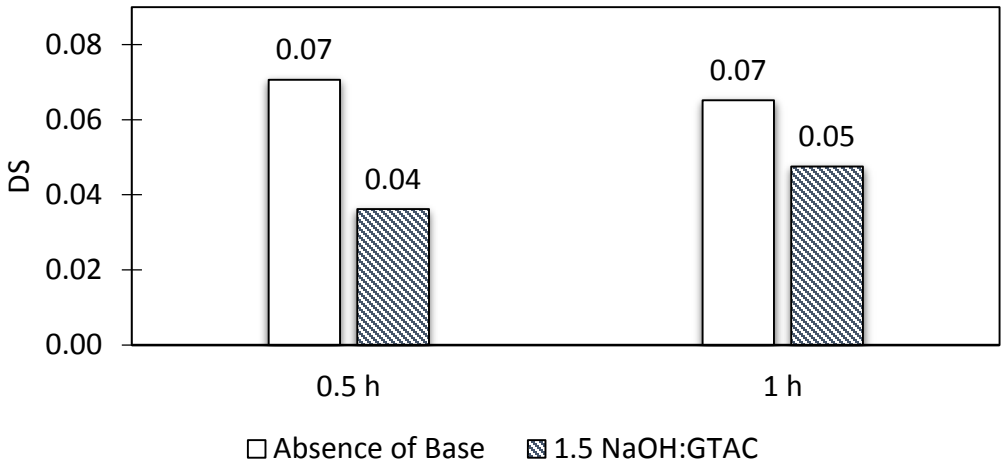

Figure 3.12. The DS for ENPs modified with GTAC in the presence and absence of a catalytic quantity of NaOH (1.5 equivalents per mol of GTAC) at 150 °C for 0.5 and 1h.

The reaction shown in Figure 3.7 was also performed in the presence of an excess amount of NaOH (1.5 mol equivalents per mol of GTAC) at oven temperatures of 60 and 150 °C for 15 - 60 min. The DS was higher for the reaction performed at 60 °C as compared to the reaction performed at 150 °C for all the reaction times as shown in Figure 3.13. At 150 °C, the reaction using 1.5 mol equivalents of NaOH yielded a similar DS to the reaction performed using 0.1 mol equivalents of NaOH. This can be explained by reagent, substrate or product decomposition that occurred at the higher temperatures which inhibited the reaction, hence the DS is independent of the NaOH concentration at the higher temperatures.

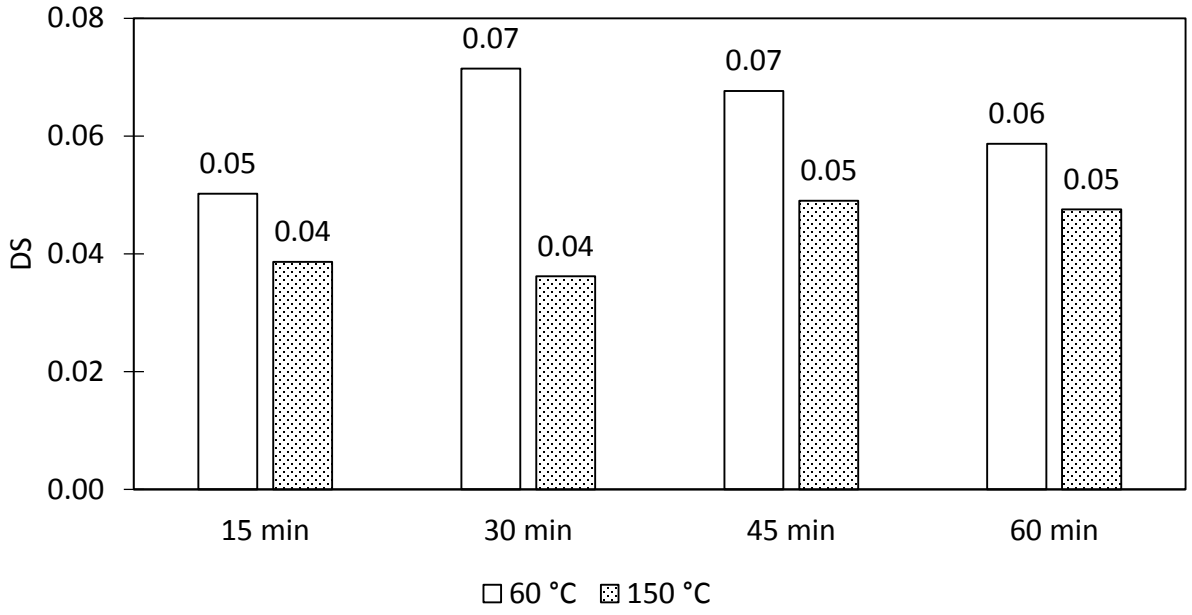

Figure 3.13. The DS for ENPs modified with GTAC in the presence of excess NaOH (1.5 mol equivalents per mol of GTAC) at 60 °C and 150 °C for 15 - 60 min.

Next, the reaction shown in Figure 3.7 was performed using 0.8 mol equivalents of NaOH per mol of GTAC at an oven temperature of 105 °C for 15 - 60 min. The DS for these reactions are illustrated in Figure 3.14. It appears that at 105 °C, the DS decreases as the reaction time

increases, but as shown with the error bars, the difference in the DS may be negligible. These reactions were performed in triplicate. The highest error was calculated to be 8.7%. This does not mean that all of the DS reported in this chapter have an error that is less than 8.7%.

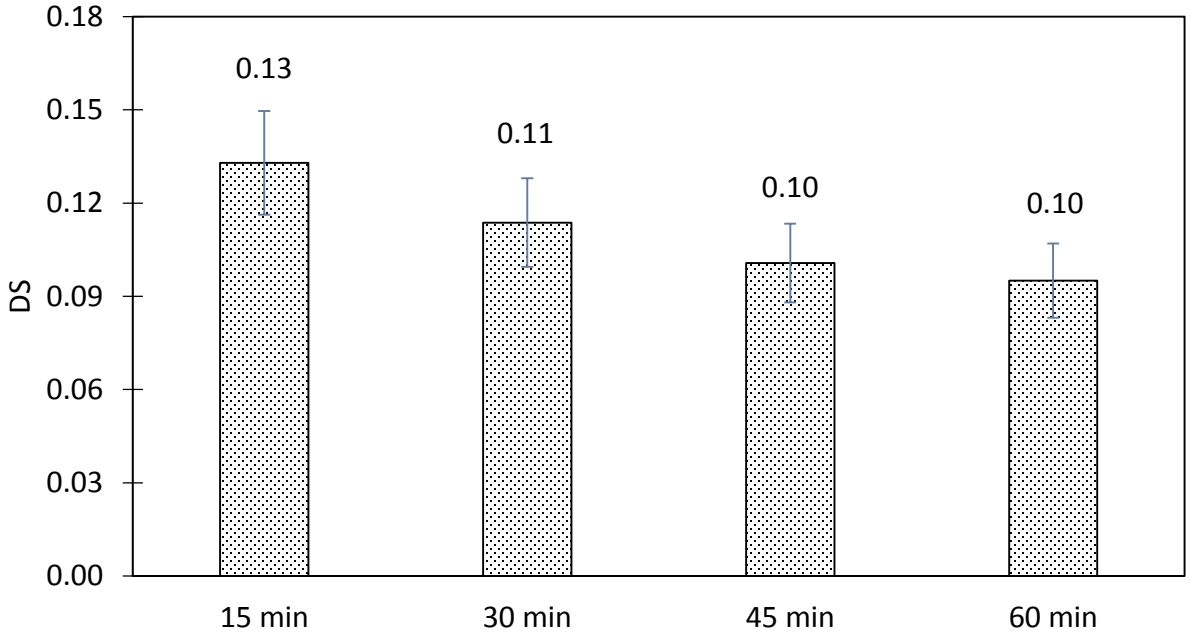

Figure 3.14. The DS for ENPs modified with GTAC in the presence of NaOH (0.8 mol equivalents per mol of GTAC) at 60 and 150 °C for 15 - 60 min.

3.3.4 Modifications with CHPTMA

The cationic modification of the ENPs using CHPTMA as the cationizing reagent was also examined (Figure 3.15). This reagent is considerably less expensive than GTAC and less prone to decomposition during storage as compared to GTAC. Hence CHPTMA is used more widely than GTAC as a reagent for cationic starch modification in commercial applications.

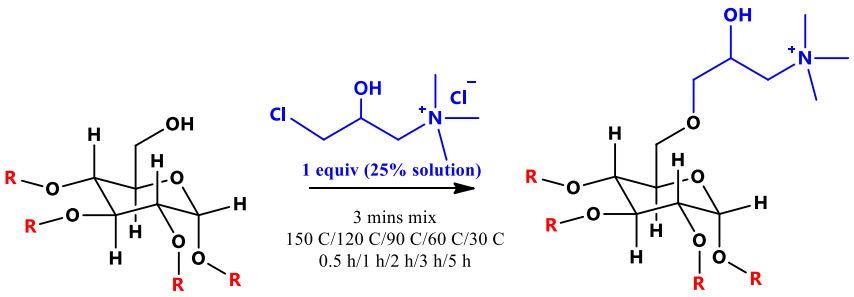

Figure 3.15. Reaction of ENPs with CHPTMA in the absence of base.

CHPTMA was purchased from a commercial source as a 25 % solution in water. One mol equivalent of CHPTMA per mol of AGU was used for all of these reactions unless stated otherwise. Although the reaction requires at least 1 mol equivalent of base per mol of CHPTMA in order to convert CHPTMA into GTAC in situ, we first attempted the reaction in the absence of base. The mixture was allowed to react in an oven at 30, 60, 90, 120, and 150 °C for 0.5, 1, 2, 3, or 5 h. Figure 3.16 illustrates the relationship between the DS and oven temperature. Figure 3.16 illustrates the relationship between the DS and reaction time. Cationically modified ENPs were only detected at 150 °C, and only when the reaction time was greater than 1 h. This indicates that the conversion of CHPTMA to GTAC proceeds spontaneously at high temperatures and logically, the longer the reaction time, the higher the conversion rate. However, at this temperature, there was evidence of decomposition because a black product was obtained and had the scent of burnt starch. The highest DS of 0.51 was obtained at an oven temperature of 150 °C and reaction time of 5 h.

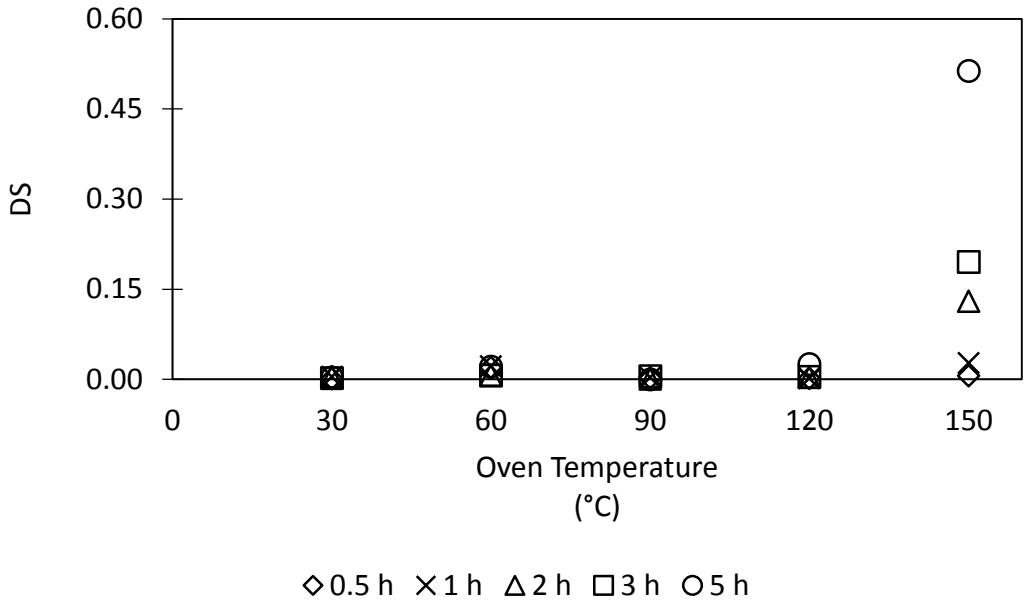

Figure 3.16. Plot of the DS vs. oven temperature for the reaction of ENPs with CHPTMA in the absence of base.

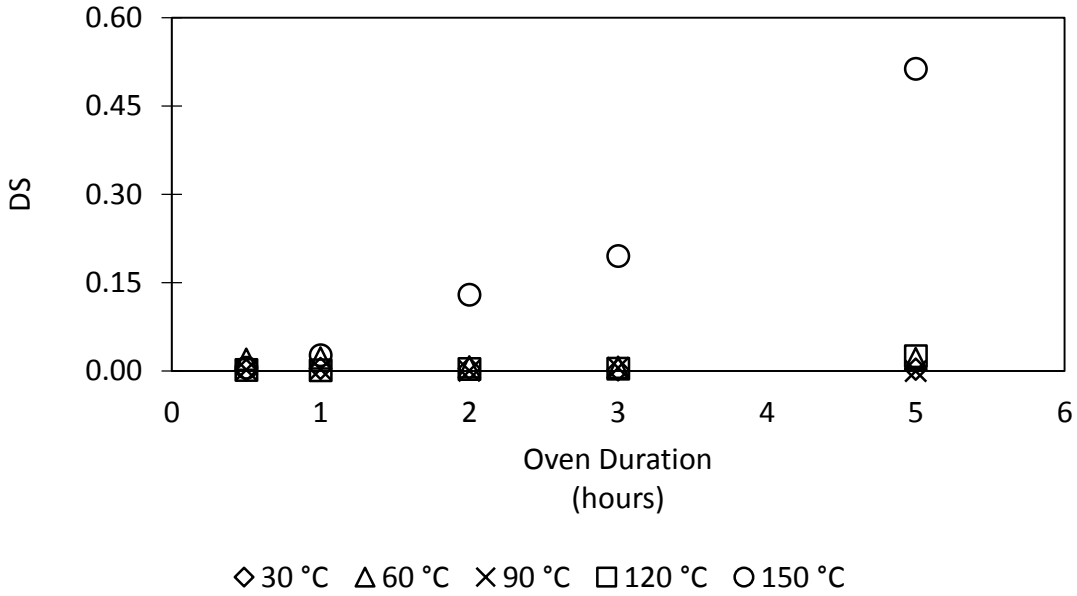

Figure 3.17. Plot of the DS vs. reaction time for the reaction of ENPs with CHPTMA in the absence of base.

The reactions shown in Figure 3.15 were performed in the presence of 2.5 mol equivalents of CaO per mol of CHPTMA. Figure 3.18 illustrates the plots of the DS versus the reaction time for these reactions. The presence of the base resulted in the formation of cationic ENPs at reaction temperatures where no product was detected when the reactions were performed in the absence of base. The exception was the reaction performed in the absence of base at 150 °C which gave a higher DS compared to the reaction performed at 150 °C in the presence of base. Although some of the results are confusing, such as the lack of a product formed after 30 min at 120 °C, it does appear that a maximum DS is reached after a short period of time (within 30 - 120 min), and longer reaction times lead to a less efficient reaction. It was evident that decomposition of the starch or the reagent occurred at the higher temperatures and longer reaction times. The maximum DS of 0.61 was obtained at a reaction time of 3 h at 30 °C.

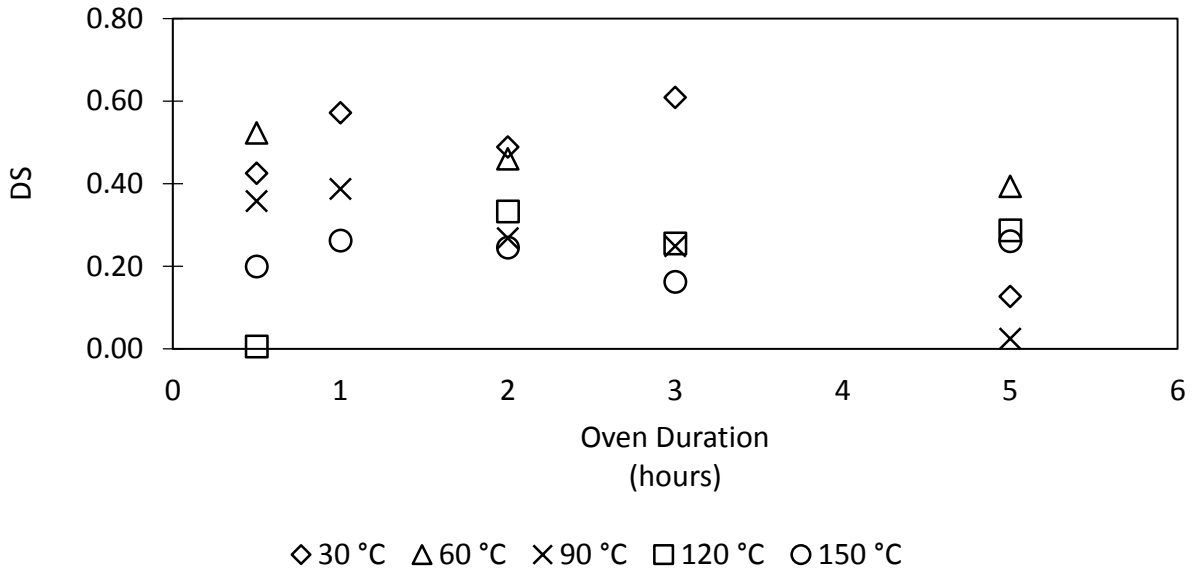

Figure 3.18. Plot of the DS vs. oven duration for the reaction of ENPs with CHPTMA in the presence of CaO (2.5 mol equivalents per mol of CHPTMA).

The modification of the ENPs with CHPTMA was also examined using NaOH as the base. These reactions were performed using 1 mol equivalent of CHPTMA (relative to AGU) and 0.1, 0.3, 1.1, and 2.7 mol equivalents of NaOH per mol of CHPTMA at 60 °C. The DS was determined every 15 min up to a maximum of 60 min. Figure 3.19 shows the plot of DS versus the reaction time for these reactions. Little or no reaction occurred with 0.1, 0.3, and 1.1 mol equivalents of NaOH. A DS of 0.2 was obtained after 15 min using 2.7 mol equivalents of NaOH. The DS did not increase significantly after the 15 min reaction time. When the reaction was performed using 2.5 mol equivalents of CaO as base (see Figure 2.18) a DS of 0.53 was obtained after 15 min. These results indicate that CaO is a more effective base than NaOH (in terms of DS).

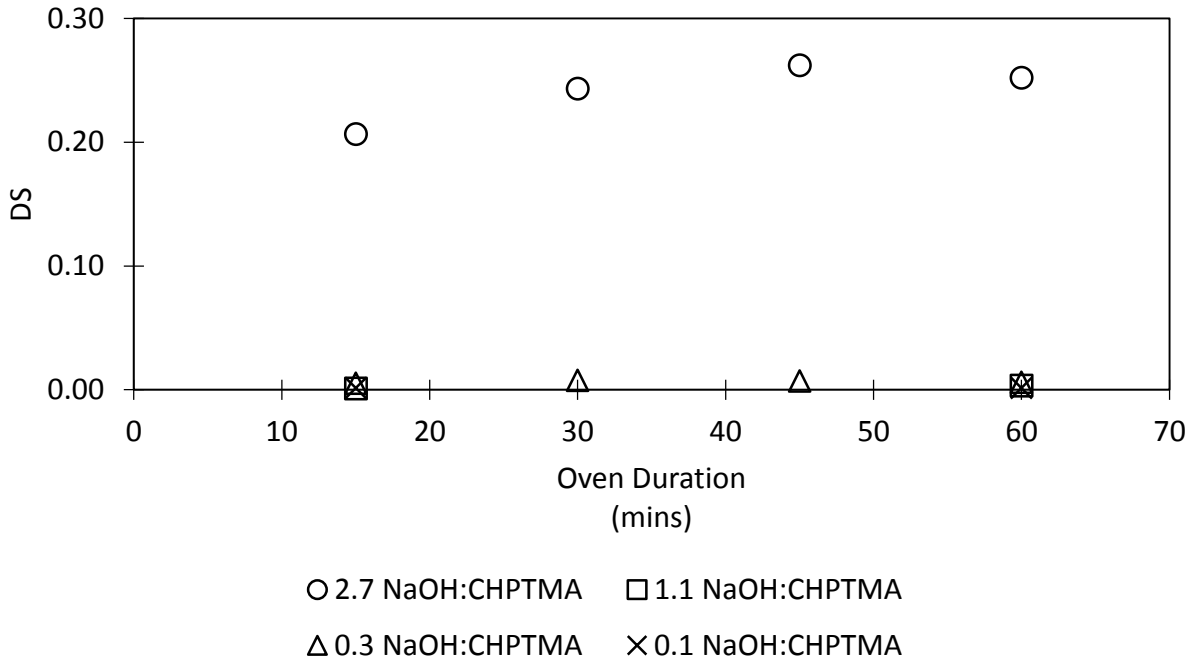

Figure 3.19. Plot of the DS vs. oven duration for the reaction of ENPs with CHPTMA in the presence of varying amounts of NaOH at 60 °C.

The reactions described in Figure 3.19 were repeated except that the reactions were performed at 150 °C. Figure 3.20 shows the plot of DS versus the reaction time for these reactions. Little or no reaction occurred with 0.1, 0.3, and 1.1 mol equivalents of NaOH. A DS of 0.09 was obtained after 15 min of using 2.7 mol equivalents of NaOH. The DS did not change significantly after the 15 min reaction time. The DS was lower when the reaction was performed at 150 °C compared to at 60 °C. This can be explained by the decomposition of the starch, starch products and the CHPTMA at the higher temperature.

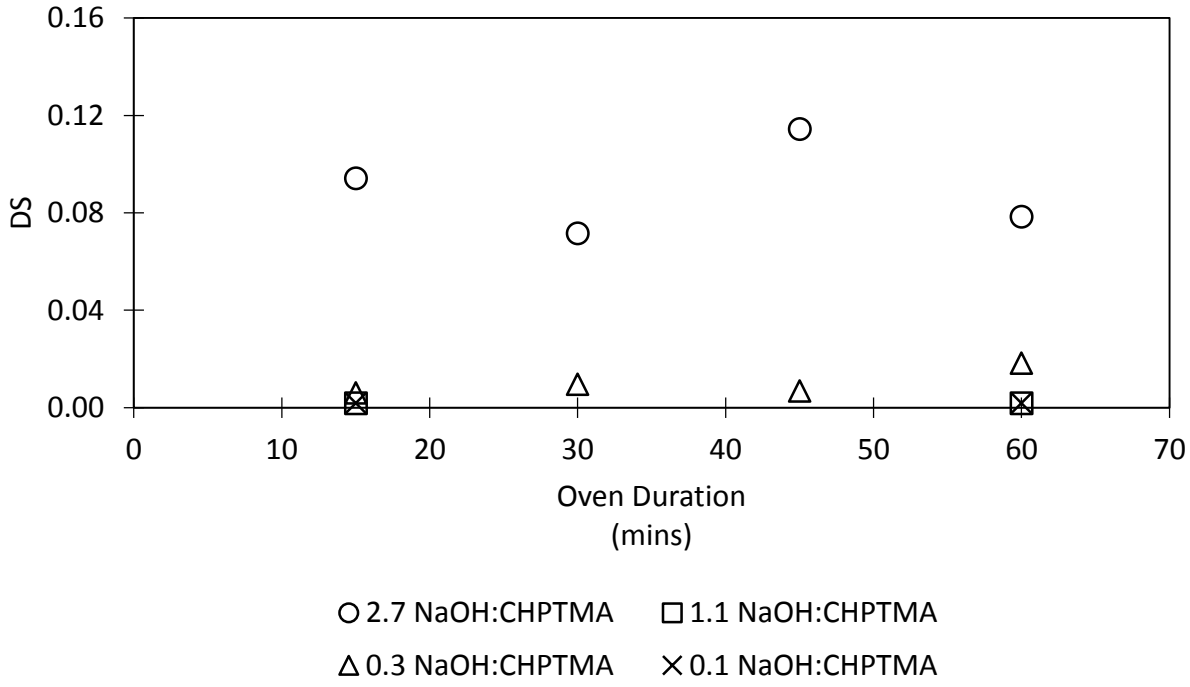

Figure 3.20. Plot of the DS vs. oven duration for the reaction of ENPs with CHPTMA in the presence of varying amounts of NaOH at 150 °C.

3.4 Summary and Future Work

This chapter describes the first cationic modification of ENPs. This was achieved using a dry process. Attempts were made to optimize the reaction. Parameters that were tested included the reaction temperature, reaction time, and base concentration. It is important to point out that, due to a lack of time and resources (i.e. NMR time), it was not possible for most of the reactions described in this chapter to be performed in triplicates (or more) and hence the errors for most the DS reported in this chapter were not determined. Since we were unable to control a variety of factors such as the temperature during mixing and our inability to agitate the mixture in the oven, it is very possible that the error for many of the DS is large. Our inability to control these factors may be the reason behind some of the confusing results obtained from some of the reactions. In spite of these issues, we believe that some trends could be determined from the data presented in this chapter. The reaction temperatures appeared to have a strong effect on the DS up until 90 °C. At higher temperatures, there was evidence of starch and possibly reagent degradation which negatively affected the DS. The reaction time did not appear to have a significant effect on DS as compared to the reaction temperature. At low temperatures, an increase in base concentration to an increase in DS. CaO performed better (in terms of the DS) than NaOH under virtually all of the reaction conditions. It is recommended to use a concentrated NaOH solution in future experiments to increase the surface area contact of the base with the ENPs. It is unlikely that a dry process will produce cationic ENPs with high enough DS to be used as flocculants for wastewater removal. However, this cannot be said with certainty since the dry reaction conditions have not yet been completely optimized.

EcoSynthetix™ would like to prepare cationically modified ENPs in an extruder using CHPTMA as the modifying reagent. Although we have not yet optimized the cationic modification of ENPs using CHPTMA, and our dry reaction conditions are different from the reaction conditions created inside an extruder, the results in this chapter are being used by researchers at EcoSynthetix™ as a foundation for their attempts to prepare cationically modified ENPs using an extruder.

3.5 Experimental

3.5.1 NMR

The ENPs were donated by EcoSynthetix Inc. (Burlington, Ontario). GTAC and CHPTMA were purchased from Sigma Aldrich Co. (Milwaukee, Wisc., USA). An Eberbach Waring® E8400 blender was used as the mixer for all of the dry cationization reactions. A Binder ED53 oven was used for all of the dry cationization reactions. Deuterium oxide (D_2O) was purchased from Sigma Aldrich Chemical Co. (Milwaukee, Wisc., USA). ^{1}H- and ^{13}C-NMR, HMQC and HMBC spectra were recorded on Bruker 500 MHz and 600 MHz instrument. The 600 MHz instrument utilized a Quattro Resonance X1+X2+X3 Decoupling Inverse Probe (QNP) and the 500 MHz instrument utilized a Triple Resonance X1+X2 Nucleus Decoupling Inverse Probe (TXI). ^{1}H-NMR chemical shifts of spectra run in D_2O were referenced to the solvent residual peak at 4.80 ppm. ^{13}C-NMR chemical shifts of spectra run in D_2O were referenced to methyl peak of 4,4-dimethyl-4-silapentane-1-sulfonic acid (0.0 ppm, external standard).

3.5.2 Dry Cationization of ENPs

GX2GY0 ENPs were added to a mixer in dry powder form along with a calculated amount of reagent (GTAC or CHPTMA) and base (CaO or NaOH). The mixture was mixed for 3 minutes and the resulting homogenous powder was transferred to a reaction vial. The vial was placed in an oven at the desired temperature. After a desired period of time, the vial was removed from the oven and the powder was dispersed in water at room temperature which took anywhere from 12 – 48 h. After the sample was dispersed, it was then transferred to a Spectra/Por® 1000 MWCO membrane and dialyzed against Milli-Q water (3 x 10^2 dilution over 24 h). After the dialysis was completed, the solution was lyophilized and the resulting powder was analyzed by NMR.

References

[1]Le Corre, D.; Bras, J.; Dufresne, A. *Biomacromolecules* **2010**, 11, 1139-1153.

[2]Cioica, N.; Fechete, R.; Cota, C.; Nagy, E.M.; David, L.; Cozar, O. *J. Mol. Struct*. **2013**, 1044, 128-133.

[3]Chakraborty, S.; Sahoo, B.; Teraoka, I.; Gross, R.A. *Carbohydr. Polym.* **2005**, 60, 475-481.

[4]Uslu, M.; Polat, S. *Carbohydr. Polym.* **2012**, 87, 1994-1999.

[5]Wang, G.; Thompson, M.R.; Liu, Q. *Starch/Stärke* **2012**, 64, 55-63.

[6]Hedin, J.; Östlund, A.; Nydén. *Carbohydr. Polym.* **2010**, 79, 606-613.

[7]Moad, G. *Prog. Polym. Sci.* **2011**, 36, 218-237.

[8]Hablot, E.; Dewasthale, S.; Zhao, Y.; Zhiguan, Y.; Shi, X.; Graiver, D.; Narayan, R. *Eur. Polym. J*. **2013**, 49, 873-881.

[9]Xu, J.; Finkenstadt, V.L. *Starch/Stärke* **2013**, 65, 984-990.

[10]Miles, M.J.; Morris, V.J.; Orford, P.D.; Ring, S.G. *Carbohydr. Res*. **1985**, 135, 271-281.

[11]Falk, H.; Stanek, M. *Monatsh. Chem.* **1997**, 784, 777-784.

[12]Liu, H.; Xie, F.; Yu, L.; Chen, L.; Li, L. *Prog. Polym. Sci.* **2009**, 34, 1348-1368.

[13]van Soesta, J.J.G.; Vliegenthartb, J.F.G. *Trends Biotechnol.* **1997**, 15, 208-213.

[14]Tavares, M.I.B.; Bathista, A.L.B.S; Silva, E.O.; Costa, P.M.; Filho, N.P.; Nogueira, J.S. *J. Appl. Polym. Sci.* **2004**, 92, 2151-2154.

[15]Shi, A.; Li, D.; Wang, L.; Li, B.; Adhikari, B. *Carbohydr. Polym.* **2011**, 83, 1604-1610.

[16]Santander-Ortega, M.J.; Stauner, T.; Loretz, B.; Ortega-Vinuesa, J.L.; Bastos-González, D.; Wenz, G.; Schaefer, U.F.; Lehr, C.M. *J. Control Release* **2010**, 141, 85-92.

[17]Tomasik, P.; Schilling, C.H. *Adv. Carbohydr. Chem. Biochem.* **2004**, 59, 175-406.

[18]Spychaj, T.; Wilpiszewska, K.; Zdanowicz, M. *Starch/Stärke* **2013**, 65, 22-33.

[19]Pal, S.; Mal, D.; Singh, R. P. *Carbohydr. Polym.* **2005**, 59, 417–423.

[20]Le Corre, D.; Bras, J.; Dufresne, *Biomacromolecules* **2010**, 11, 1139–1153.

[21]Bendoraitienė, J.; Klimaviciute, R.; Zemaitaitis, A. *Starch/Stärke* **2012**, 64, 696-703.

[22]Kweon, M. R.; Bhirud, P. R.; Sosulski, F. W. *Starch/Stärke* **1996**, 48, 214-220.

[23]Wei, Y.; Cheng, F.; Zheng, H. *Carbohydr. Polym.* **2008**, 74, 673-679.

[24]Krentz, D.-O,; Lohmann, C.; Schwarz. S.; Bratskaya, S.; Liebert, T.; Laube, J.; Heinze, T.; Kulicke, W-M. Starch/*Stärke* **2006**, 58, 161-169.

[25]Haack, V.; Heinze, T.; Oelmeyer, G.; Kulicke, W-M. *Macromol. Mater. Eng.* **2002**, 287, 495-502.

[26]Heinze, T.; Haack, V.; Rensing, S. *Starch/Stärke* **2004**, 56, 288-296.

[27]Nyström, R.; Backfolk, K.; Rosenholm, J. B.; Nurmi, K. *Colloid Surface, A* **2003**, 219, 55–66.

[28]Bratskaya, S.; Schwartz, S.; Liebert, T.; Heinze, T. *Colloids Surface* **2005**, 254, 75-80.

[29]Carr, M.E. *J. Appl. Polym. Sci.* **1994**, 54, 1855-1861.

[30]Tara, A.; Berzin, F.; Tighzert.; Vergnes, B. *J. Appl. Polym. Sci*. **2004**, 93, 201-208.

[31]Kavaliauskaite, R.; Klimaviciute, R.; Zemaitaitis, A. *Carbohydr. Polym.* **2008**, 665-675.

[32]Reddy, N.; Yang, Y. *Food Chem*. **2010**, 118, 702-711.

[33]Seker, M.; Hanna, M.A. *Carbohydr. Polym.* **2005**, 59, 541-544.

[34]Namazi, H.; Fathi, F.; Dadkhah, A. *Sci. Iran.* **2011**, 18, 439-445.

[35]Lee, D.I.; Bloembergen, S.; van Leeuwen, J. *PaperCon*. **2010**. 1-19.

[36]Bloembergen, S.; McLennan, I.J.; van Leeuwen, J. *PTS Advanced Coating Fundamentals Symposium*. **2010**, 1-19.

[37]Chakraborty, S.; Sahoo, B.; Teraoka, I.; Miller, L.M.; Gross, R.A. *Macromolecules* **2005**, 38, 61-68

[38]Chiou, H.; Fellows, C.M.; Gilbert, R.G.; Fitzgerald, M.A. *Carbohydr. Polym.* **2005**, 61, 61-71.

[39]Ma, X.; Jian, R.; Chang, P.R; Yu, J. *Biomacromolecules* **2008**, 9, 3314-3320.

[40]Rabiller, C. *New J. Chem.* **1987**, 11, 419-429.

[41]Chastrette, F.; Bracoud, C.; Chastrette, M.; Mattioda, G.; Christidis, Y. *B. Soc. Chim. Fr.* **1983**, 1-2, 11-39.

[42]Whipple, E.B. *J. Am. Chem. Soc.* **1970**, 92, 7183-7186.

[43]Kliegman, J.M; Barnes, R.K. *J. Org. Chem.* **1974**, 39, 1772-1776.

[44]Paalme, T.; Olivson, A.; Vilu, R. *Biochim. Biophys. Acta*, **1982**, 720, 303-310.

[45]Mora-Guiterrez, A.; Baianu, I.C. *J. Agri. Food Chem*, **1991**, 39, 1057-1062.

[46]McIntyre, D.D.; Ho, C.; Vogel, H.J. *Starch/Stärke* **1990**, 42, 260-267.

[47]Mattioda, G.; Blanc, A. (**1989**). *Ullmann's Enclopedia of Industrial Chemistry*. Weinheim, New York: Verlag Chemie.

[48]Chastrette, F.; Bracoud, C.; Chastrette, M.; Mattioda, G.; Christidis, Y. *Bull. Soc. Chim. Fr.* **1983**, 33-40.

[49]Fratzke, A.R.; Reilly, P.J. *Int. J. Chem. Kinet.* **1986**, 18, 775-789.

[50]Trincado, M.; Kühlein, K.; Grützmacher, H. *Chem. Eur. J.* **2011**, 17, 11905-11913.

[51]Zhang, Y.; Zhu, P.C.; Edgren, D. *J. Polym. Res.* **2010**, 17, 725-730.

[52]Nyström, R.; Rosenholm, J.B. *Colloid Surface A* **2005**, 252, 135-141.

[53]Maniruzzaman, M.; Douroumis, D.; Boateng, J.S.; Snowden, M.J. *Recent Advances in Novel Drug Carrier Systems* **2012**, 3-16.

[54]Pack, S.; Bobo, E.; Muir, N.; Yang, K.; Swaraj, S.; Ade, H.; Cao, C.; Korach, C.S.; Kashiwagi, T.; Rafailovich, M.H. *Polymer* **2012**, 53, 4787-4799.

[55]Alissandratos, A.; Halling, P.J. *Bioresour. Technol.* **2012**, 115, 41-47.

[56]Bubb, W. A. *Concepts Magnetic Res*. **2003**, 19A, 1–19.

[57]Kim, H.; Hwang, D.; Kim, B.; Baik, M. *Food Chem*. **2012**, 130, 977-980.

[58]Brigger, I.; Dubernet, C.; Couvreur, P. *Adv. Drug Delivery Rev*. **2002**, 54, 631-651.

[59]Rutledge, J.E.; Islam, M.N.; James, W.H. *Cereal Chem*. **1974**, 51, 46-51.

[60]Goclik, V.; Stach, S.; Mischnick, P. *J. Chromatogr.* **2004**, 1038, 283-289.